

Electronic Supplementary Information

A Cross-Conjugation Approach for High-Performance Diaryl-Hemithioindigo Photoswitches

Max Zitzmann,[§] Frank Hampel,[§] Henry Dube^{§*}

[§] Friedrich-Alexander-Universität Erlangen-Nürnberg, Department of Chemistry and Pharmacy, Nikolaus-Fiebiger-Str. 10, 91058 Erlangen, Germany.

Table of Contents

Synthesis	2
General Procedures, Instrumentation and Materials	2
Synthesis Overview	4
Synthetic Protocols	6
Synthesis of Thioethers 12-14	6
General procedure for the synthesis of (3-hydroxybenzo[<i>b</i>]thiophen-2-yl)methanones 15-17	9
Synthesis of vinyl chlorides 18-20.....	11
Synthesis of Diaryl-HTIs 1-10.....	15
UV/Vis Spectroscopic Measurements	25
Determination of the UV/Vis Spectra of Pure <i>Z</i> and <i>E</i> Isomers	25
Molar Extinction Coefficients of Diaryl-HTIs	27
NMR Irradiation experiments	34
Thermal Double Bond Isomerization.....	44
Quantum Yield Determination.....	57
Molecular Logic Application of Diaryl-HTIs 3 and 8 in Logic Gates and Keypad Locks.....	66
Theoretical Description of Diaryl-HTI 3 and Diaryl-HTI 8	75
1D NOE NMR Spectra for Determination of Isomer Configuration.....	78
Crystal Structural Data.....	84
NMR spectra	87
References.....	106

Synthesis

General Procedures, Instrumentation and Materials

General. All reactions involving oxygen- or moisture-sensitive compounds were carried out in dry reaction vessels under an inert atmosphere of nitrogen using anhydrous solvents and standard Schlenk techniques. All oxygen- and moisture-sensitive liquids and anhydrous solvents were transferred *via* a syringe or a stainless-steel cannula. Analytical TLC analysis was performed on aluminum plates coated with 0.20 mm silica gel containing a fluorescent indicator (Macherey-Nagel, ALUGRAM®, Sil G/UV₂₅₄) or on aluminum plates coated with 0.20 mm aluminum oxide containing a fluorescent indicator (Macherey-Nagel, ALUGRAM®, ALOX N/UV₂₅₄). For visualization TLC plates were exposed to ultraviolet light ($\lambda = 254$ nm and 366 nm). Column chromatography was performed on silica gel (Macherey-Nagel, M-N Silica Gel 60A, 230-400 mesh) or aluminum oxide (Macherey-Nagel, M-N Aluminum oxide neutral, 90A, 50-200 mesh).

Solvents and Reagents. Reagents were purchased at reagent grade from commercial suppliers and used without further purification. MgSO₄ was used as the drying agent after aqueous workup.

Instrumentation. ¹H- and ¹³C-NMR spectra were recorded on a Bruker Avance Neo HD 400 (Bruker, 400 MHz for ¹H, 101 MHz for ¹³C), a Bruker Avance Neo HD 500 (Bruker, 500 MHz for ¹H, 126 MHz for ¹³C), and a Bruker Avance Neo HD 600 (Bruker, 601 MHz for ¹H, 151 MHz for ¹³C) spectrometer. Chemical shifts (δ) are reported in ppm and were referenced to the residual solvent signal as an internal reference (CDCl₃: 7.26 ppm for ¹H and 77.16 ppm for ¹³C, (CD₃)₂CO: 2.05 ppm for ¹H and 29.84 ppm for ¹³C, CD₂Cl₂: 5.32 ppm for ¹H and 54.00 ppm for ¹³C, (CD₃)₂SO: 2.50 ppm for ¹H and 39.52 ppm for ¹³C, toluene-*d*₈: 2.09 ppm for ¹H, benzene-*d*₆: 7.16 ppm for ¹H, THF-*d*₈: 3.58 ppm for ¹H). Coupling constants (*J*) are given in Hz as observed and the apparent resonance multiplicity is reported as s (singlet), d (doublet), t (triplet), q (quartet), dd (doublet of doublets), dt (doublet of triplets), td (triplet of doublets) and ddd (doublet of doublets of doublets) or m (multiplet).^[1]

All signals of solvents and impurities are assigned according to literature. CDCl₃ (Deutero GmbH, 99.8%), toluene-*d*₈ (Deutero GmbH, 99.5%), (CD₃)₂CO (Deutero GmbH, 99.8%), (CD₃)₂SO (Deutero GmbH, 99.0%), CD₂Cl₂ (Deutero GmbH, 99.6%) and benzene-*d*₆ (Deutero GmbH, 99.5%) were used to dissolve the samples. All spectra were recorded at ambient probe temperatures if not otherwise stated.

Medium pressure liquid chromatography was performed on a Biotage Isolera One or on a Biotage Selekt instrument. As stationary phase a CHROMABOND® Flash RS 40 SiOH column (particle size 40-63 μm), a CHROMABOND® Flash RS 25 SiOH column (particle size 40-63 μm), a CHROMABOND® Flash RS 15 SiOH column (particle size 40-63 μm), and a CHROMABOND® Flash RS 4 SiOH column (particle size 40-63 μm) were used.

Mass spectra were obtained from a MicroTOF II (Bruker, HR ESI and APPI) or a UltraflexTOF/TOF (Bruker, HR MALDI) mass spectrometer.

IR spectra were recorded on a 660-IR (Varian, ATR mode) spectrometer and characteristic IR absorptions were reported in cm^{-1} and labeled as strong (s), medium (m) and weak (w).

UV/Vis absorption measurements were acquired on a Cary 60 UV-Vis (Agilent Technologies) or on a Cary 500 UV-Vis NIR (Varian) spectrophotometer in a quartz cuvette (1 cm) at room temperature. The absorption maxima (λ_{max}) are reported in nm with the extinction coefficient (ϵ) in $\text{M}^{-1}\text{cm}^{-1}$.

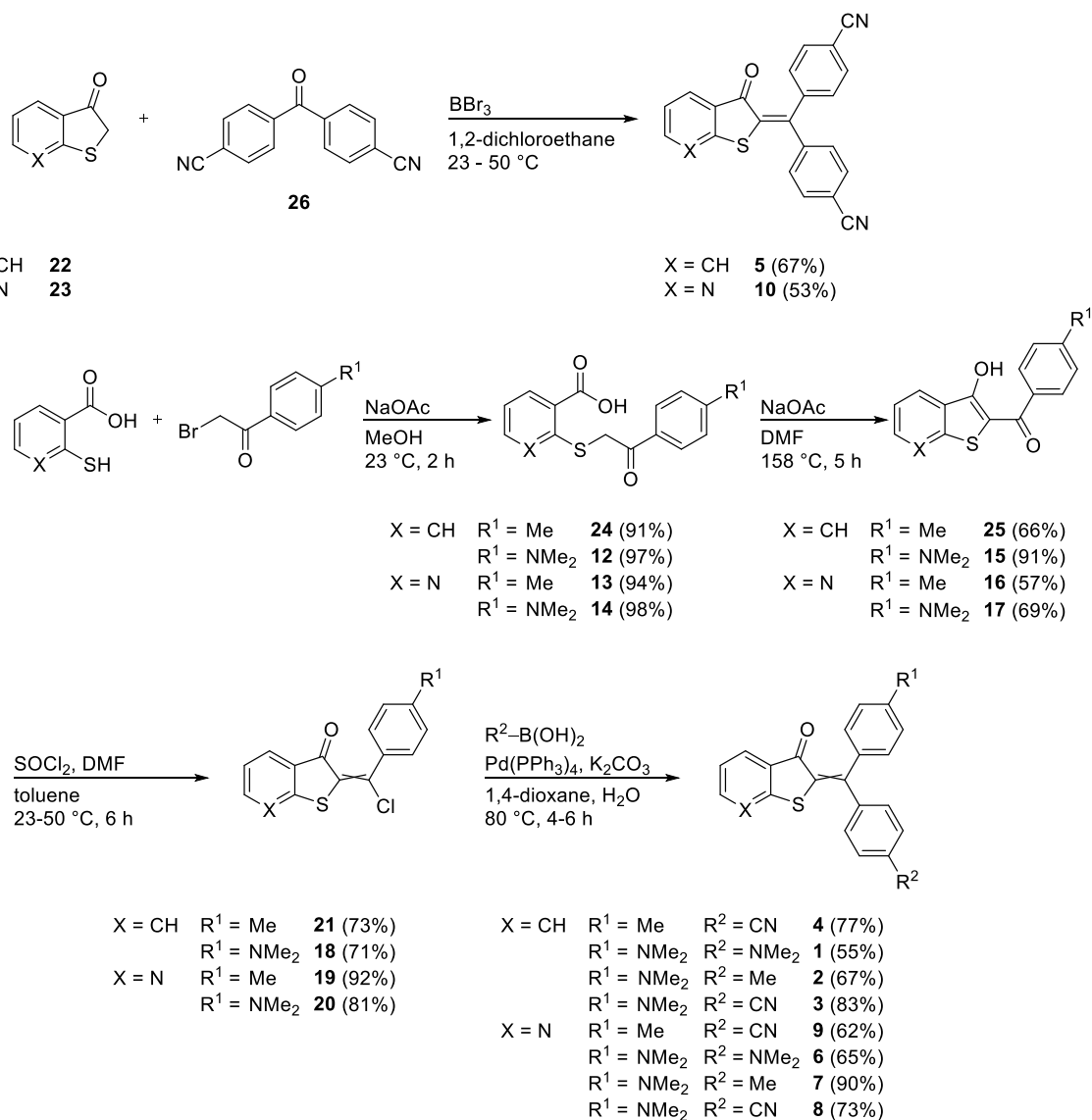
Melting Points (m.p.) were measured on a Büchi B-540 melting point apparatus in open capillaries.

Irradiation experiments. LEDs for irradiation were purchased from Thorlabs GmbH and Roithner Lasertechnik GmbH (405 nm, 430 nm, 450 nm, 470 nm, 490 nm, 505 nm, 515 nm, 530 nm, 554 nm, 565 nm, 590 nm, 617 nm, 625 nm, 650 nm).

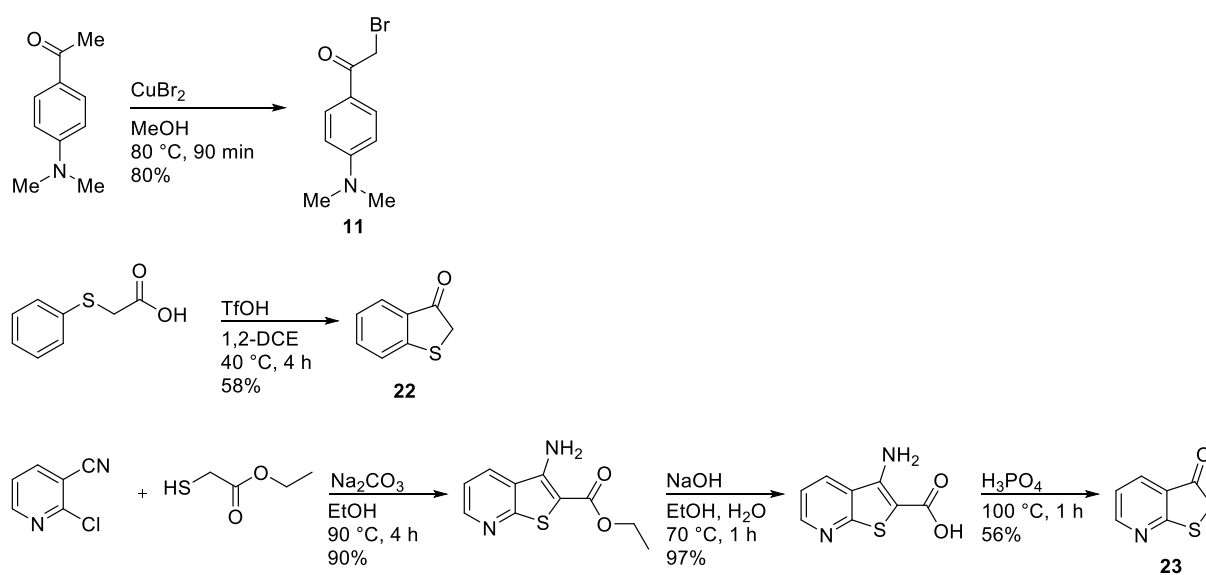
X-ray diffraction of a single crystal was performed on a *SuperNova Atlas* diffractometer using Cu-K α -radiation.

Synthesis Overview

Synthesis of diaryl-HTIs **1-4** and **6-9** followed a published protocol.^[2] Diaryl-HTIs **5** and **10** were obtained from condensation of benzothiophenones **22** and **23** with ketone **26**. Precursors **11**, **22**, and **23** were synthesized according to established synthetic protocols.^[3-5]



Scheme S1: Synthetic pathway towards substituted diaryl-HTIs **1-10**.

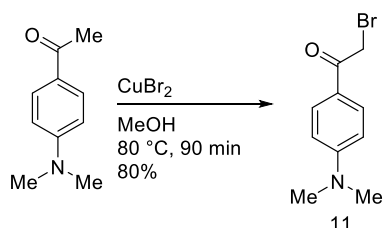


Scheme 2: Synthesis of precursors **11**, **22**, and **23**.

Synthetic Protocols

Synthesis of Thioethers 12-14

Alpha-brominated ketone **11** was synthesized according to a previously published protocol.^[3]

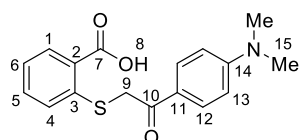


Scheme S3: Synthesis of alpha-brominated ketone **11**.

General procedure for the synthesis of thioethers 12-14

Thioethers **12-14** were synthesized according to a published procedure:^[2] Thiosalicylic acid or 2-mercaptonicotinic acid were suspended in methanol before sodium acetate and the alpha-bromination products of the corresponding ketones were added. The suspension was stirred at $20\text{ }^\circ\text{C}$ for 45 min and poured into ice water. The precipitate was filtered off and dried *in vacuo*.

2-((2-(4-(Dimethylamino)phenyl)-2-oxoethyl)thio)benzoic acid (**12**)



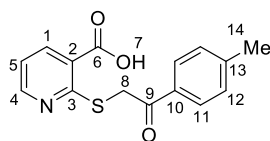
2-((2-(4-(Dimethylamino)phenyl)-2-oxoethyl)thio)benzoic acid (**12**) was prepared from 2-bromo-1-(4-(dimethylamino)phenyl)ethan-1-one (2.90 g, 12.0 mmol), thiosalicylic acid (1.85 g, 12.0 mmol), and sodium acetate (1.97 g, 24.0 mmol) in methanol (50 mL) according to the general procedure. The title compound was obtained as colorless solid (3.66 g, 97%).

m.p.: $170\text{--}171\text{ }^\circ\text{C}$

$^1\text{H-NMR}$ (400 MHz, $(\text{CD}_3)_2\text{SO}$): $\delta = 13.05$ (s, 1H, H-C(8)), $7.92\text{--}7.87$ (m, 3H, H-C(1 and 12)), $7.51\text{--}7.45$ (m, 2H, H-C(4 and 5)), 7.20 (ddd, $J = 7.8, 5.8, 2.6$ Hz, 1H, H-C(6)), $6.75\text{--}6.70$ (m, 2H, H-C(13)), 4.46 (s, 2H, H-C(9)), 3.03 (s, 6H, H-C(15))

^{13}C -NMR (101 MHz, $(\text{CD}_3)_2\text{SO}$): δ = 191.9 (C(10)), 167.5 (C(7)), 153.5 (C(14)), 140.8 (C(3)), 132.3 (C(5)), 130.9 (C(1)), 130.7 (C(12)), 127.8 (C(2)), 126.0 (C(4)), 124.0 (C(6)), 122.8 (C(11)), 110.7 (C(13)), 38.2 (C(9)), (C(15)) is superimposed by the solvent signal at 39.5 ppm
IR: $\tilde{\nu}$ = 3435 (m), 2893 (w), 1676 (w), 1648 (w), 1583 (s), 1538 (m), 1382 (m), 1323 (w), 1249 (m), 1166 (m), 1042 (w), 998 (w), 977 (w), 819 (w), 771 (S), 741 (m)
HRMS (APPI, CH_2Cl_2 , positive mode) calcd. for $\text{C}_{17}\text{H}_{18}\text{NO}_3\text{S}$ $[\text{M}+\text{H}]^+$ 316.1002, found 316.1005

2-((2-Oxo-2-(*p*-tolyl)ethyl)thio)nicotinic acid (**13**)



2-((2-Oxo-2-(*p*-tolyl)ethyl)thio)nicotinic acid (**13**) was prepared by reacting 2-bromo-1-(*p*-tolyl)ethan-1-one (6.87 g, 32.2 mmol), 2-mercaptonicotinic acid (5.00 g, 32.2 mmol), and sodium acetate (5.29 g, 64.4 mmol) in methanol (100 mL) according to the general procedure. The title compound was obtained as colorless solid (8.67 g, 94%).

m.p.: 216-217 °C

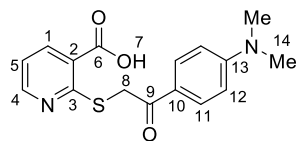
^1H -NMR (400 MHz, $(\text{CD}_3)_2\text{SO}$): δ = 13.49 (s, 1H, H-C(7)), 8.39 (dd, J = 4.7, 1.8 Hz, 1H, H-C(4)), 8.22 (dd, J = 7.7, 1.8 Hz, 1H, H-C(1)), 7.96 – 7.93 (m, 2H, H-C(11)), 7.37 – 7.34 (m, 2H, H-C(12)), 7.19 (dd, J = 7.8, 4.8 Hz, 1H, H-C(5)), 4.64 (s, 2H, H-C(8)), 2.40 (s, 3H, H-C(14))

^{13}C -NMR (101 MHz, $(\text{CD}_3)_2\text{SO}$): δ = 194.1 (C(9)), 166.4 (C(6)), 159.7 (C(3)), 151.6 (C(4)), 143.5 (C(13)), 139.1 (C(1)), 134.1 (C(10)), 129.3 (C(12)), 128.3 (C(11)), 123.3 (C(2)), 119.1 (C(5)), 37.0 (C(8)), 21.2 (C(14))

IR: $\tilde{\nu}$ = 3174 (m), 2909 (w), 1705 (w), 1665 (m), 1601 (w), 1572 (w), 1554 (w), 1400 (m), 1352 (m), 1200 (m), 1133 (m), 1070 (m), 800 (m), 763 (m), 695 (m)

HRMS (APPI, CH_2Cl_2 , positive mode) calcd. for $\text{C}_{15}\text{H}_{14}\text{NO}_3\text{S}$ $[\text{M}+\text{H}]^+$ 288.0689, found 288.0693

2-((2-(4-(Dimethylamino)phenyl)-2-oxoethyl)thio)nicotinic acid (14)



2-((2-(4-(Dimethylamino)phenyl)-2-oxoethyl)thio)nicotinic acid (**14**) was prepared from 2-bromo-1-(4-(dimethylamino)phenyl)ethan-1-one (3.46 g, 14.3 mmol), 2-mercaptonicotinic acid (2.22 g, 14.3 mmol), and sodium acetate (2.34 g, 28.6 mmol) in methanol (50 mL) according to the general procedure. The title compound was obtained as colorless solid (4.44 g, 98%).

m.p.: 215-216 °C

¹H-NMR (400 MHz, (CD₃)₂SO): δ = 13.46 (s, 1H, H-C(7)), 8.47 (dd, J = 4.8, 1.8 Hz, 1H, H-C(4)), 8.21 (dd, J = 7.7, 1.9 Hz, 1H, H-C(1)), 7.90 – 7.86 (m, 2H, H-C(11)), 7.20 (dd, J = 7.8, 4.8 Hz, 1H, H-C(5)), 6.76 – 6.72 (m, 2H, H-C(12)), 4.58 (s, 2H, H-C(8)), 3.03 (s, 6H, H-C(14))

¹³C-NMR (101 MHz, (CD₃)₂SO): δ = 191.8 (C(9)), 166.4 (C(6)), 160.1 (C(3)), 153.4 (C(13)), 151.7 (C(4)), 139.0 (C(1)), 130.3 (C(11)), 123.7 (C(10)), 123.3 (C(2)), 119.0 (C(5)), 110.7 (C(12)), 36.4 (C(8)), (C(14)) is superimposed by the solvent signal at 39.5 ppm

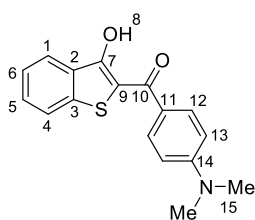
IR: $\tilde{\nu}$ = 3464 (m), 2910 (w), 1700 (m), 1556 (s), 1538 (s), 1438 (m), 1326 (m), 1248 (w), 1168 (s), 1071 (m), 1004 (m), 820 (m), 765 (s)

HRMS (APPI, methanol, positive mode) calcd. for C₁₆H₁₇N₂O₃S [M+H]⁺ 317.0954, found 317.0958

General procedure for the synthesis of (3-hydroxybenzo[*b*]thiophen-2-yl)methanones 15-17

Compounds **15-17** were synthesized according to a published protocol:^[2] Thioethers **12-14** were dissolved in DMF and sodium acetate was added. The mixture was heated to 158 °C for 4 h. After cooling to 23 °C the solvent was removed under reduced pressure and the crude product was purified by column chromatography or MPLC.

(4-(Dimethylamino)phenyl)(3-hydroxybenzo[*b*]thiophen-2-yl)methanone (**15**)



(4-(Dimethylamino)phenyl)(3-hydroxybenzo[*b*]thiophen-2-yl)methanone (**15**) was prepared from 2-((2-(4-(dimethylamino)phenyl)-2-oxoethyl)thio)benzoic acid (**12**) (2.00 g, 6.34 mmol), and sodium acetate (1.56 g, 19.0 mmol) in DMF (5 mL) according to the general procedure. The crude product was purified by MPLC (SiO₂, hexanes to hexanes/ethyl acetate 4:1) to afford **15** as orange solid (1.71 g, 91%).

m.p.: 151-152 °C

*R*_f = 0.81 (SiO₂, ethyl acetate)

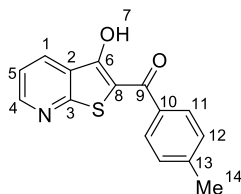
¹H-NMR (400 MHz, CDCl₃): δ = 14.17 (s, 1H, H-C(8)), 8.11 (d, *J* = 8.6 Hz, 2H, H-C(12)), 8.04 (d, *J* = 7.9 Hz, 1H, H-C(1)), 7.74 (d, *J* = 8.1 Hz, 1H, H-C(4)), 7.52 (t, *J* = 7.4 Hz, 1H, H-C(5)), 7.41 (t, *J* = 7.5 Hz, 1H, H-C(6)), 6.76 (d, *J* = 8.6 Hz, 2H, H-C(13)), 3.10 (s, 6H, H-C(15))

¹³C-NMR (101 MHz, CDCl₃): δ = 189.3 (C(10)), 165.2 (C(7)), 153.4 (C(14)), 140.3 (C(3)), 131.2 (C(12)), 130.7 (C(2)), 129.6 (C(5)), 125.2 (C(11)), 124.6 (C(6)), 123.8 (C(1)), 122.9 (C(4)), 111.2 (C(13)), 109.1 (C(9)), 40.3 (C(15))

IR: $\tilde{\nu}$ = 2905 (w), 1595 (w), 1560 (m), 1508 (s), 1376 (m), 1234 (m), 1196 (w), 1168 (w), 1092 (w), 886 (m), 821 (m), 750 (s), 722 (s), 701 (m)

HRMS (APPI, CH₂Cl₂, positive mode) calcd. for C₁₇H₁₅NO₂S [M]⁺ 297.0818, found 297.0815

(3-Hydroxythieno[2,3-b]pyridin-2-yl)(*p*-tolyl)methanone (**16**)



(3-Hydroxythieno[2,3-b]pyridin-2-yl)(*p*-tolyl)methanone (**16**) was prepared from 2-((2-oxo-2-(*p*-tolyl)ethyl)thio)nicotinic acid (**13**) (2.00 g, 6.96 mmol), and sodium acetate (1.71 g, 20.9 mmol) in DMF (5 mL) according to the general procedure. The crude product was purified by MPLC (SiO₂, hexanes to hexanes/ethyl acetate 4:1) to afford **16** as yellow solid (1.07 g, 57%).

m.p.: 152-153 °C

*R*_f = 0.60 (SiO₂, hexanes/ethyl acetate 2:1)

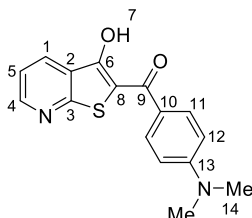
¹H-NMR (400 MHz, CDCl₃): δ = 13.54 (s, 1H, H-C(7)), 8.76 (dd, *J* = 4.6, 1.7 Hz, 1H, H-C(4)), 8.33 (dd, *J* = 8.1, 1.7 Hz, 1H, H-C(1)), 7.98 – 7.95 (m, 2H, H-C(11)), 7.40 (dd, *J* = 8.1, 4.6 Hz, 1H, H-C(5)), 7.38 – 7.35 (m, 2H, H-C(12)), 2.47 (s, 3H, H-C(14))

¹³C-NMR (101 MHz, CDCl₃): δ = 192.2 (C(9)), 162.8 (C(6)), 161.1 (C(3)), 152.2 (C(4)), 144.1 (C(13)), 135.3 (C(10)), 132.2 (C(1)), 129.7 (C(12)), 128.8 (C(11)), 124.8 (C(2)), 120.1 (C(5)), 109.5 (C(8)), 21.9 (C(14))

IR: $\tilde{\nu}$ = 3038 (w), 1585 (m), 1558 (m), 1506 (m), 1458 (w), 1327 (m), 1245 (w), 1174 (m), 1073 (w), 968 (w), 828 (m), 786 (m), 750 (s)

HRMS (APPI, CH₂Cl₂/toluene, positive mode) calcd. for C₁₅H₁₂NO₂S [M+H]⁺ 270.0583, found 270.0586

(4-(Dimethylamino)phenyl)(3-hydroxythieno[2,3-b]pyridin-2-yl)methanone (**17**)



(4-(Dimethylamino)phenyl)(3-hydroxythieno[2,3-b]pyridin-2-yl)methanone (**17**) was prepared from 2-((2-(4-(dimethylamino)phenyl)-2-oxoethyl)thio)nicotinic acid (**14**) (2.00 g, 6.32 mmol), and sodium acetate (1.56 g, 19.0 mmol) in DMF (8 mL) according to the

general procedure. The crude product was purified by column chromatography (SiO₂, ethyl acetate/hexanes 7:1) to afford **17** as orange solid (1.30 g, 69%).

m.p.: 190-191 °C

*R*_f = 0.79 (SiO₂, ethyl acetate)

¹H-NMR (400 MHz, (CD₃)₂CO): δ = 8.79 (dd, *J* = 4.6, 1.7 Hz, 1H, H-C(4)), 8.36 (dd, *J* = 8.1, 1.7 Hz, 1H, H-C(1)), 8.11 – 8.07 (m, 2H, H-C(11)), 7.55 (dd, *J* = 8.1, 4.6 Hz, 1H, H-C(5)), 6.91 – 6.87 (m, 2H, H-C(12)), 3.15 (s, 6H, H-C(14))

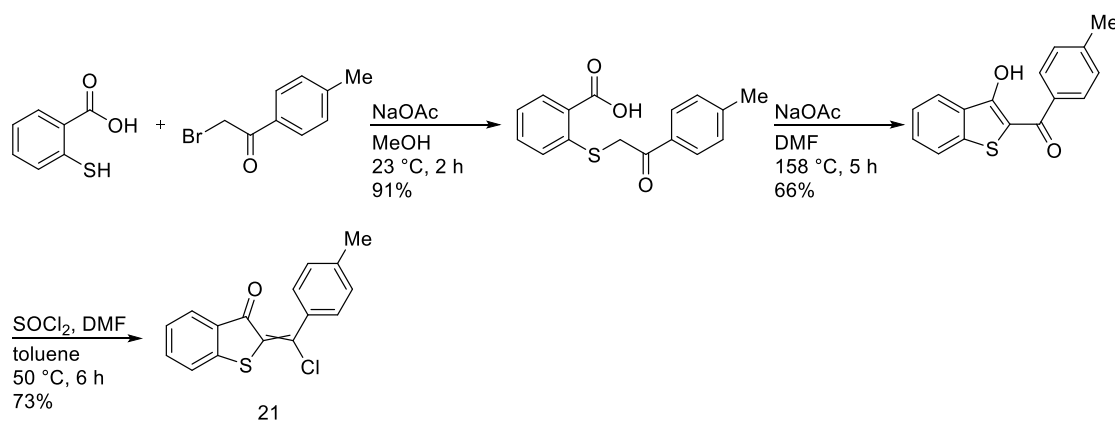
¹³C-NMR (101 MHz, (CD₃)₂CO): δ = 189.9 (C(9)), 163.5 (C(6)), 161.4 (C(3)), 155.0 (C(13)), 153.1 (C(4)), 132.2 (C(1)), 131.9 (C(11)), 125.3 (C(2)), 124.8 (C(10)), 121.2 (C(5)), 112.0 (C(12)), 108.9 (C(8)), 40.1 (C(14))

IR: $\tilde{\nu}$ = 3060 (w), 2913 (w), 1607 (w), 1557 (m), 1504 (s), 1373 (m), 1330 (m), 1260 (w), 1161 (w), 1074 (m), 894 (m), 806 (s), 755 (s)

HRMS (APPI, CH₂Cl₂, positive mode) calcd. for C₁₆H₁₅N₂O₂S [M+H]⁺ 299.0849, found 299.0853

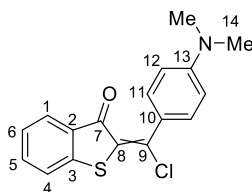
Synthesis of vinyl chlorides 18-20

Chloride **21** was synthesized according to a published protocol.^[2]



Scheme S4: Synthesis of vinyl chloride **21**.

2-(Chloro(4-(dimethylamino)phenyl)methylene)benzo[b]thiophen-3(2H)-one (18)



To a solution of (4-(dimethylamino)phenyl)(3-hydroxybenzo[b]thiophen-2-yl)methanone (**15**) (400 mg, 1.35 mmol) in toluene (10 mL) was added thionyl chloride (800 mg, 488 μ L, 6.73 mmol) and *N,N*-dimethylformamide (98.3 mg, 105 μ L, 1.35 mmol) and the mixture was stirred at 23 °C for 24 h. The reaction mixture was neutralized with sat. aq. NaHCO₃, extracted with CH₂Cl₂ and dried (MgSO₄). The solvent was removed *in vacuo* and the crude product was purified by column chromatography (Al₂O₃, CH₂Cl₂) to afford **18** as red solid (303 mg, 71%).
m.p.: 143-144 °C

R_f = 0.56 (SiO₂, hexanes/ethyl acetate 2:1)

Z-isomer:

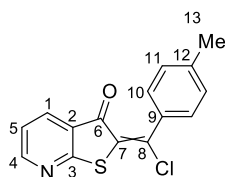
¹H-NMR (500 MHz, CD₂Cl₂): δ = 7.73 (ddd, J = 7.7, 1.4, 0.7 Hz, 1H, H-C(1)), 7.60 – 7.57 (m, 2H, H-C(11)), 7.56 – 7.54 (m, 1H, H-C(5)), 7.47 (dt, J = 7.9, 0.9 Hz, 1H, H-C(4)), 7.26 (ddd, J = 8.0, 7.2, 1.0 Hz 2H, H-C(6)), 6.71 – 6.65 (m, 2H, H-C(12)), 3.07 (s, 6H, H-C(14))

¹³C-NMR (101 MHz, CD₂Cl₂): δ = 183.3 (C(7)), 152.7 (C(13)), 145.6 (C(9)), 144.3 (C(3)), 135.1 (C(5)), 134.1 (C(2)), 132.0 (C(11)), 127.0 (C(1)), 125.6 (C(6)), 123.7 (C(4)), 122.4 (C(10)), 110.6 (C(12)), 40.3 (C(14)), (C(8)) could not be clearly assigned

IR: $\tilde{\nu}$ = 2894 (w), 1663 (m), 1598 (m), 1548 (w), 1509 (s), 1442 (m), 1368 (m), 1280 (w), 1235 (m), 1184 (m), 1058(m), 947 (w), 866 (w), 784 (m), 775 (m), 734 (s)

HRMS (APPI, CH₂Cl₂, positive mode) calcd. for C₁₇H₁₅ClNOS [M+H]⁺ 316.0557, found 316.0564.

2-(Chloro(*p*-tolyl)methylene)thieno[2,3-*b*]pyridin-3(2H)-one (19)



To a solution of (3-hydroxythieno[2,3-*b*]pyridin-2-yl)(*p*-tolyl)methanone (**16**) (300 mg, 1.11 mmol) in toluene (10 mL) was added thionyl chloride (663 mg, 404 μ L, 5.57 mmol), and

N,N-dimethylformamide (81.4 mg, 86.6 μ L, 1.11 mmol) and the mixture was heated to 50 $^{\circ}$ C for 4 h. After cooling to 23 $^{\circ}$ C, the mixture was neutralized with sat. aq. NaHCO_3 , extracted with CH_2Cl_2 and dried (MgSO_4). The solvent was removed *in vacuo* and the crude product was purified by column chromatography (Al_2O_3 , CH_2Cl_2) to afford **19** as yellow solid (294 mg, 92%).

m.p.: 187-188 $^{\circ}$ C

R_f = 0.29 (SiO_2 , hexanes/ethyl acetate 5:1)

Z-Isomer:

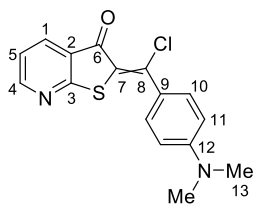
$^1\text{H-NMR}$ (400 MHz, CD_2Cl_2): δ = 8.67 (dd, J = 4.8, 1.8 Hz, 1H, H-C(4)), 7.93 (dd, J = 7.7, 1.8 Hz, 1H, H-C(1)), 7.49 – 7.45 (m, 2H, H-C(10)), 7.29 – 7.25 (m, 2H, H-C(11)), 7.23 (dd, J = 7.7, 4.8 Hz, 1H, H-C(5)), 2.43 (s, 3H, H-C(13))

$^{13}\text{C-NMR}$ (101 MHz, CD_2Cl_2): δ = 182.3 (C(6)), 166.4 (C(3)), 156.3 (C(4)), 144.8 (C(8)), 141.9 (C(12)), 134.7 (C(1)), 133.4 (C(9)), 132.3 (C(7)), 129.5 (C(10)), 129.2 (C(11)), 127.7 (C(2)), 121.2 (C(5)), 21.7 (C(13))

IR: $\tilde{\nu}$ = 3025 (w), 2916 (w), 1671 (s), 1565 (m), 1538 (s), 1502 (w), 1461 (w), 1395 (s), 1288 (m), 1231 (m), 1185 (w), 1092 (w), 1060 (m), 870 (w), 838 (w), 771 (s), 757 (s)

HRMS (APPI, CH_2Cl_2 /acetonitrile, positive mode) calcd. for $\text{C}_{15}\text{H}_{11}\text{ClNOS}$ $[\text{M}+\text{H}]^+$ 288.0244, found 288.0248

2-(Chloro(4-(dimethylamino)phenyl)methylene)thieno[2,3-b]pyridin-3(2H)-one (**20**)



To a solution of (4-(dimethylamino)phenyl)(3-hydroxythieno[2,3-b]pyridin-2-yl)methanone (**17**) (150 mg, 0.503 mmol) in toluene (4 mL) was added thionyl chloride (299 mg, 182 μ L, 2.51 mmol) and *N,N*-dimethylformamide (36.8 mg, 39.1 μ L, 0.503 mmol) and the mixture was stirred at 23 $^{\circ}$ C for 24 h. The reaction mixture was neutralized with sat. aq. NaHCO_3 , extracted with CH_2Cl_2 and dried (MgSO_4). The solvent was removed *in vacuo* and the crude product was purified by column chromatography (Al_2O_3 , CH_2Cl_2) to afford **20** as red solid (129 mg, 81%).

m.p.: 171-172 $^{\circ}$ C

R_f = 0.50 (SiO_2 , hexanes/ethyl acetate 1:1)

E-Isomer:

¹H-NMR (601 MHz, CDCl₃): δ = 8.66 (dd, J = 4.8, 1.8 Hz, 1H, H-C(4)), 7.97 (dd, J = 7.7, 1.8 Hz, 1H, H-C(1)), 7.65 – 7.63 (m, 2H, H-C(10)), 7.19 (dd, J = 7.7, 4.8 Hz, 1H, H-C(5)), 6.74 – 6.70 (m, 2H, H-C(11)), 3.08 (s, 6H, H-C(13))

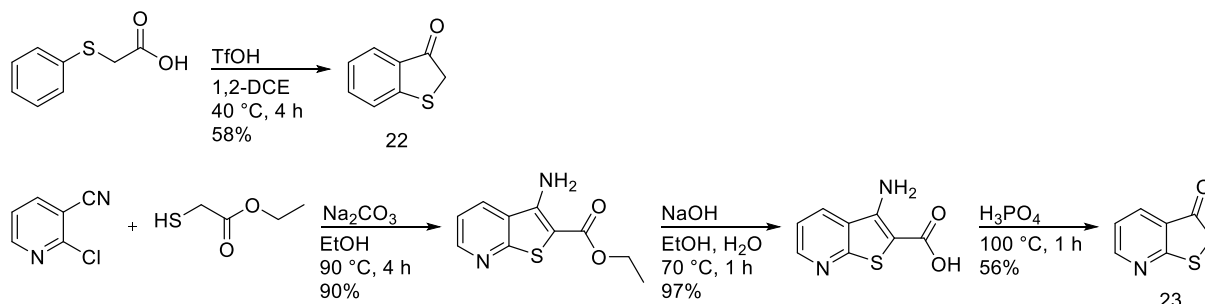
¹³C-NMR (151 MHz, CDCl₃): δ = 181.6 (C(6)), 166.3 (C(3)), 155.4 (C(4)), 152.2 (C(12)), 147.3 (C(8)), 134.4 (C(1)), 131.9 (C(10)), 128.2 (C(2)), 122.9 (C(9)), 120.5 (C(5)), 111.0 (C(11)), 40.5 (C(13)), (C(7)) could not be clearly assigned

IR: $\tilde{\nu}$ = 2908 (w), 2818 (w), 1656 (s), 1606 (s), 1578 (m), 1566 (m), 1552 (m), 1504 (s), 1408 (m), 1370 (m), 1286 (m), 1192 (m), 1095 (w), 1058 (s), 945 (w), 869 (w), 809 (m), 785 (m), 758 (w)

HRMS (APPI, CH₂Cl₂/acetonitrile, positive mode) calcd. for C₁₆H₁₄ClN₂OS [M+H]⁺ 317.0510, found 317.0513

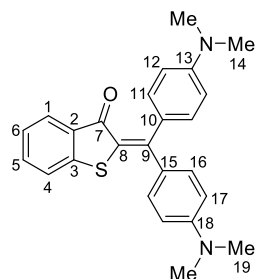
Synthesis of Diaryl-HTIs 1-10

Benzothiophenones **22** and **23** were synthesized according to published protocols.^[4,5]



Scheme S5: Synthesis of benzothiophenones **22** and **23**.

2-(Bis(4-(dimethylamino)phenyl)methylene)benzo[b]thiophen-3(2H)-one (**1**)



2-(Bis(4-(dimethylamino)phenyl)methylene)benzo[b]thiophen-3(2H)-one (**1**) was prepared from chloride (**18**) (200 mg, 0.633 mmol) and (4-(dimethylamino)phenyl)boronic acid (157 mg, 0.950 mmol). The crude product was purified by column chromatography (Al_2O_3 , hexanes/ethyl acetate 3:1) and recrystallized from ethyl acetate to afford **1** (138 mg, 55%) as red crystals.

m.p.: 244-245 °C

R_f = 0.32 (SiO_2 , hexanes/ethyl acetate 3:1)

E-Isomer:

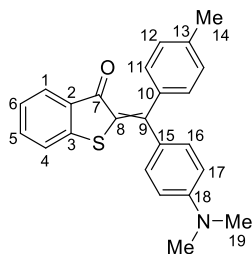
$^1\text{H-NMR}$ (601 MHz, CD_2Cl_2): δ = 7.76 (ddd, J = 7.8, 1.4, 0.7 Hz, 1H, H-C(1)), 7.49 (ddd, J = 7.9, 7.1, 1.3 Hz, 1H, H-C(5)), 7.41 (dt, J = 7.9, 0.9 Hz, 1H, H-C(4)), 7.31 – 7.29 (m, 2H, H-C(16)), 7.22 (ddd, J = 7.7, 7.1, 1.0 Hz, 1H, H-C(6)), 7.19 – 7.16 (m, 2H, H-C(11)), 6.70 – 6.68 (m, 2H, H-C(17)), 6.67 – 6.64 (m, 2H, H-C(12)), 3.03 (s, 6H, H-C(14 or 19)), 3.03 (s, 6H, H-C(14 or 19))

^{13}C -NMR (151 MHz, CD_2Cl_2): δ = 185.8 (C(7)), 154.8 (C(9)), 151.8 (C(13)), 151.7 (C(18)), 146.0 (C(3)), 134.5 (C(2)), 133.8 (C(5)), 133.20 (C(11)), 133.17 (C(16)), 130.2 (C(15)), 127.5 (C(10)), 126.7 (C(8)), 125.8 (C(1)), 124.7 (C(6)), 123.5 (C(4)), 111.3 (C(17)), 111.0 (C(12)), 40.4 (C(14 or 19)), 40.3 (C(14 or 19))

IR: $\tilde{\nu}$ = 2794 (w), 1649 (w), 1597 (s), 1552 (w), 1521 (w), 1476 (s), 1442 (m), 1359 (s), 1311 (m), 1214 (m), 1167 (m), 1123 (w), 1048 (s), 958 (m), 864 (w), 820 (s), 741 (s), 688 (m)

HRMS (APPI, $\text{CH}_2\text{Cl}_2/\text{acetonitrile}$, positive mode) calcd. for $\text{C}_{25}\text{H}_{25}\text{N}_2\text{OS}$ $[\text{M}+\text{H}]^+$ 401.1682, found 401.1689

2-((4-(Dimethylamino)phenyl)(*p*-tolyl)methylene)benzo[*b*]thiophen-3(2H)-one (**2**)



2-((4-(Dimethylamino)phenyl)(*p*-tolyl)methylene)benzo[*b*]thiophen-3(2H)-one (**2**) was prepared from chloride (**18**) (200 mg, 0.633 mmol) and *p*-tolylboronic acid (129 mg, 0.950 mmol). The crude product was purified by MPLC (Al_2O_3 , hexanes to hexanes/ethyl acetate 9:1) and recrystallized from methanol to afford **2** (157 mg, 67%) as red crystals.

m.p.: 171-172 °C

R_f = 0.70 (SiO_2 , hexanes/ethyl acetate 2:1)

Z-Isomer:

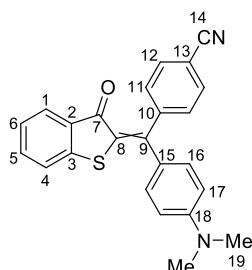
^1H -NMR (601 MHz, CD_2Cl_2): δ = 7.72 (ddd, J = 7.7, 1.4, 0.7 Hz, 1H, H-C(1)), 7.53 – 7.48 (m, 1H, H-C(5)), 7.44 (dt, J = 7.9, 0.9 Hz, 1H, H-C(4)), 7.32 – 7.30 (m, 2H, H-C(16)), 7.24 – 7.18 (m, 3H, H-C(6 and 12)), 7.13 – 7.11 (m, 2H, H-C(11)), 6.69 – 6.66 (m, 2H, H-C(17)), 3.02 (s, 6H, H-C(19)), 2.42 (s, 3H, H-C(14))

^{13}C -NMR (151 MHz, CD_2Cl_2): δ = 186.5 (C(7)), 152.6 (C(9)), 151.6 (C(18)), 146.1 (C(3)), 139.0 (C(13)), 138.1 (C(10)), 134.34 (C(5)), 133.6 (C(2)), 132.6 (C(16)), 130.4 (C(11)), 129.3 (C(15)), 129.1 (C(12)), 126.80 (C(1)), 125.04 (C(6)), 123.6 (C(4)), 111.4 (C(17)), 40.28 (C(19)), 21.6 (C(14)), (C(8)) could not be clearly assigned

IR: $\tilde{\nu}$ = 2888 (w), 2811 (w), 1654 (m), 1600 (s), 1501 (s), 1441 (m), 1364 (m), 1310 (w), 1280 (m), 1221 (w), 1198 (m), 1154 (w), 1050 (s), 959 (w), 815 (s), 746 (s), 649 (w)

HRMS (APPI, CH₂Cl₂, positive mode) calcd. for C₂₄H₂₁NOS [M]⁺ 371.1338, found 371.1338

4-((4-(Dimethylamino)phenyl)(3-oxobenzo[b]thiophen-2(3H)-ylidene) methyl) benzonitrile (3)



4-((4-(Dimethylamino)phenyl)(3-oxobenzo[b]thiophen-2(3H)-ylidene) methyl) benzonitrile (**3**) was prepared from chloride (**18**) (200 mg, 0.633 mmol) and (4-cyanophenyl)boronic acid (140 mg, 0.950 mmol). The crude product was purified by column chromatography (Al₂O₃, hexanes/ethyl acetate 2:1) and recrystallized from ethanol to afford **3** (200 mg, 83%) as red crystals.

m.p.: 178-179 °C

R_f = 0.60 (SiO₂, hexanes/ethyl acetate 2:1)

Z-Isomer:

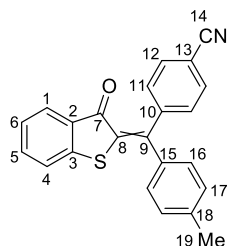
¹H-NMR (601 MHz, CD₂Cl₂): δ = 7.71 – 7.68 (m, 3H, H-C(1 and 12)), 7.54 (ddd, J = 7.9, 7.2, 1.3 Hz, 1H, H-C(5)), 7.47 (dt, J = 7.9, 0.9 Hz, 1H, H-C(4)), 7.35 – 7.33 (m, 2H, H-C(11)), 7.31 – 7.29 (m, 2H, H-C(16)), 7.24 (ddd, J = 7.7, 7.2, 1.0 Hz, 1H, H-C(6)), 6.69 – 6.67 (m, 2H, H-C(17)), 3.03 (s, 6H, H-C(19))

¹³C-NMR (151 MHz, CD₂Cl₂): δ = 186.8 (C(7)), 151.7 (C(18)), 148.9 (C(9)), 146.4 (C(10)), 146.0 (C(3)), 134.8 (C(5)), 132.9 (C(2)), 132.4 (C(16)), 132.3 (C(12)), 130.8 (C(11)), 127.4 (C(15)), 126.9 (C(1)), 125.4 (C(6)), 123.8 (C(4)), 119.3 (C(14)), 111.9 (C(13)), 111.6 (C(17)), 40.2 (C(19)), (C(8)) could not be clearly assigned

IR: ν̄ = 2818 (w), 2224 (w), 1664 (m), 1601 (m), 1548 (m), 1521 (s), 1494 (m), 1440 (m), 1371 (m), 1280 (m), 1221 (w), 1200 (m), 1166 (w), 1119 (w), 1059 (s), 1019 (w), 949 (m), 819 (s), 745 (s), 647 (m)

HRMS (APPI, CH₂Cl₂, positive mode) calcd. for C₂₄H₁₈N₂OS [M+H]⁺ 383.1213, found 383.1224

4-((3-Oxobenzo[b]thiophen-2(3H)-ylidene)(*p*-tolyl)methyl)benzonitrile (**4**)



4-((3-Oxobenzo[b]thiophen-2(3H)-ylidene)(*p*-tolyl)methyl)benzonitrile (**4**) was prepared from chloride (**21**) (184 mg, 0.642 mmol) and (4-cyanophenyl)boronic acid (141 mg, 0.962 mmol). The crude product was purified by column chromatography (Al_2O_3 , hexanes/ethyl acetate 3:1) and recrystallized from *n*-heptane to afford **4** (174 mg, 77%) as orange crystals.

m.p.: 155-156 °C

R_f = 0.55 (SiO_2 , hexanes/ethyl acetate 3:1)

Z-isomer:

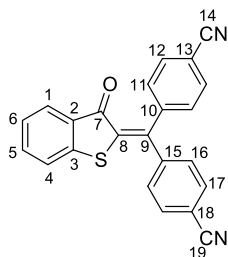
$^1\text{H-NMR}$ (601 MHz, $(\text{CD}_3)_2\text{CO}$): δ = 7.81 – 7.79 (m, 2H, H-C(12)), 7.70 (ddd, J = 7.8, 1.3, 0.7 Hz, 1H, H-C(1)), 7.67 (ddd, J = 8.4, 7.2, 1.3 Hz, 1H, H-C(5)), 7.60 (dt, J = 7.9, 0.9 Hz, 1H, H-C(4)), 7.52 – 7.50 (m, 2H, H-C(11)), 7.37 – 7.33 (m, 3H, H-C(6 and 16)), 7.32 – 7.30 (m, 2H, H-C(17)), 2.38 (s, 3H, H-C(19))

$^{13}\text{C-NMR}$ (151 MHz, $(\text{CD}_3)_2\text{CO}$): δ = 186.9 (C(7)), 148.4 (C(9)), 146.2 (C(3)), 146.0 (C(10)), 140.9 (C(18)), 139.1 (C(15)), 136.27 (C(5)), 132.81 (C(12)), 132.78 (C(2)), 131.23 (C(11)), 130.33 (C(16)), 130.27 (C(17)), 127.4 (C(1)), 126.4 (C(6)), 124.7 (C(4)), 119.4 (C(14)), 112.4 (C(13)), 21.3 (C(19)), (C(8)) could not be clearly assigned

IR: $\tilde{\nu}$ = 2227 (m), 1666 (s), 1587 (m), 1529 (m), 1497 (w), 1448 (m), 1403 (w), 1280 (m), 1218 (w), 1047 (s), 1016 (m), 951 (w), 823 (m), 741 (s)

HRMS (APPI, CH_2Cl_2 , positive mode) calcd. for $\text{C}_{23}\text{H}_{16}\text{NOS}$ $[\text{M}+\text{H}]^+$ 354.0947, found 354.0956

4,4'-((3-Oxobenzo[b]thiophen-2(3H)-ylidene)methylene)dibenzonitrile (**5**)



To a solution of 4,4'-carbonyldibenzonitrile (110 mg, 0.476 mmol) in dry 1,2-dichloroethane (3 mL) was added BBr_3 (1.0 M in CH_2Cl_2 , 536 mg, 0.536 mL, 2.14 mmol) under inert atmosphere. The mixture was subsequently transferred to a solution of benzo[b]thiophen-3(2H)-one (**22**) (100 mg, 0.666 mmol) in dry 1,2-dichloroethane (3 mL) and stirred at 23 °C for 24 h under inert atmosphere. After the reaction was quenched by the addition of sat. aq. NH_4Cl , the aqueous phase was extracted with ethyl acetate and dried (MgSO_4). The crude product was purified by MPLC (Al_2O_3 , hexanes to hexanes/ethyl acetate 7:3) and recrystallization from methanol to afford **5** as orange crystals (116 mg, 67%).

m.p.: 208-209 °C

R_f = 0.58 (SiO_2 , hexanes/ethyl acetate 2:1)

$^1\text{H-NMR}$ (601 MHz, CDCl_3): δ = 7.76 (ddd, J = 7.7, 1.4, 0.7 Hz, 1H, H-C(1)), 7.74 – 7.72 (m, 2H, H-C(17)), 7.71 – 7.69 (m, 2H, H-C(12)), 7.59 (ddd, J = 7.9, 7.2, 1.3 Hz, 1H, H-C(5)), 7.53 – 7.51 (m, 2H, H-C(16)), 7.40 (dt, J = 8.0, 0.8 Hz, 1H, H-C(4)), 7.38 – 7.35 (m, 2H, H-C(11)), 7.28 (ddd, J = 7.8, 7.3, 0.9 Hz, 1H, H-C(6))

$^{13}\text{C-NMR}$ (151 MHz, CDCl_3): δ = 186.8 (C(7)), 145.1 (C(15)), 144.9 (C(3)), 144.6 (C(9)), 143.4 (C(10)), 136.0 (C(5)), 134.1 (C(8)), 132.7 (C(17)), 132.5 (C(12)), 131.6 (C(2)), 130.3 (C(16)), 130.2 (C(11)), 127.5 (C(1)), 126.1 (C(6)), 123.7 (C(4)), 118.6 (C(14)), 118.2 (C(19)), 113.4 (C(18)), 112.8 (C(13))

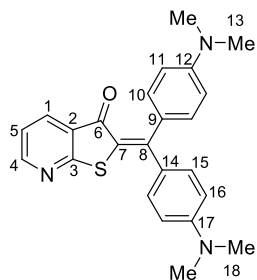
IR: $\tilde{\nu}$ = 2224 (m), 1673 (s), 1586 (m), 1563 (m), 1495 (w), 1450 (m), 1403 (w), 1280 (s), 1217 (w), 1053 (s), 1016 (m), 835 (s), 745 (s), 636 (w), 568 (m), 553 (s)

HRMS (APPI, CH_2Cl_2 , positive mode) calcd. for $\text{C}_{23}\text{H}_{12}\text{N}_2\text{OS}$ $[\text{M}]^+$ 364.0665, found 364.0667

Diaryl-HTIs **1-4** and **6-9** were synthesized *via Suzuki-Miyaura* cross-coupling adopting a published protocol:^[2] Chlorides **18-21** (1.0 equiv.), boronic acid (1.5 equiv.) and K_2CO_3 (2.0 equiv.) were dissolved in 1,4-dioxane and water (10 vol%). The solution was degassed with nitrogen (15 min) before $\text{Pd}(\text{PPh}_3)_4$ (5 mol%) was added. The reaction mixture was heated to 80 °C for 4 to 8 h under inert gas atmosphere. After cooling to 23 °C, sat. aq. Na_2CO_3 was

added. The aqueous phase was extracted with CH₂Cl₂, dried (MgSO₄) and the solvent removed *in vacuo*. The crude product was purified by column chromatography, MPLC and/or recrystallization.

2-(Bis(4-(dimethylamino)phenyl)methylene)thieno[2,3-b]pyridin-3(2H)-one (6)



2-(Bis(4-(dimethylamino)phenyl)methylene)thieno[2,3-b]pyridin-3(2H)-one (**6**) was prepared from chloride (**20**) (200 mg, 0.631 mmol) and (4-(dimethylamino)phenyl)boronic acid (156 mg, 947 μmol). The crude product was purified by column chromatography (Al₂O₃, hexanes/ethyl acetate 2:1) and recrystallized from methanol to afford **6** (166 mg, 65%) as red crystals.

m.p.: 222-223 °C

R_f = 0.56 (SiO₂, hexanes/ethyl acetate 1:1)

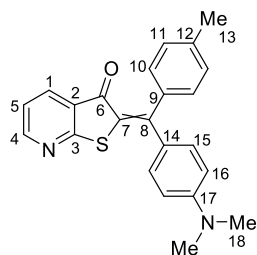
¹H-NMR (601 MHz, CD₂Cl₂): δ = 8.59 (dd, J = 4.8, 1.8 Hz, 1H, H-C(4)), 7.99 (dd, J = 7.7, 1.8 Hz, 1H, H-C(1)), 7.33 – 7.30 (m, 2H, H-C(10)), 7.19 – 7.16 (m, 3H, H-C(5 and 15)), 6.71 – 6.69 (m, 2H, H-C(11)), 6.66 – 6.64 (m, 2H, H-C(16)), 3.04 (s, 6H, H-C(13 or 18)), 3.04 (s, 6H, H-C(13 or 18))

¹³C-NMR (151 MHz, CD₂Cl₂): δ = 184.1 (C(6)), 167.9 (C(3)), 156.4 (C(8)), 154.6 (C(4)), 152.1 (C(17)), 151.9 (C(12)), 134.0 (C(1)), 133.5 (C(10)), 133.4 (C(15)), 129.6 (C(9)), 128.6 (C(2)), 127.4 (C(14)), 124.9 (C(7)), 120.0 (C(5)), 111.3 (C(11)), 111.0 (C(16)), 40.4 (C(13 or 18)), 40.3 (C(13 or 18))

IR: $\tilde{\nu}$ = 2224 (m), 1673 (s), 1586 (m), 1563 (m), 1495 (w), 1450 (m), 1403 (w), 1280 (s), 1217 (w), 1053 (s), 1016 (m), 835 (s), 745 (s), 636 (w), 568 (m), 553 (s)

HRMS (APPI, CH₂Cl₂, positive mode) calcd. for C₂₄H₂₃N₃OS [M]⁺ 401.1556, found 401.1561

2-((4-(Dimethylamino)phenyl)(*p*-tolyl)methylene)thieno[2,3-*b*]pyridin-3(2H)-one (7)



2-((4-(Dimethylamino)phenyl)(*p*-tolyl)methylene)thieno[2,3-*b*]pyridin-3(2H)-one (7) was prepared from chloride (20) (150 mg, 0.473 mmol) and *p*-tolylboronic acid (96.6 mg, 0.710 mmol). The crude product was purified by MPLC (SiO₂, hexanes to hexanes/ethyl acetate 1:1) and recrystallized from methanol to afford 7 (159 mg, 90%) as red crystals.

m.p.: 161-162 °C

R_f = 0.63 (SiO₂, hexanes/ethyl acetate 1:1)

Z-Isomer:

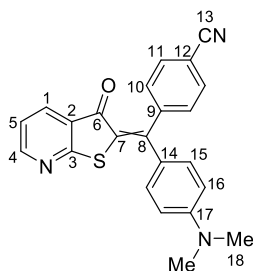
¹H-NMR (601 MHz, CD₂Cl₂): δ = 8.61 (dd, J = 4.7, 1.8 Hz, 1H, H-C(4)), 7.94 (dd, J = 7.7, 1.8 Hz, 1H, H-C(1)), 7.33 – 7.31 (m, 2H, H-C(15)), 7.21 – 7.19 (m, 2H, H-C(11)), 7.18 (dd, J = 7.7, 4.8 Hz, 1H, H-C(5)), 7.14 – 7.12 (m, 2H, H-C(10)), 6.70 – 6.67 (m, 2H, H-C(16)), 3.03 (s, 6H, H-C(18)), 2.42 (s, 3H, H-C(13))

¹³C-NMR (151 MHz, CD₂Cl₂): δ = 185.0 (C(6)), 168.2 (C(3)), 155.1 (C(4)), 154.2 (C(8)), 151.8 (C(17)), 139.3 (C(12)), 138.1 (C(9)), 134.2 (C(1)), 132.8 (C(15)), 130.4 (C(10)), 129.1 (C(11)), 128.7 (C(14)), 127.8 (C(6)), 120.4 (C(5)), 111.4 (C(16)), 40.3 (C(18)), 21.6 (C(13)), (C(7)) could not be clearly assigned

IR: $\tilde{\nu}$ = 2915 (w), 2852 (w), 2818 (w), 1662 (m), 1644 (w), 1603 (m), 1567 (m), 1491 (m), 1411 (m), 1368 (w), 1277 (w), 1204 (w), 1091 (m), 959 (w), 865 (m), 763 (s)

HRMS (APPI, CH₂Cl₂, positive mode) calcd. for C₂₃H₂₀N₂OS [M]⁺ 372.1291, found 372.1291

4-((4-(Dimethylamino)phenyl)(3-oxothieno[2,3-*b*]pyridin-2(3H)-ylidene)methyl)benzonitrile (8)



4-((4-(Dimethylamino)phenyl)(3-oxothieno[2,3-b]pyridin-2(3H)-ylidene)methyl) benzonitrile (**8**) was prepared from chloride (**20**) (300 mg, 0.947 mmol) and (4-cyanophenyl)boronic acid (209 mg, 1.42 mmol). The crude product was purified by column chromatography (Al₂O₃, hexanes/ethyl acetate 1:1) and recrystallized from ethyl acetate to afford **8** (266 mg, 73%) as red crystals.

m.p.: 247-248 °C

*R*_f = 0.55 (SiO₂, hexanes/ethyl acetate 1:1)

Z-Isomer:

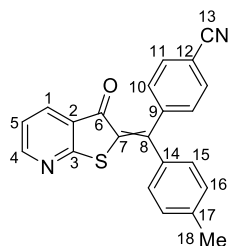
¹H-NMR (601 MHz, (CD₃)₂CO): δ = 8.70 (dd, *J* = 4.8, 1.8 Hz, 1H, H-C(4)), 7.97 (dd, *J* = 7.7, 1.8 Hz, 1H, H-C(1)), 7.83 – 7.80 (m, 2H, H-C(11)), 7.48 – 7.45 (m, 2H, H-C(10)), 7.37 (dd, *J* = 7.7, 4.8 Hz, 1H, H-C(5)), 7.33 – 7.30 (m, 2H, H-C(15)), 6.81 – 6.78 (m, 2H, H-C(16)), 3.07 (s, 6H, H-C(18))

¹³C-NMR (151 MHz, (CD₃)₂CO): δ = 185.1 (C(6)), 168.1 (C(3)), 156.1 (C(4)), 152.5 (C(17)), 150.7 (C(8)), 146.8 (C(9)), 134.6 (C(1)), 132.7 (C(15 and 11)), 131.4 (C(10)), 127.34 (C(14)), 127.28 (C(2)), 121.5 (C(5)), 119.4 (C(13)), 112.3 (C(12)), 112.2 (C(16)), 40.0 (C(18)), (C(7)) could not be clearly assigned

IR: ν̄ = 2906 (w), 2223 (m), 1652 (m), 1600 (m), 1485 (s), 1429 (m), 1394 (m), 1371 (m), 1319 (m), 1274 (m), 1208 (s), 1123 (m), 1057 (s), 957 (s), 852 (m), 813 (m), 757 (s), 580 (s)

HRMS (APPI, CH₂Cl₂, positive mode) calcd. for C₂₃H₁₇N₃OS [M]⁺ 383.1087, found 383.1084

4-((3-Oxothieno[2,3-b]pyridin-2(3H)-ylidene)(*p*-tolyl)methyl)benzonitrile (**9**)



4-((3-Oxothieno[2,3-b]pyridin-2(3H)-ylidene)(*p*-tolyl)methyl)benzonitrile (**9**) was prepared from chloride (**19**) (239 mg, 0.831 mmol) and (4-cyanophenyl)boronic acid (183 mg, 1.25 mmol). The crude product was purified by MPLC (Al₂O₃, hexanes to hexanes/ethyl acetate 4:1) and recrystallized from methanol to afford **9** (182 mg, 62%) as orange crystals.

m.p.: 169-170 °C

*R*_f = 0.62 (SiO₂, hexanes/ethyl acetate 2:1)

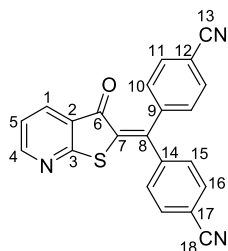
E-Isomer:

¹H-NMR (500 MHz, (CD₃)₂CO): δ = 8.71 (dd, J = 4.8, 1.8 Hz, 1H, H-C(4)), 8.01 (dd, J = 7.7, 1.8 Hz, 1H, H-C(1)), 7.83 – 7.80 (m, 2H, H-C(11)), 7.54 – 7.52 (m, 2H, H-C(10)), 7.39 (dd, J = 7.8, 4.8 Hz, 1H, H-C(5)), 7.38 – 7.34 (m, 2H, H-C(15)), 7.34 – 7.31 (m, 2H, H-C(16)), 2.39 (s, 3H, H-C(18))

¹³C-NMR (126 MHz, (CD₃)₂CO): δ = 185.6 (C(6)), 168.1 (C(3)), 156.8 (C(4)), 149.7 (C(8)), 145.9 (C(9)), 141.3 (C(17)), 138.8 (C(14)), 135.03 (C(1)), 132.9 (C(11)), 131.16 (C(10)), 130.38 (C(16)), 130.35 (C(15)), 127.1 (C(2)), 121.88 (C(5)), 119.3 (C(13)), 112.6 (C(12)), 21.4 (C(18)), (C(7)) could not be clearly assigned

IR: $\tilde{\nu}$ = 2918 (w), 2224 (w), 1665 (s), 1604 (w), 1571 (s), 1527 (m), 1497 (m), 1452 (w), 1395 (s), 1279 (m), 1201 (w), 1125 (m), 1089 (m), 1050 (s), 1018 (m), 824 (s), 759 (s), 729 (m)
HRMS (APPI, CH₂Cl₂, positive mode) calcd. for C₂₂H₁₅N₂OS [M+H]⁺ 355.0900, found 355.0907

4,4'-((3-Oxothieno[2,3-b]pyridin-2(3H)-ylidene)methylene)dibenzonitrile (**10**)



To a solution of 4,4'-carbonyldibenzonitrile (46.1 mg, 0.198 mmol) in dry 1,2-dichloroethane (1 mL) was added BBr₃ (1.0 M in CH₂Cl₂, 224 mg, 0.893 mL, 0.893 mmol) under inert atmosphere. The mixture was subsequently transferred to a solution of thieno[2,3-b]pyridin-3(2H)-one (**23**) (30.0 mg, 0.198 mmol) in dry 1,2-dichloroethane (1 mL) and heated to 50 °C for 5 h. The reaction was quenched by the addition of sat. aq. NH₄Cl. The aqueous phase was extracted with ethyl acetate and dried (MgSO₄). The crude product was purified by column chromatography (SiO₂, hexanes/ethyl acetate 1:1) and recrystallization from methanol to afford **10** as yellow crystals (38.7 mg, 53%).

m.p.: 188-189 °C

R_f = 0.53 (SiO₂, hexanes/ethyl acetate 1:1)

¹H-NMR (601 MHz, CDCl₃): δ = 8.69 (dd, J = 4.8, 1.8 Hz, 1H, H-C(4)), 7.98 (dd, J = 7.7, 1.8 Hz, 1H, H-C(1)), 7.75 – 7.73 (m, 2H, H-C(16)), 7.73 – 7.71 (m, 2H, H-C(11)),

7.53 – 7.51 (m, 2H, H-C(15)), 7.38 – 7.36 (m, 2H, H-C(10)), 7.26 (dd, $J = 7.9, 4.8$ Hz, 1H, H-C(5))

^{13}C -NMR (151 MHz, CDCl_3): $\delta = 185.4$ (C(6)), 167.3 (C(3)), 156.4 (C(4)), 146.3 (C(8)), 144.6 (C(14)), 143.3 (C(9)), 134.8 (C(1)), 133.5 (C(7)), 132.9 (C(16)), 132.6 (C(11)), 130.3 (C(15)), 130.1 (C(10)), 126.0 (C(2)), 121.2 (C(5)), 118.5 (C(13)), 118.1 (C(18)), 113.9 (C(17)), 113.1 (C(12))

IR: $\tilde{\nu} = 3056$ (w), 2232 (m), 1683 (s), 1575 (s), 1541 (m), 1500 (m), 1456 (w), 1400 (s), 1286 (m), 1261 (w), 1202 (w), 1091 (m), 1053 (s), 1019 (m), 961 (m), 847 (m), 761 (s), 569 (s), 553 (s)

HRMS (APPI, CH_2Cl_2 , positive mode) calcd. for $\text{C}_{22}\text{H}_{12}\text{N}_3\text{OS}$ $[\text{M}+\text{H}]^+$ 366.0696, found 366.0702

UV/Vis Spectroscopic Measurements

Determination of the UV/Vis Spectra of Pure *Z* and *E* Isomers

UV/Vis absorption spectra of pure *E/Z* isomer were obtained by subtraction of a *E/Z* mix absorption spectrum with known isomeric composition from a second different *E/Z* mix spectrum with known isomeric composition. Determination of the isomeric compositions of the *E/Z* isomer mixtures was based on the integration of indicative signals in the ¹H-NMR spectra recorded immediately after measurement of the *E/Z* mix absorption spectra.

Stock solutions of diaryl-HTIs **2**, **3**, **4**, **7**, **8**, and **9** were prepared from 1.44 mg – 2.06 mg substance and 0.8 mL – 2.5 mL toluene-*d*₈ or DMSO-*d*₆. The NMR-tube was filled with 0.8 mL of the stock solution and the UV/Vis cuvette (1 cm) was filled with 2.5 mL toluene or DMSO (spectroscopic grade) mixed with 14.9 μL – 60.4 μL stock solution. The ¹H-NMR spectrum and the UV/Vis spectrum were recorded simultaneously. After the first measurement, the NMR sample was irradiated with 435 nm, 450 nm, or 470 nm to change the isomeric composition. For the second measurement 14.9 μL – 60.4 μL of the irradiated NMR solution was mixed with 2.5 mL of spectroscopic solvent in the UV/Vis cuvette. Again, the ¹H-NMR spectrum and the UV/Vis spectrum were recorded simultaneously.

Furthermore, the following conditions must be fulfilled:

- The photosystem must consist of only two isomers and the interconversion of the *E/Z* isomers under irradiation with light must proceed without formation of side-products
- The total concentration in the UV/Vis cuvette remains constant throughout the measurement to obtain defined isosbestic points
- The *E/Z* mix spectra result from the addition of the pure *E* and *Z* spectra

Absorption spectra of pure *E* and *Z* isomer are defined as:

$$S(E) = S(X_E; Y_E) \quad (\text{eq. 1})$$

$$S(Z) = S(X_Z; Y_Z) \quad (\text{eq. 2})$$

with the absorption intensity Y_E and Y_Z at wavelengths X_E and X_Z , respectively. The *E/Z* mix absorption spectra with one isomer enriched (*E*⁺ or *Z*⁺) are described as addition of pure *E* and *Z* spectra with different weighting factors for each isomer:

$$S_{mix}(E+) = S(E) \cdot z_1 + S(Z) \cdot z_2 \quad (\text{eq. 3})$$

$$S_{mix}(Z+) = S(E) \cdot z_3 + S(Z) \cdot z_4 \quad (\text{eq. 4})$$

with z_1 , z_2 , z_3 and z_4 as weighting factors accounting for the relative concentration of each isomer in the enriched mixtures derived from integration of characteristic signals of the E or Z isomer in the corresponding $^1\text{H-NMR}$ spectra.

	E isomer	Z isomer
E enriched spectrum ($S(E+)$)	z_1	z_2
Z enriched spectrum ($S(Z+)$)	z_3	z_4

$S(E)$ and $S(Z)$ can be expressed as

$$S(E) = \frac{S_{mix}(E+) \cdot z_4 - S_{mix}(Z+) \cdot z_2}{z_1 \cdot z_4 - z_3 \cdot z_2} \quad (\text{eq. 5})$$

$$S(Z) = \frac{S_{mix}(Z+) \cdot z_1 - S_{mix}(E+) \cdot z_3}{z_1 \cdot z_4 - z_2 \cdot z_3} \quad (\text{eq. 6})$$

by solving linear equations eq. 3 and eq. 4.

With the calculated absorptions of the pure E and Z isomer and known concentration in the cuvette in hand the molar extinction coefficients can be calculated according to the *Lambert-Beer* Law:

$$A = \varepsilon \cdot c \cdot d \quad (\text{eq. 7})$$

with the absorption A , the concentration c , path length of the cuvette d and the molar extinction coefficient ε .

Molar Extinction Coefficients of Diaryl-HTIs

UV/Vis absorption spectra of diaryl-HTIs **1**, **5**, **6**, and **10** were recorded in toluene and DMSO (spectroscopic grade). Therefore, stock solutions with defined concentrations ($3.45 \cdot 10^{-5} - 1.30 \cdot 10^{-4} \text{ mol} \cdot \text{L}^{-1}$) were prepared. The UV/Vis cuvette was filled with 2.5 mL of stock solution. Molar extinction coefficients were calculated according to the *Lambert-Beer* law (eq. 7).

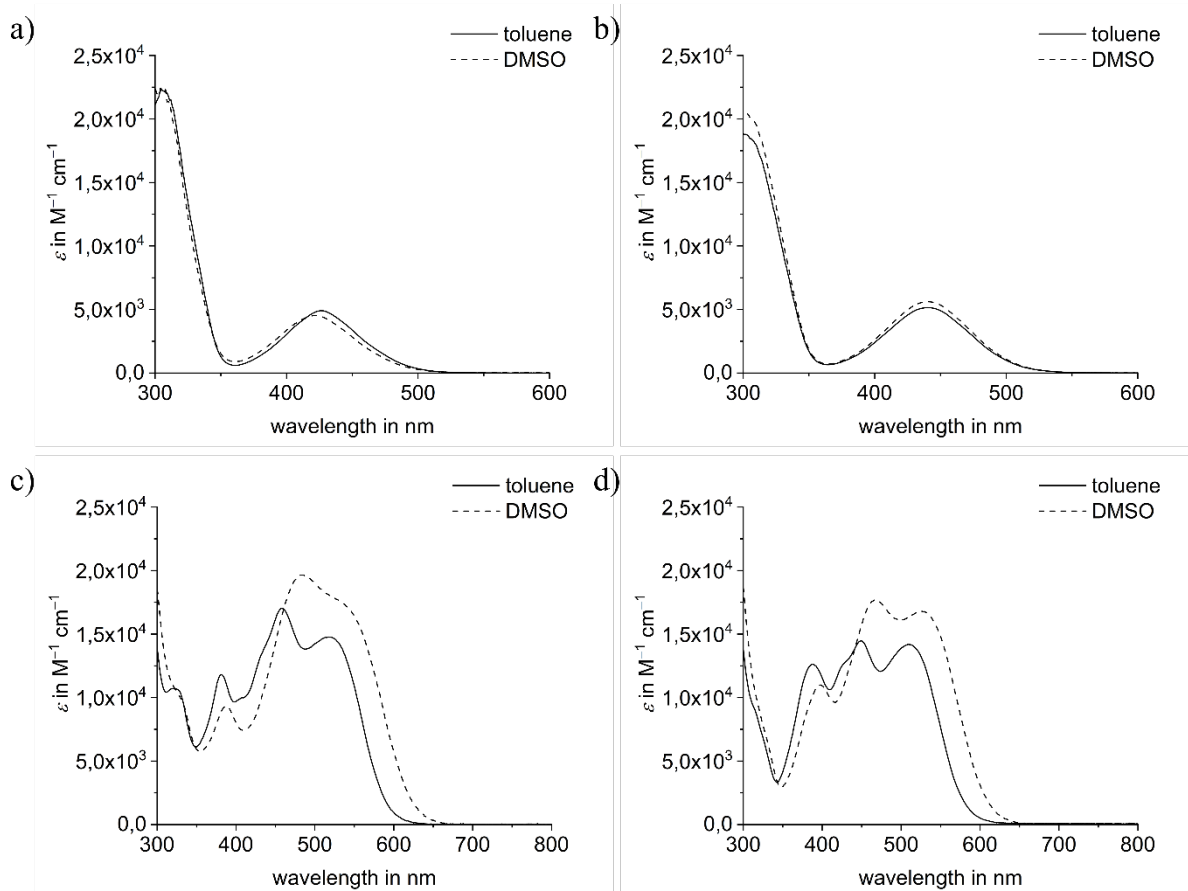


Figure S1: Molar extinction coefficients of diaryl-HTIs **1**, **5**, **6** and **10** in toluene and DMSO; a) molar extinction coefficients of **10** in toluene (solid line) and DMSO (dotted line); b) molar extinction coefficients of **5** in toluene (solid line) and DMSO (dotted line); c) molar extinction coefficients of **6** in toluene (solid line) and DMSO (dotted line); d) molar extinction coefficients of **1** in toluene (solid line) and DMSO (dotted line).

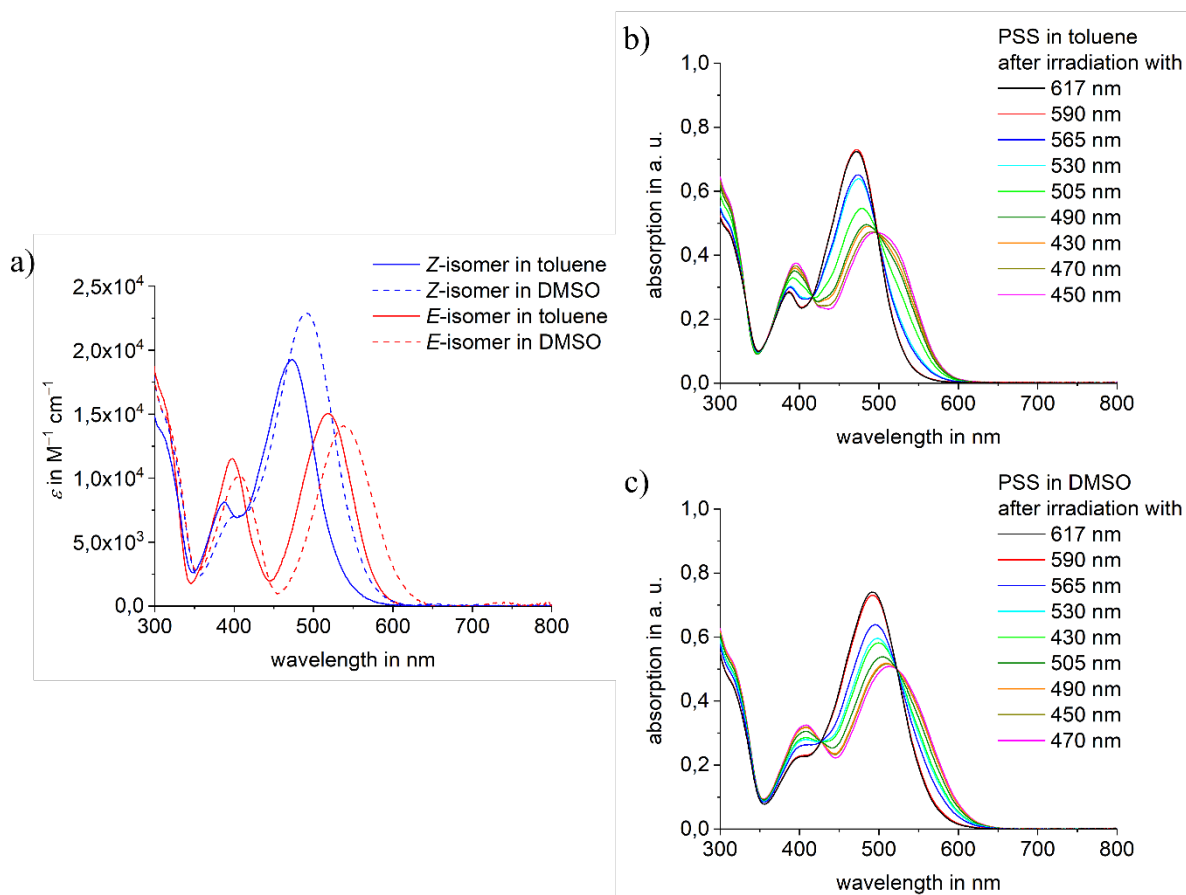


Figure S2: Molar extinction coefficients and irradiation behavior of diaryl-HTI 2 in toluene and DMSO; a) molar extinction coefficients of pure *E* (red) and *Z* isomer (blue) in toluene (solid line) and DMSO (dashed line); b) UV/Vis absorption spectra of enriched *E* or *Z* isomer measured in toluene at 23 °C after irradiation with 617 nm, 590 nm, 565 nm, 530 nm, 505 nm, 490 nm, 470 nm, 450 nm and 430 nm light; c) UV/Vis absorption spectra of enriched *E* or *Z* isomer measured in DMSO at 23 °C after irradiation with 617 nm, 590 nm, 565 nm, 530 nm, 505 nm, 490 nm, 470 nm, 450 nm and 430 nm light.

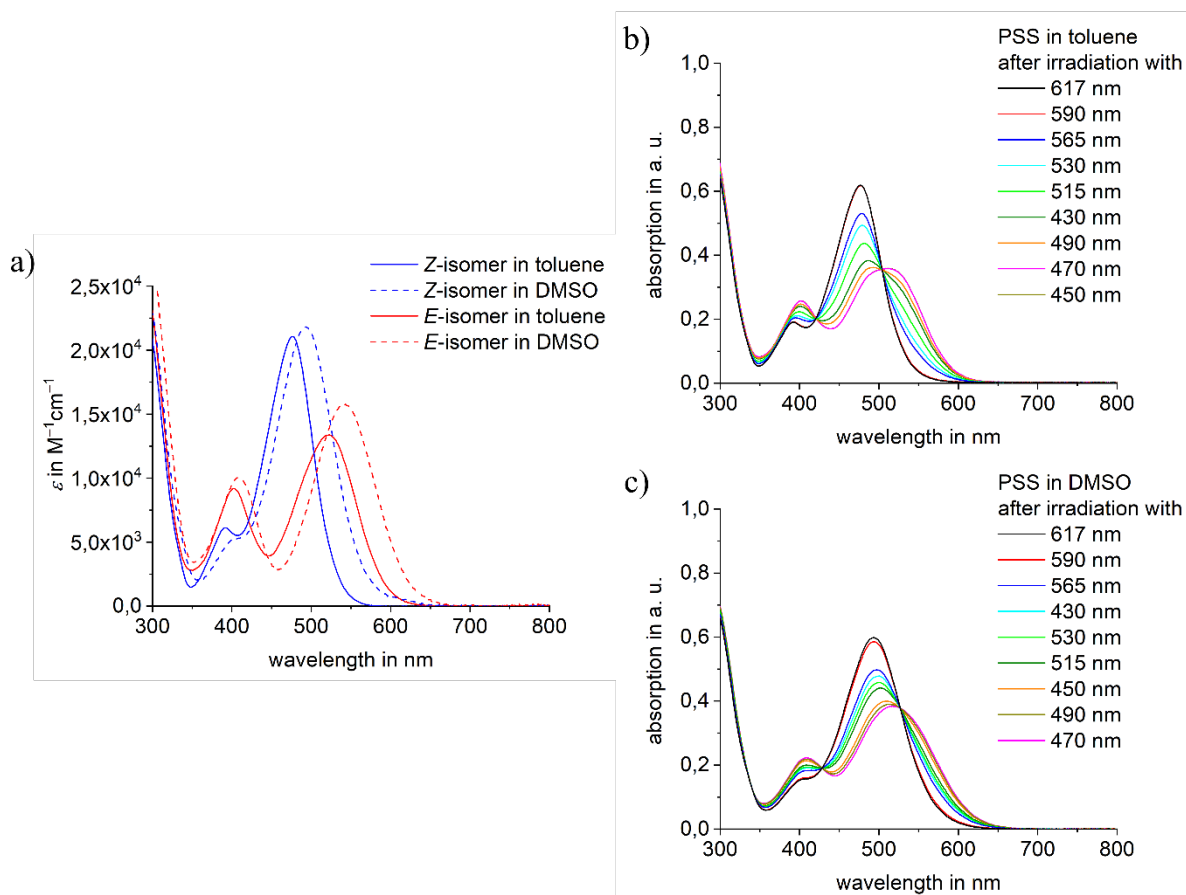


Figure S3: Molar extinction coefficients and irradiation behavior of diaryl-HTI **3** in toluene and DMSO; a) molar extinction coefficients of pure *E* (red) and *Z* isomer (blue) in toluene (solid line) and DMSO (dashed line); b) UV/Vis absorption spectra of enriched *E* or *Z* isomer measured in toluene at 23 °C after irradiation with 617 nm, 590 nm, 565 nm, 530 nm, 515 nm, 490 nm, 470 nm, 450 nm and 430 nm light; c) UV/Vis absorption spectra of enriched *E* or *Z* isomer measured in DMSO at 23 °C after irradiation with 617 nm, 590 nm, 565 nm, 530 nm, 515 nm, 490 nm, 470 nm, 450 nm and 430 nm light.

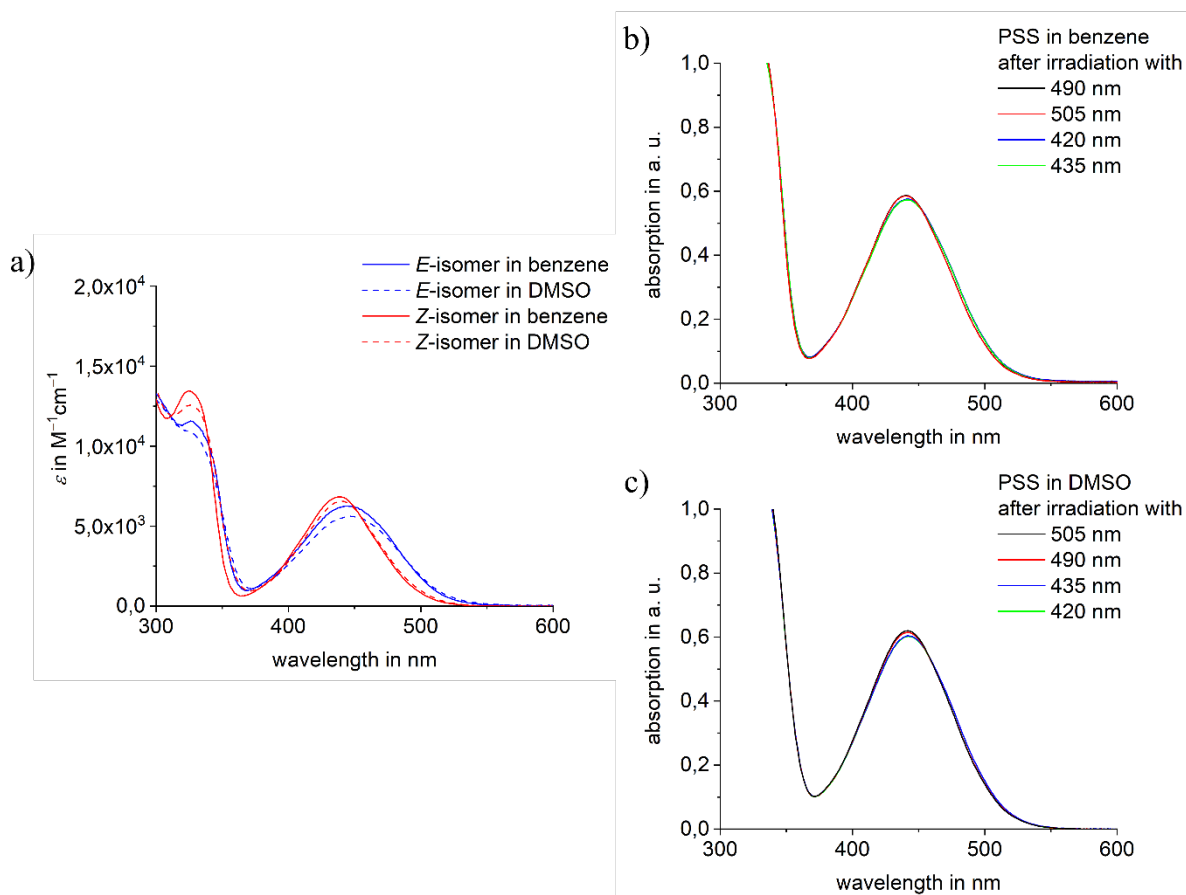


Figure S4: Molar extinction coefficients and irradiation behavior of diaryl-HTI 4 in benzene and DMSO; a) molar extinction coefficients of pure E and Z isomer in toluene (solid line) and DMSO (dashed line); b) UV/Vis absorption spectra of enriched E or Z isomer measured in toluene at 23 °C after irradiation with 505 nm, 490 nm, 435 nm and 420 nm light; c) UV/Vis absorption spectra of enriched E or Z isomer measured in DMSO at 23 °C after irradiation with 505 nm, 490 nm, 435 nm and 420 nm light.

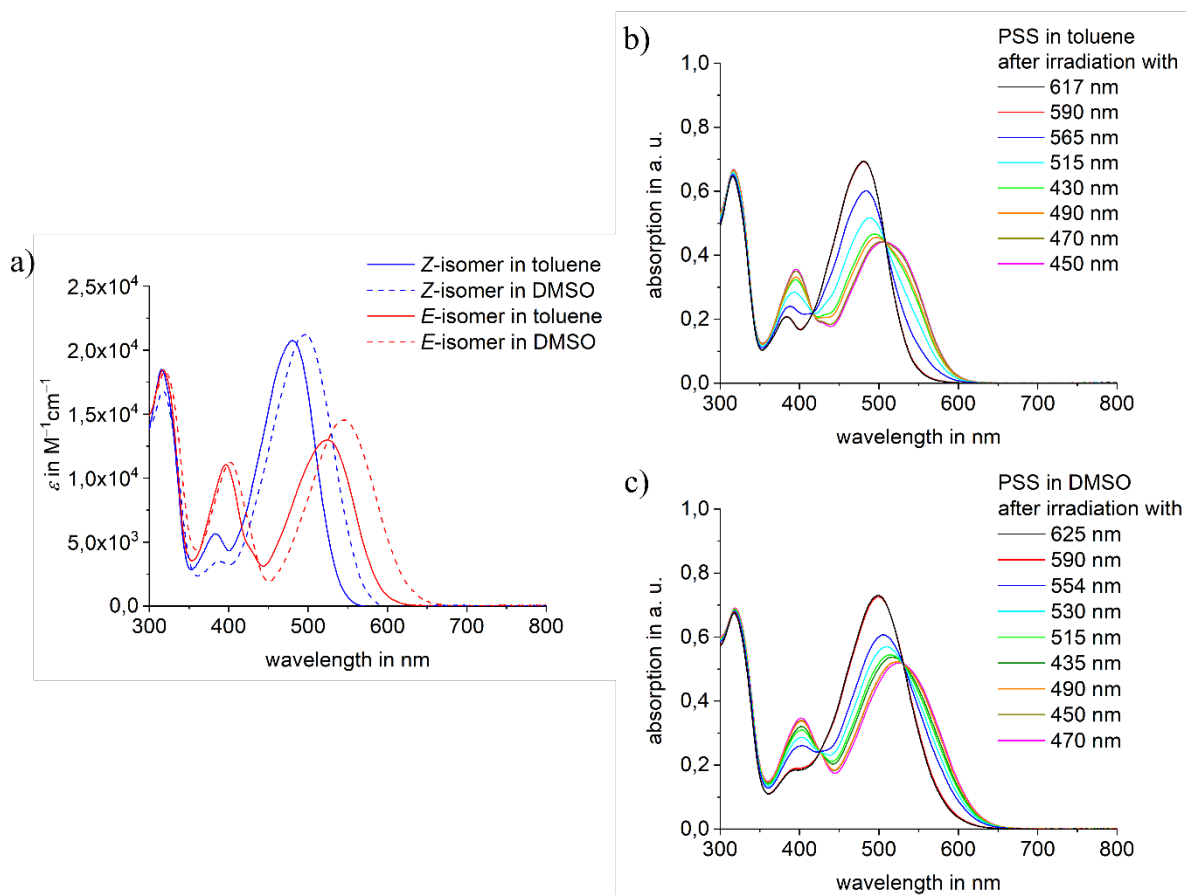


Figure S5: Molar extinction coefficients and irradiation behavior of diaryl-HTI **7** in toluene and DMSO; a) molar extinction coefficients of pure *E* (red) and *Z* isomer (blue) in toluene (solid line) and DMSO (dashed line); b) UV/Vis absorption spectra of enriched *E* or *Z* isomer measured in toluene at 23 °C after irradiation with 617 nm, 590 nm, 565 nm, 515 nm, 490 nm, 470 nm, 450 nm and 430 nm light; c) UV/Vis absorption spectra of enriched *E* or *Z* isomer measured in DMSO at 23 °C after irradiation with 625 nm, 590 nm, 554 nm, 530 nm, 515 nm, 490 nm, 470 nm, 450 nm and 435 nm light.

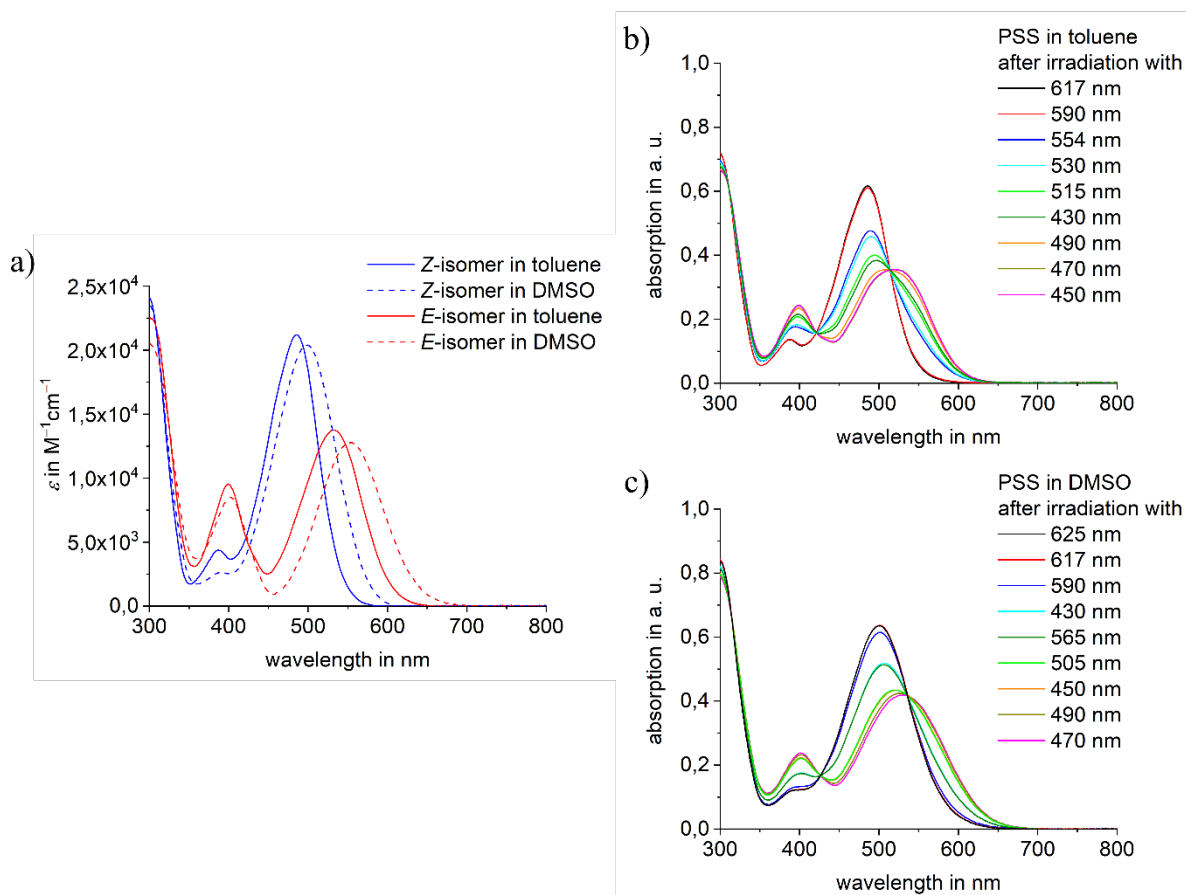


Figure S6: Molar extinction coefficients and irradiation behavior of diaryl-HTI **8** in toluene and DMSO; a) molar extinction coefficients of pure *E* (red) and *Z* isomer (blue) in toluene (solid line) and DMSO (dashed line); b) UV/Vis absorption spectra of enriched *E* or *Z* isomer measured in toluene at 23 °C after irradiation with 617 nm, 590 nm, 554 nm, 530 nm, 515 nm, 490 nm, 470 nm, 450 nm and 430 nm light; c) UV/Vis absorption spectra of enriched *E* or *Z* isomer measured in DMSO at 23 °C after irradiation with 625 nm, 617 nm, 590 nm, 565 nm, 505 nm, 490 nm, 470 nm, 450 nm and 430 nm light.

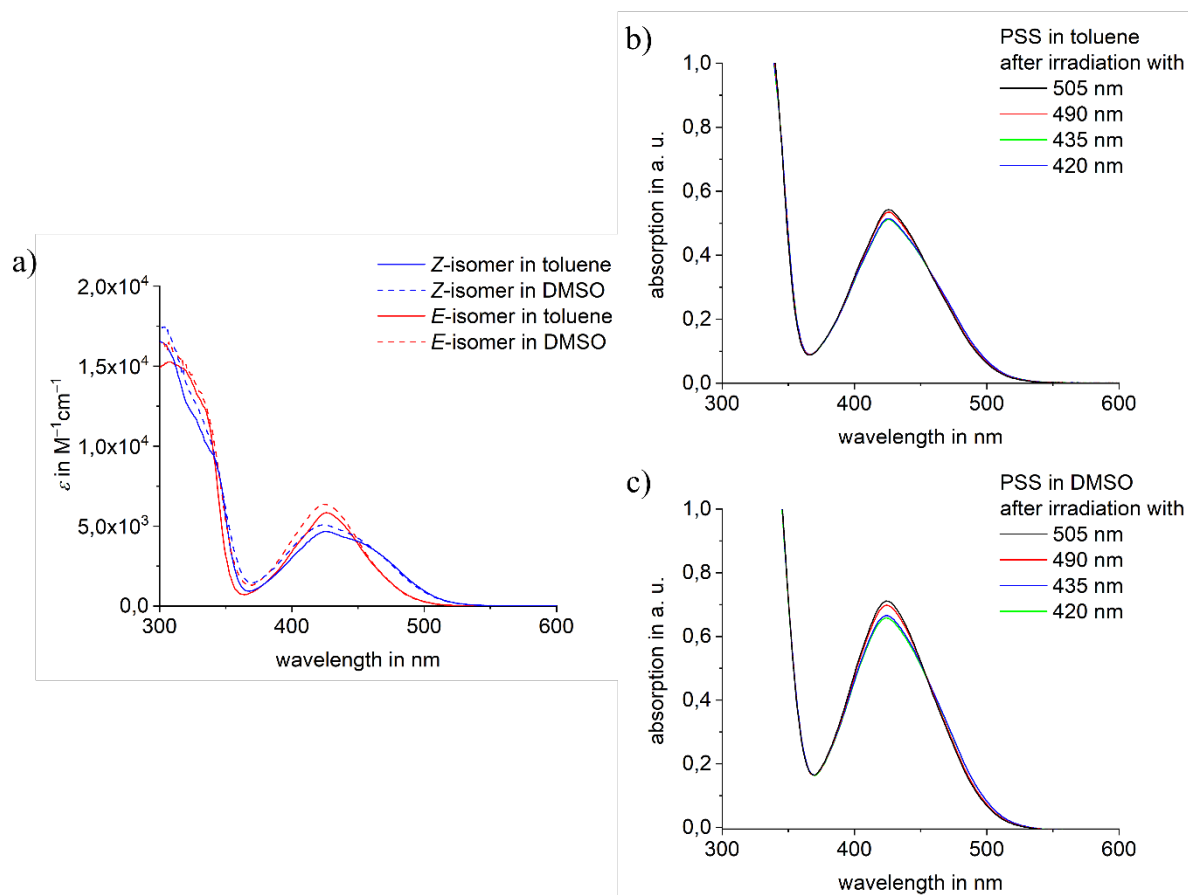


Figure S7: Molar extinction coefficients and irradiation behavior of diaryl-HTI **9** in toluene and DMSO; a) molar extinction coefficients of pure *E* (red) and *Z* isomer (blue) in toluene (solid line) and DMSO (dashed line); b) UV/Vis absorption spectra of enriched *E* or *Z* isomer measured in toluene at 23 °C after irradiation with 505 nm, 490 nm, 435 nm and 420 nm light; c) UV/Vis absorption spectra of enriched *E* or *Z* isomer measured in DMSO at 23 °C after irradiation with 505 nm, 490 nm, 435 nm and 420 nm light.

NMR Irradiation experiments

The *E/Z* isomeric ratio obtained after light irradiation was determined by ¹H NMR spectroscopy. NMR tubes were charged with 0.27 – 2.6 mg substance and 0.7 mL of toluene-*d*₈, DMSO-*d*₆ or benzene-*d*₆. The NMR samples were irradiated with various wavelengths in defined time intervals and ¹H-NMR spectra were recorded afterwards until no change of the *E/Z* isomeric ratio was observed. Suitable signals for the *E* and *Z* isomer in the ¹H-NMR spectrum were integrated and the integral of one signal was set to 1. The *E/Z* isomeric ratio was then calculated according to

$$\frac{I_1}{I_2} = \frac{1}{1+i} \quad (\text{eq. 8})$$

with *I*₁ and *I*₂ as isomer 1 and isomer 2 abundance and *i* as the second integral, which was not set to 1.

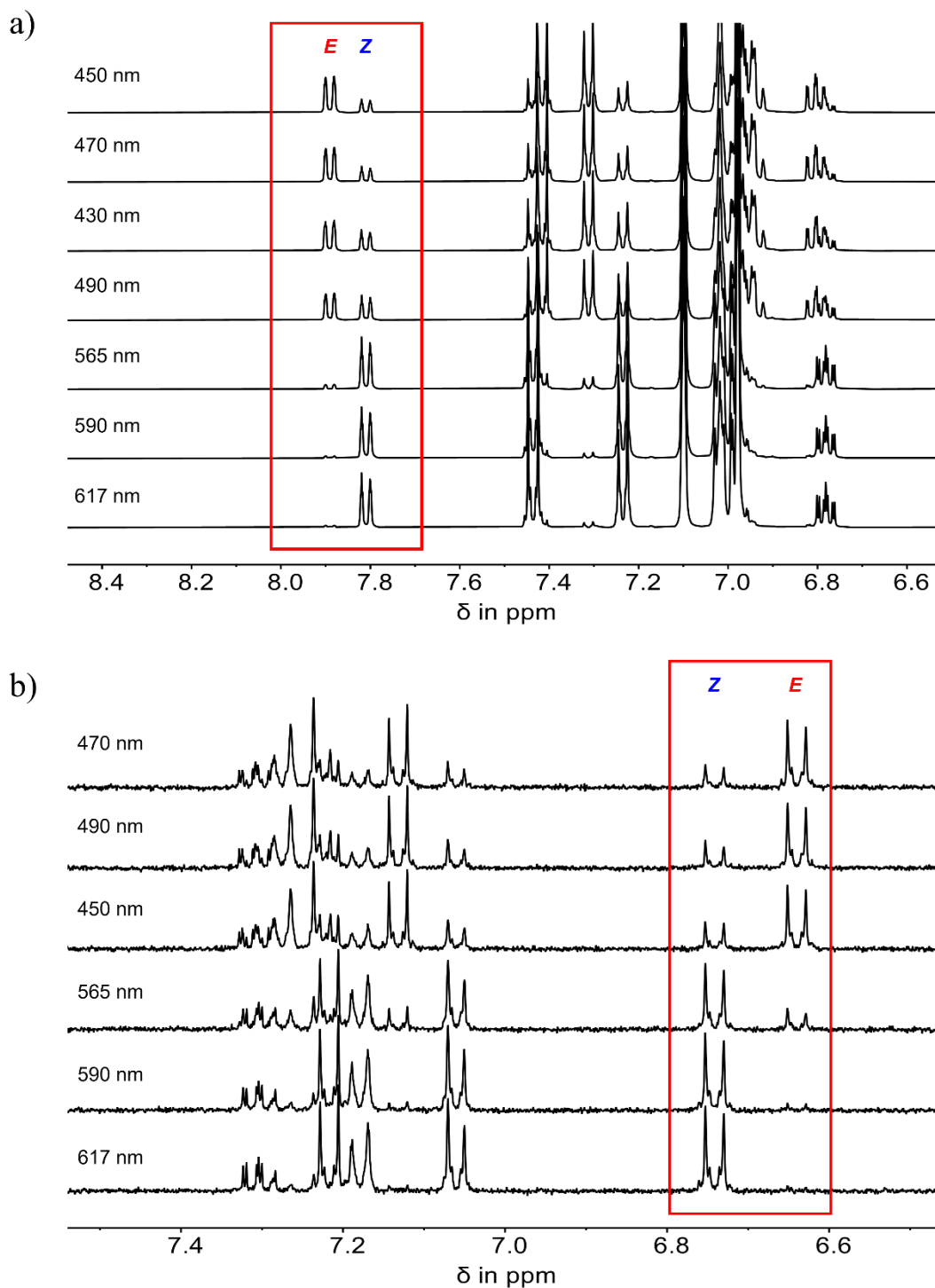


Figure S8: Partial ^1H -NMR spectra of diaryl-HTI **2** recorded after irradiation with light of different wavelengths to enrich the *E* or *Z* isomer; a) partial ^1H -NMR spectra (400 MHz, toluene- d_8 , 20 °C) of enriched *E* and *Z* isomer after irradiation to the pss with 430 nm, 450 nm, 470 nm, 490 nm, 565 nm, 590 nm, or 617 nm light; b) partial ^1H -NMR spectra (400 MHz, DMSO- d_6 , 20 °C) of enriched *E* and *Z* isomer after irradiation to the pss with 450 nm, 470 nm, 490 nm, 565 nm, 590 nm, or 617 nm light.

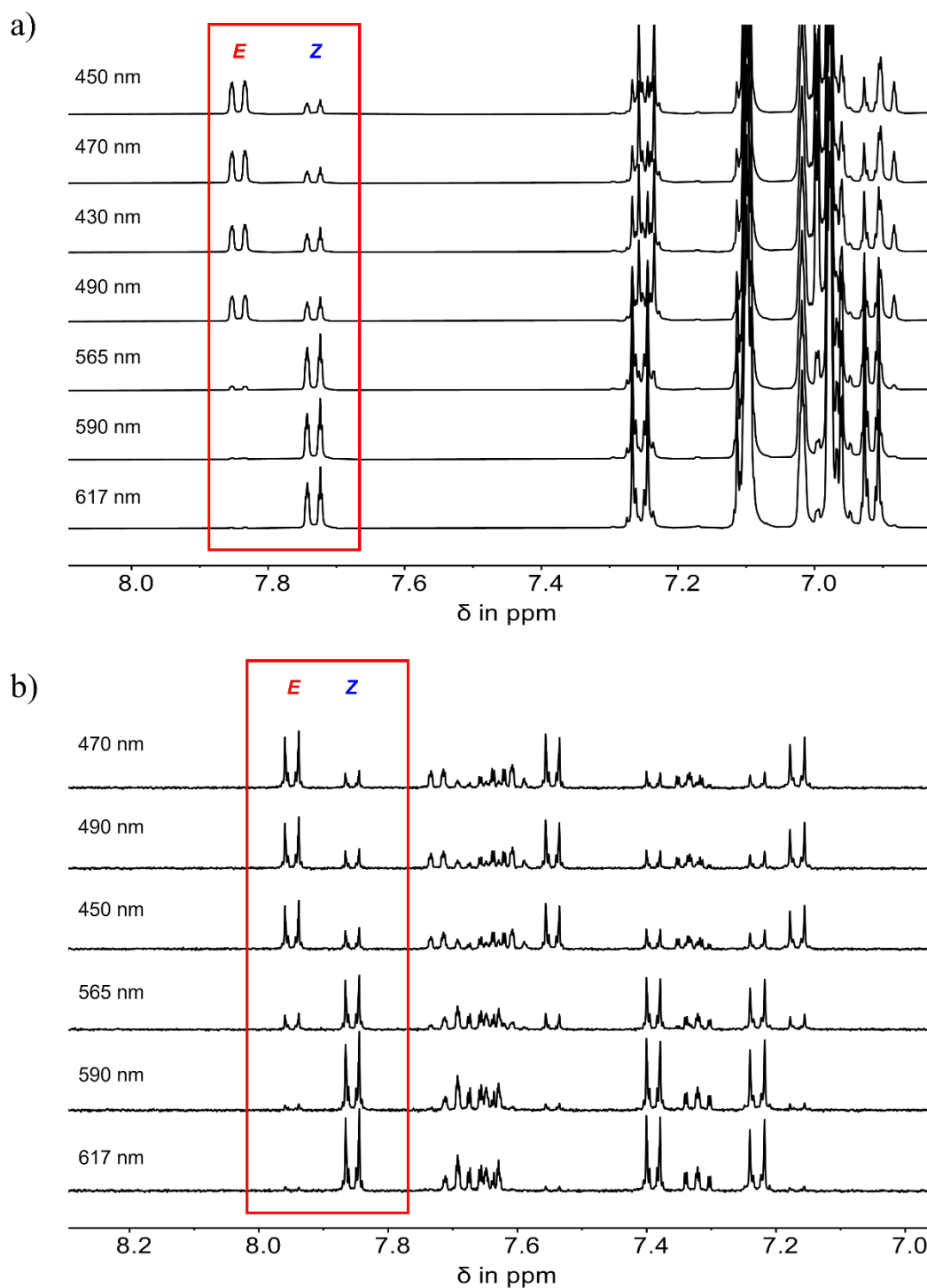


Figure S9: Partial ^1H -NMR spectra of diaryl-HTI **3** recorded after irradiation with light of different wavelengths to enrich the *E* or *Z* isomer; a) partial ^1H -NMR spectra (400 MHz, toluene- d_8 , 20 °C) of enriched *E* and *Z* isomer after irradiation to the pss with 430 nm, 450 nm, 470 nm, 490 nm, 565 nm, 590 nm, or 617 nm light; b) partial ^1H -NMR spectra (400 MHz, DMSO- d_6 , 20 °C) of enriched *E* and *Z* isomer after irradiation with 450 nm, 470 nm, 490 nm, 565 nm, 590 nm, or 617 nm light.

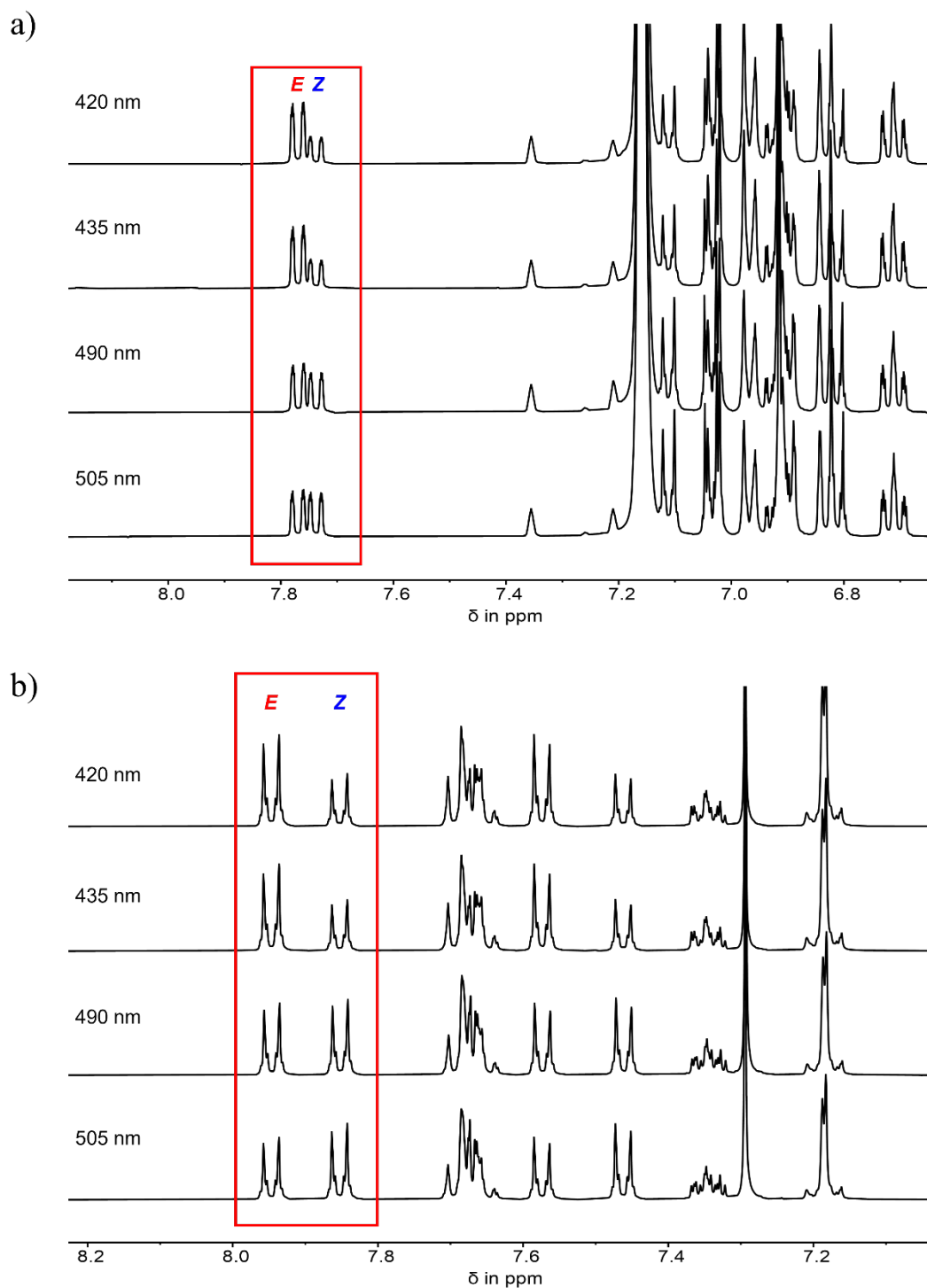


Figure S10: Partial ^1H -NMR spectra of diaryl-HTI **4** recorded after irradiation with light of different wavelengths to enrich the *E* or *Z* isomer; a) partial ^1H -NMR spectra (400 MHz, benzene- d_6 , 20 °C) of enriched *E* and *Z* isomer after irradiation to the pss with 420 nm, 435 nm, 490 nm, or 505 nm light; b) partial ^1H -NMR spectra (400 MHz, DMSO- d_6 , 20 °C) of enriched *E* and *Z* isomer after irradiation to the pss with 420 nm, 435 nm, 490 nm, or 505 nm light.

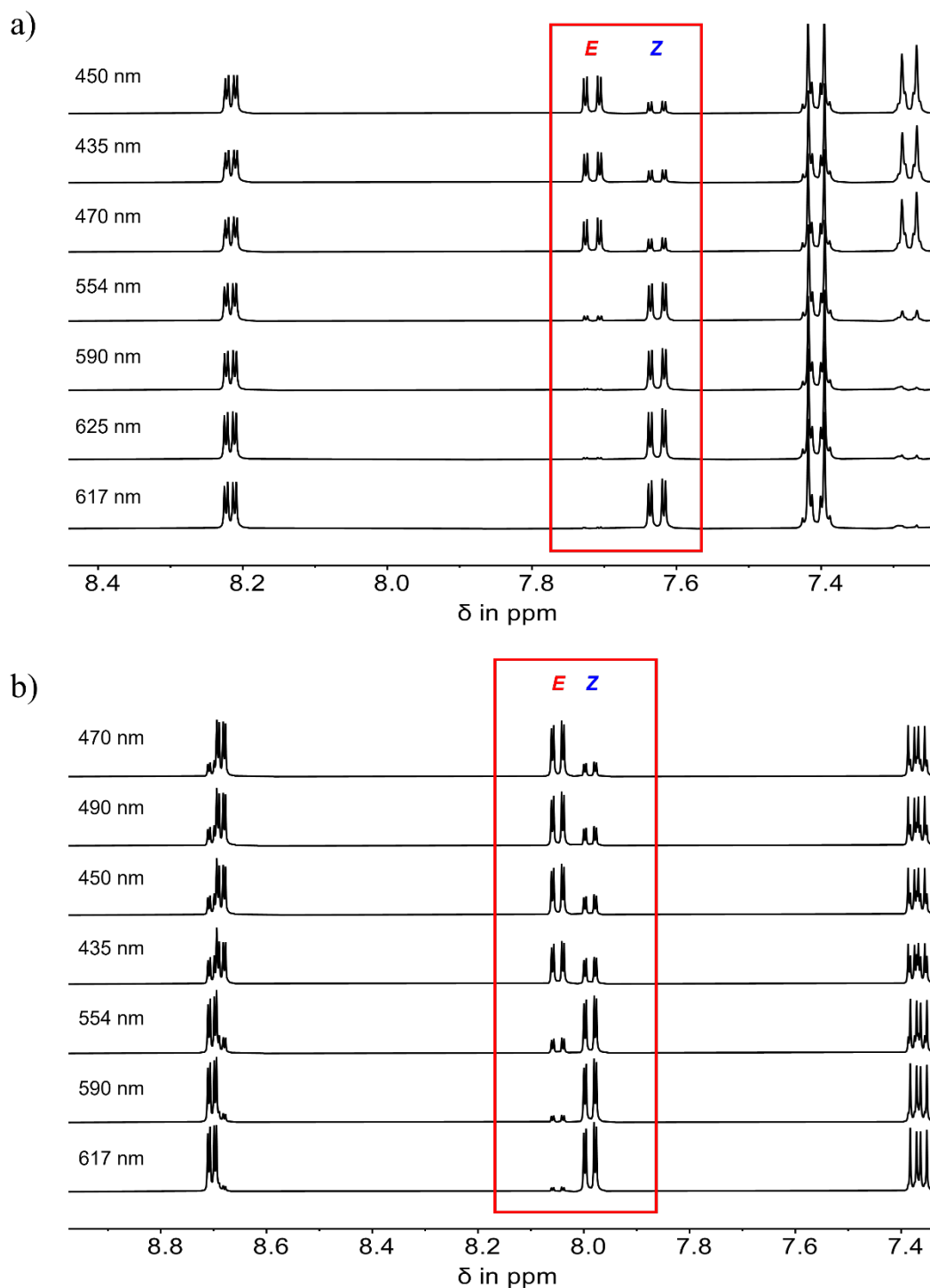


Figure S11: Partial ^1H -NMR spectra of diaryl-HTI **7** recorded after irradiation with light of different wavelengths to enrich the *E* or *Z* isomer; a) partial ^1H -NMR spectra (400 MHz, toluene- d_8 , 20 °C) of enriched *E* and *Z* isomer after irradiation to the pss with 435 nm, 450 nm, 470 nm, 554 nm, 590 nm, 617 nm, or 625 nm light; b) partial ^1H -NMR spectra (400 MHz, DMSO- d_6 , 20 °C) of enriched *E* and *Z* isomer after irradiation to the pss with 435 nm, 450 nm, 470 nm, 490 nm, 554 nm, 590 nm, or 617 nm light.

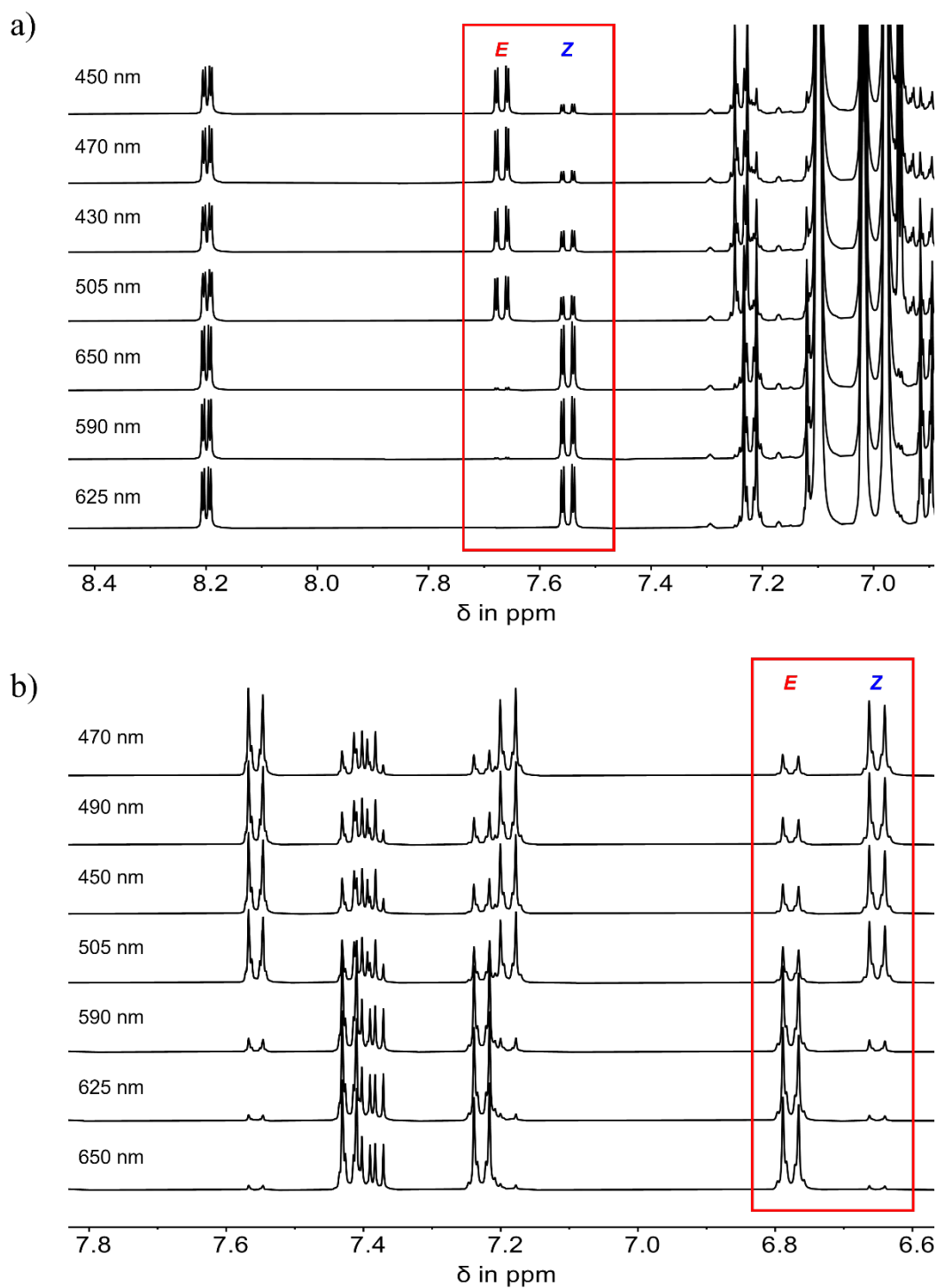


Figure S12: Partial ^1H -NMR spectra of diaryl-HTI **8** recorded after irradiation with light of different wavelengths to enrich the *E* or *Z* isomer; a) Partial ^1H -NMR spectra (400 MHz, toluene- d_8 , 20 °C) of enriched *E* and *Z* isomer after irradiation to the pss with 430 nm, 450 nm, 470 nm, 505 nm, 590 nm, 625 nm, or 650 nm light; b) Partial ^1H -NMR spectra (400 MHz, DMSO- d_6 , 20 °C) of enriched *E* and *Z* isomer after irradiation to the pss with 450 nm, 470 nm, 490 nm, 505 nm, 590 nm, 625 nm, or 650 nm light.

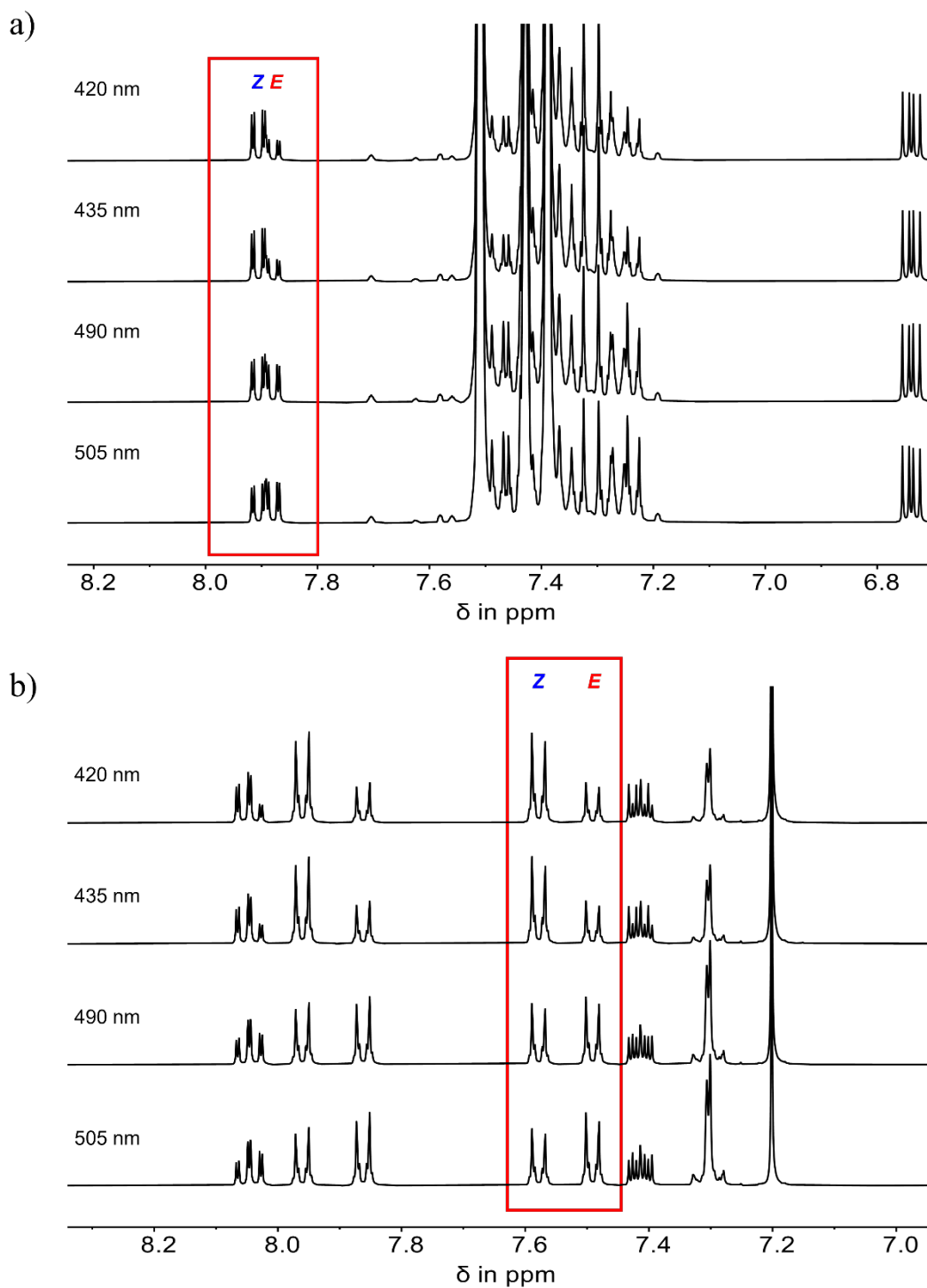


Figure S13: Partial ^1H -NMR spectra of diaryl-HTI **9** recorded after irradiation with light of different wavelengths to enrich the *E* or *Z* isomer; a) partial ^1H -NMR spectra (400 MHz, toluene- d_8 , 20 °C) of enriched *E* and *Z* isomer after irradiation to the pss with 420 nm, 435 nm, 490 nm, or 505 nm light; b) partial ^1H -NMR spectra (400 MHz, DMSO- d_6 , 20 °C) of enriched *E* and *Z* isomer after irradiation to the pss with 420 nm, 435 nm, 490 nm, and 505 nm light.

Table S1: Isomeric composition obtained from integration of specific signals in the ^1H NMR spectra after irradiation to the pss of the NMR samples with different wavelengths of light in different solvents.

Hemithioindigo	Solvent	Wavelength	% <i>Z</i>-isomer	% <i>E</i>-isomer
2	toluene- d_8	430 nm	35	65
		450 nm	24	76
		470 nm	28	72
		490 nm	44	56
		565 nm	90	10
		590 nm	95	5
		617 nm	96	4
	DMSO- d_6	450 nm	27	73
		470 nm	25	75
		490 nm	30	70
		565 nm	78	22
		590 nm	93	7
		617 nm	97	3
		3	toluene- d_8	430 nm
450 nm	25			75
470 nm	26			74
490 nm	42			58
565 nm	90			10
590 nm	97			3
617 nm	97			3
DMSO- d_6	450 nm		30	70
	470 nm		23	77
	490 nm		27	73
	565 nm		77	23
	590 nm		93	7
	617 nm		96	4
	4		benzene- d_6	420 nm
435 nm		31		69
490 nm		45		55
505 nm		49		51

7	DMSO- <i>d</i> ₆	420 nm	36	64
		435 nm	37	63
		490 nm	51	49
		505 nm	55	45
	toluene- <i>d</i> ₈	435 nm	30	70
		450 nm	25	75
		470 nm	30	70
		554 nm	87	13
		590 nm	96	4
		617 nm	97	3
	DMSO- <i>d</i> ₆	625 nm	96	4
		435 nm	39	61
		450 nm	29	71
		470 nm	21	79
490 nm		26	74	
554 nm		78	22	
590 nm		90	10	
617 nm		94	6	
8	toluene- <i>d</i> ₈	650 nm	84	16
		430 nm	33	67
		450 nm	17	83
		470 nm	18	82
		505 nm	35	65
		590 nm	97	3
	DMSO- <i>d</i> ₆	625 nm	98	2
		650 nm	96	4
		450 nm	30	70
		470 nm	22	78
		490 nm	27	73
9	toluene- <i>d</i> ₈	505 nm	37	63
		590 nm	88	12
		625 nm	94	6
		650 nm	96	4
		420 nm	71	29

	435 nm	71	29
	490 nm	55	45
	505 nm	51	49
DMSO- <i>d</i> ₆	420 nm	69	31
	435 nm	68	32
	490 nm	48	52
	505 nm	44	46

Thermal Double Bond Isomerization

Thermal double bond isomerization of diaryl-HTIs **2**, **3**, **4**, **7**, **8**, and **9** was investigated by heating experiments in the dark. First NMR-tubes were charged with 0.19 to 2.30 mg of the particular diaryl-HTI and 0.7 mL of toluene-*d*₈ or DMSO-*d*₆. For enrichment of the metastable isomers in solution, the NMR-samples were irradiated with 435 nm, 450 nm, or 470 nm. Afterwards, the NMR-tubes were heated (30 to 100 °C) in the dark and the kinetics of thermal isomerizations were followed by ¹H-NMR spectra measured in defined time intervals. Concentrations of *E* and *Z* isomer were determined by integration of indicative ¹H-NMR signals. The measurements were stopped after reaching the thermal equilibrium between the *E* and *Z* isomer.

Equation 9 describes the thermal double bond isomerization process of a unimolecular first order reaction towards an equilibrium between the two isomers isomer 1 and isomer 2:

$$\ln \left(\frac{[I_1]_{t_0} - [I_1]_{eq}}{[I_1]_t - [I_1]_{eq}} \right) = (k_{I_1/I_2} + k_{I_2/I_1})t \quad (\text{eq. 9})$$

with $[I_1]_{t_0}$ as the initial concentration of isomer 1 at time $t = 0$, $[I_1]_{eq}$ as the concentration of isomer 1 in the equilibrium, $[I_1]_t$ as the concentration of isomer 1 at a defined time t , k_{I_1/I_2} as the rate constant for the isomerization of isomer 1 to isomer 2, k_{I_2/I_1} as the rate constant for the isomerization of isomer 2 to isomer 1 and t as the elapsed time. The slope $m = k_{I_1/I_2} + k_{I_2/I_1}$ obtained from the plot of the logarithmic part in equation 9 against time t contains the rate constants for both isomerization processes. Consequently, the rate constant can be calculated according to:

$$k_{I_1/I_2} = \frac{m}{1 + \frac{[I_1]_{eq}}{[I_2]_{eq}}} \quad (\text{eq. 10})$$

when the law of mass action (eq. 11) is considered:

$$\frac{[I_1]_{eq}}{[I_2]_{eq}} = \frac{k_{I_2/I_1}}{k_{I_1/I_2}} \quad (\text{eq. 11})$$

The Gibbs energy of activation ΔG^\ddagger can then be calculated from the rate constants by using the Eyring equation (eq. 12):

$$k = \frac{k_B \cdot T}{h} \cdot e^{\frac{-\Delta G^\ddagger}{R \cdot T}} \quad (\text{eq. 12})$$

with the *Boltzmann* constant k_B ($1.381 \cdot 10^{-23} \text{ J} \cdot \text{K}^{-1}$), temperature T , *Planck* constant h ($6.626 \cdot 10^{-34} \text{ J} \cdot \text{s}$) and the rate constant k . After rearrangement of equation 12 the Gibbs energy of activation ΔG^\ddagger is obtained:

$$\Delta G^\ddagger = -R \cdot T \cdot \ln\left(\frac{k \cdot h}{k_B \cdot T}\right) \quad (\text{eq. 13})$$

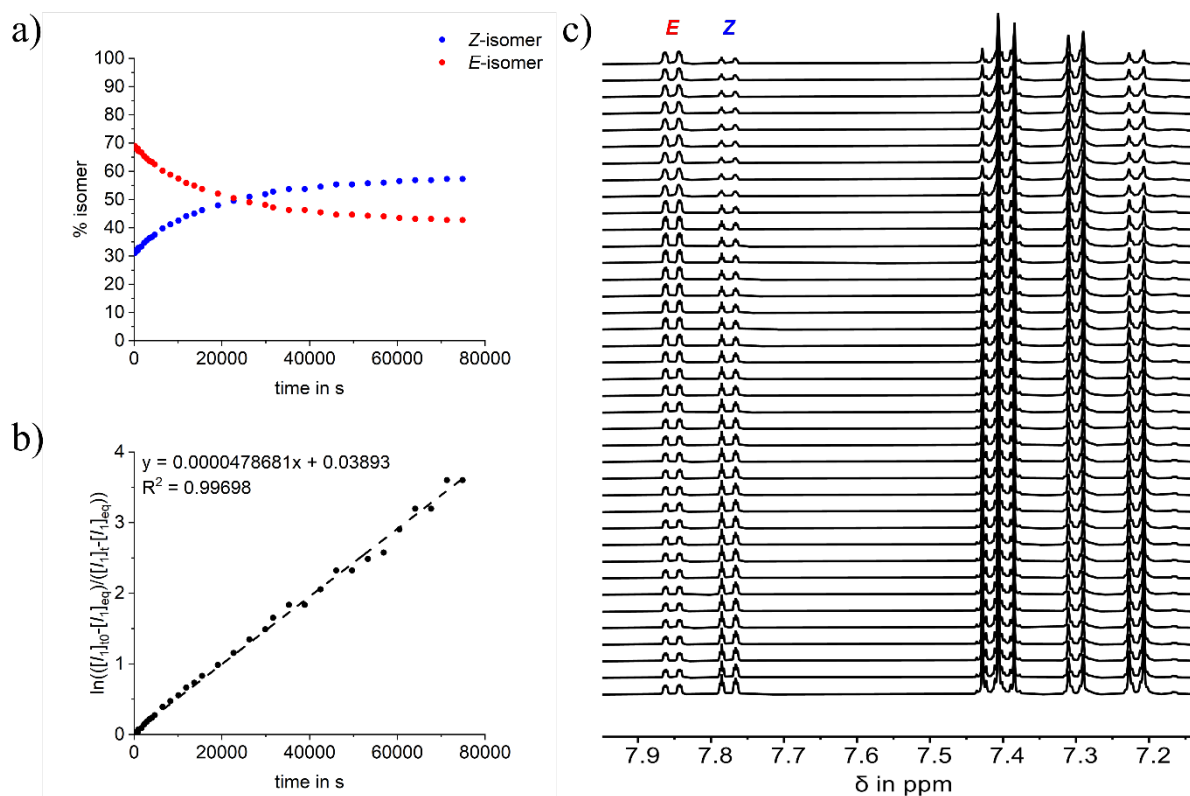


Figure S14: Thermal *E* to *Z* isomerization of diaryl-HTI **2** at 50 °C in toluene-*d*₈ solution in the dark. The metastable *E*-isomer was enriched with 470 nm light irradiation before the measurement; a) temporal change of the isomeric composition while heating at 50 °C; b) first order kinetic analysis of the thermal *E* to *Z* isomerization by plotting equation 9. The rate constant $k_{E/Z}$ is obtained from the slope of the linear fit; c) partial ¹H NMR spectra (400 MHz, toluene-*d*₈, 50 °C) measured in defined time intervals while heating the NMR-sample at 50 °C.

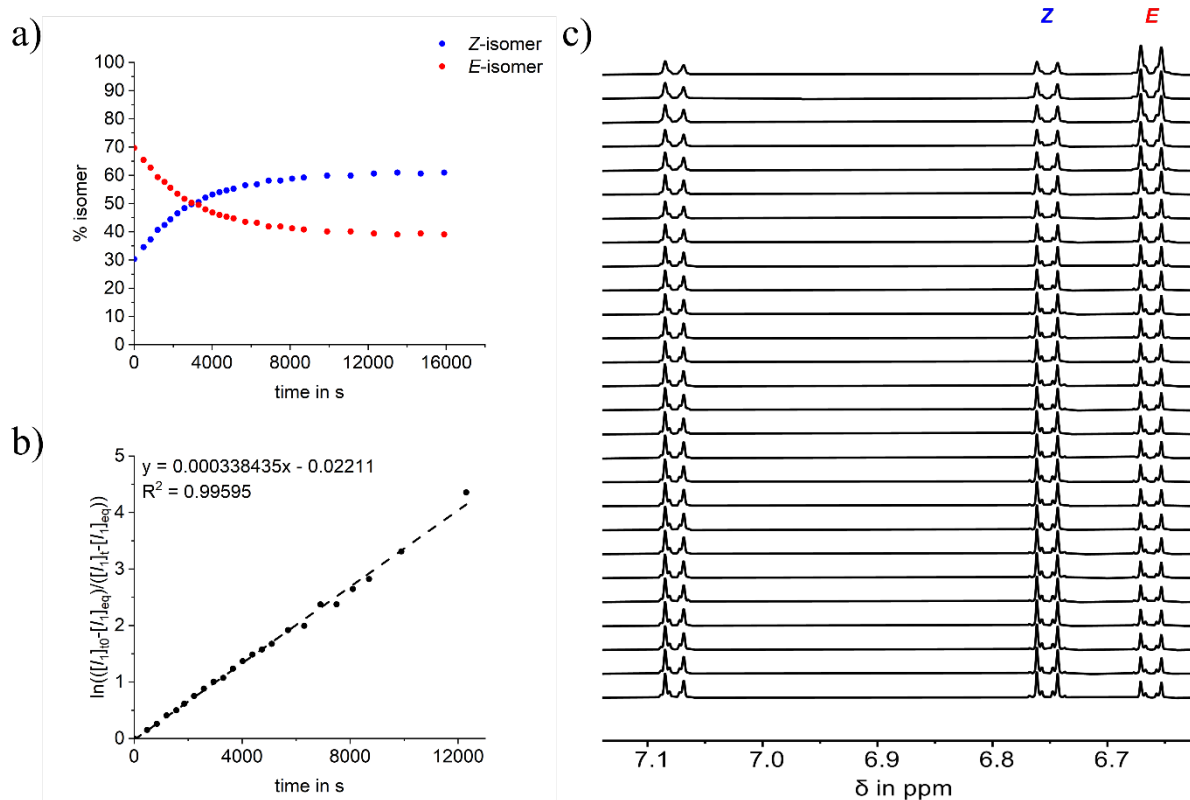


Figure S15: Thermal *E* to *Z* isomerization of diaryl-HTI **2** at 100 °C in DMSO-*d*₆ solution in the dark. The metastable *E*-isomer was enriched with 470 nm light irradiation before the measurement; a) temporal change of the isomeric composition while heating at 100 °C; b) first order kinetic analysis of the thermal *E* to *Z* isomerization by plotting equation 9. The rate constant $k_{E/Z}$ is obtained from the slope of the linear fit; c) partial ¹H NMR spectra (500 MHz, DMSO-*d*₆, 100 °C) measured in defined time intervals while heating the NMR-sample at 100 °C.

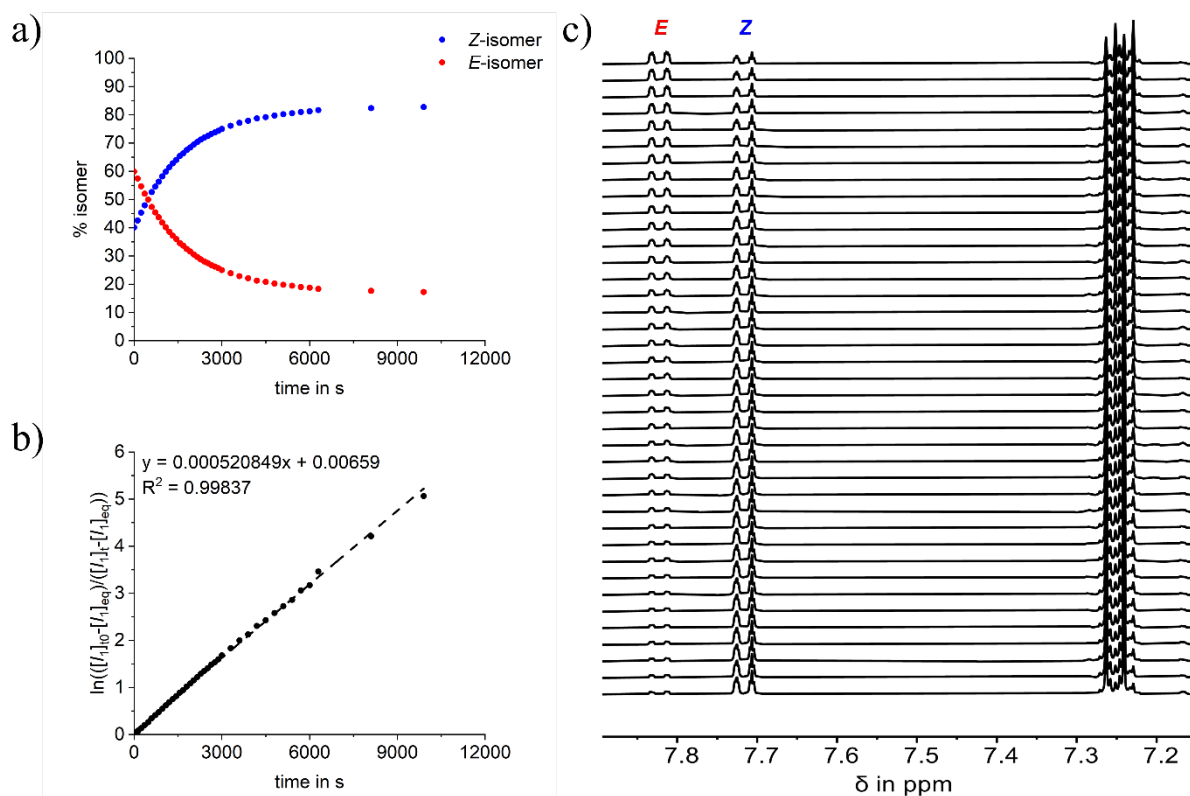


Figure S16: Thermal *E* to *Z* isomerization of diaryl-HTI **3** at 40 °C in toluene-*d*₈ solution in the dark. The metastable *E*-isomer was enriched with 470 nm light irradiation before the measurement; a) temporal change of the isomeric composition while heating at 40 °C; b) first order kinetic analysis of the thermal *E* to *Z* isomerization by plotting equation 9. The rate constant $k_{E/Z}$ is obtained from the slope of the linear fit; c) partial ¹H NMR spectra (400 MHz, toluene-*d*₈, 40 °C) measured in defined time intervals while heating the NMR-sample at 40 °C.

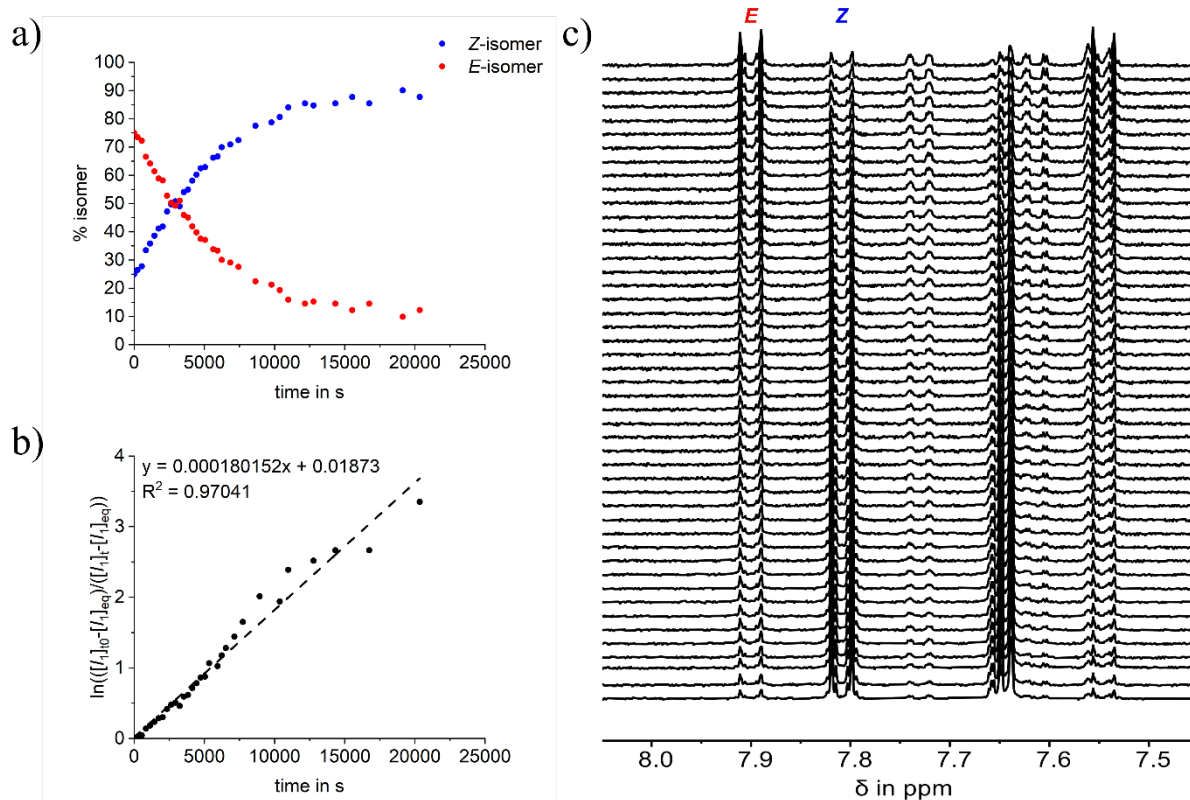


Figure S17: Thermal *E* to *Z* isomerization of diaryl-HTI **3** at 90 °C in DMSO-*d*₆ solution in the dark. The metastable *E*-isomer was enriched with 470 nm light irradiation before the measurement; a) temporal change of the isomeric composition while heating at 90 °C; b) first order kinetic analysis of the thermal *E* to *Z* isomerization by plotting equation 9. The rate constant $k_{E/Z}$ is obtained from the slope of the linear fit; c) partial ¹H NMR spectra (400 MHz, DMSO-*d*₆, 90 °C) measured in defined time intervals while heating the NMR-sample at 90 °C.

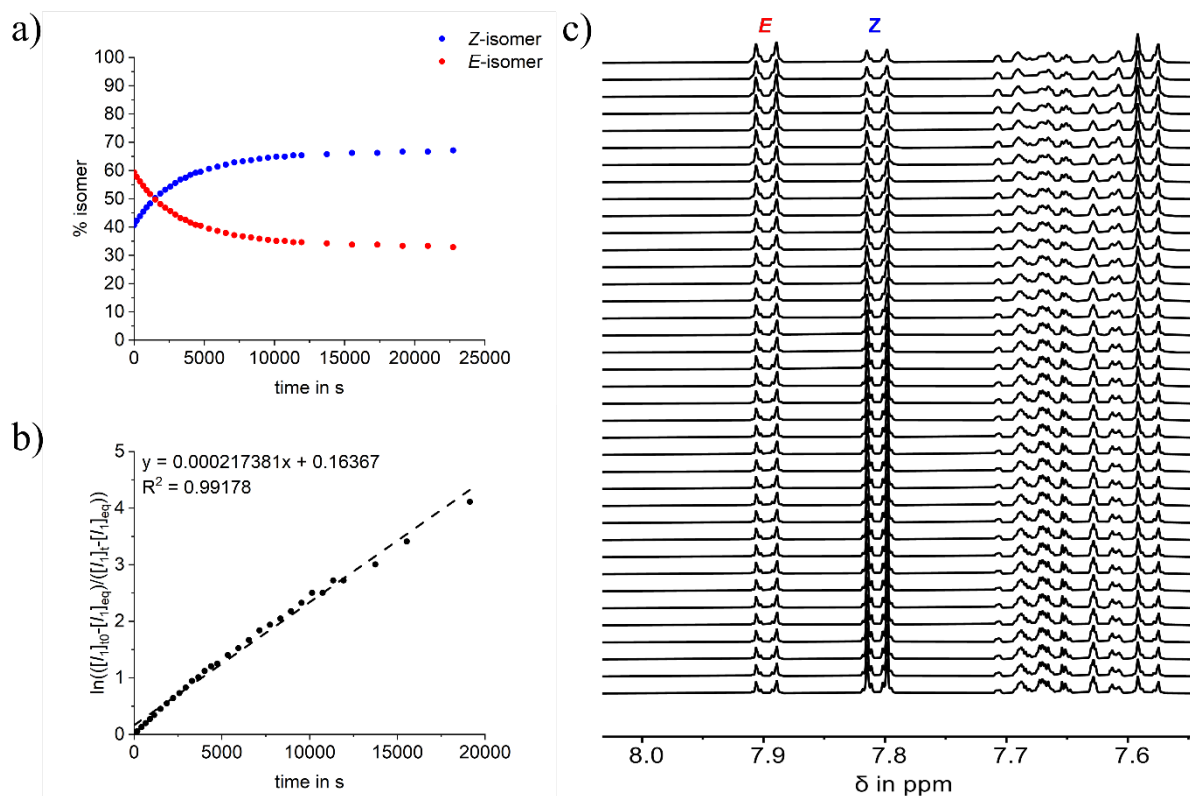


Figure S18: Thermal *E* to *Z* isomerization of diaryl-HTI **4** at 90 °C in DMSO-*d*₆ solution in the dark. The metastable *E*-isomer was enriched with 420 nm light irradiation before the measurement; a) temporal change of the isomeric composition while heating at 90 °C; b) first order kinetic analysis of the thermal double bond isomerization by plotting equation 9. The rate constant $k_{E/Z}$ is obtained from the slope of the linear fit; c) partial ¹H NMR spectra (500 MHz, DMSO-*d*₆, 90 °C) measured in defined time intervals while heating the NMR-sample at 90 °C.

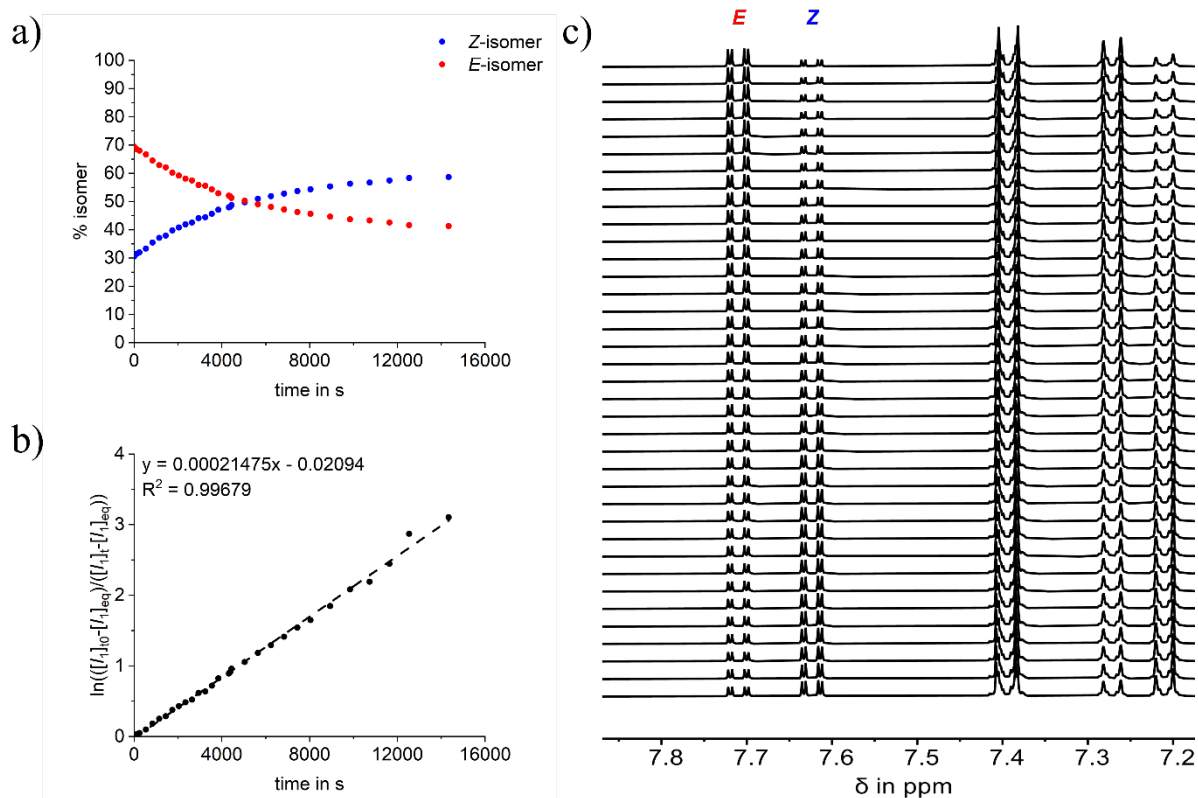


Figure S19: Thermal *E* to *Z* isomerization of diaryl-HTI 7 at 40 °C in toluene- d_8 solution in the dark. The metastable *E*-isomer was enriched with 470 nm light irradiation before the measurement; a) temporal change of the isomeric composition while heating at 40 °C; b) first order kinetic analysis of the thermal *E* to *Z* isomerization by plotting equation 9. The rate constant $k_{E/Z}$ is obtained from the slope of the linear fit; c) partial ^1H NMR spectra (400 MHz, toluene- d_8 , 40 °C) measured in defined time intervals while heating the NMR-sample at 40 °C.

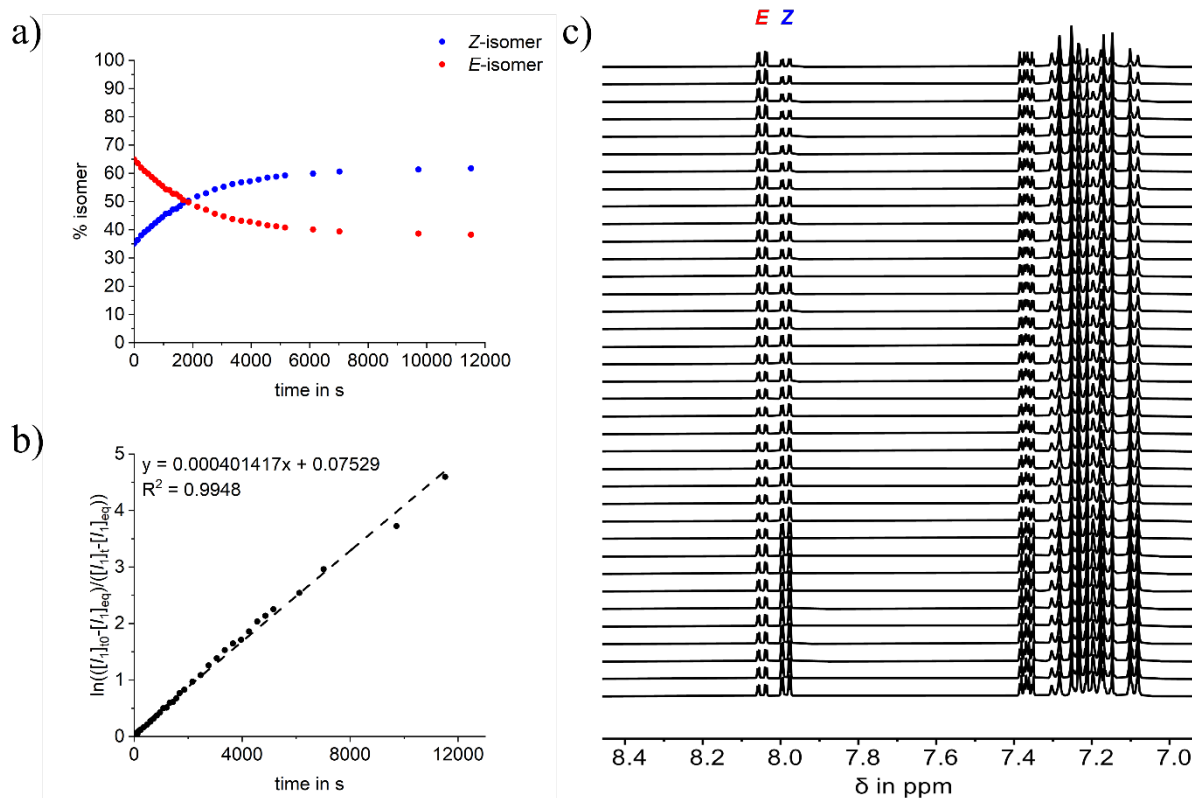


Figure S20: Thermal *E* to *Z* isomerization of diaryl-HTI 7 at 30 °C in DMSO- d_6 solution in the dark. The metastable *E*-isomer was enriched with 470 nm light irradiation before the measurement; a) temporal change of the isomeric composition while heating at 30 °C; b) first order kinetic analysis of the thermal *E* to *Z* isomerization by plotting equation 9. The rate constant $k_{E/Z}$ is obtained from the slope of the linear fit; c) partial ^1H NMR spectra (400 MHz, DMSO- d_6 , 30 °C) measured in defined time intervals while heating the NMR-sample at 30 °C.

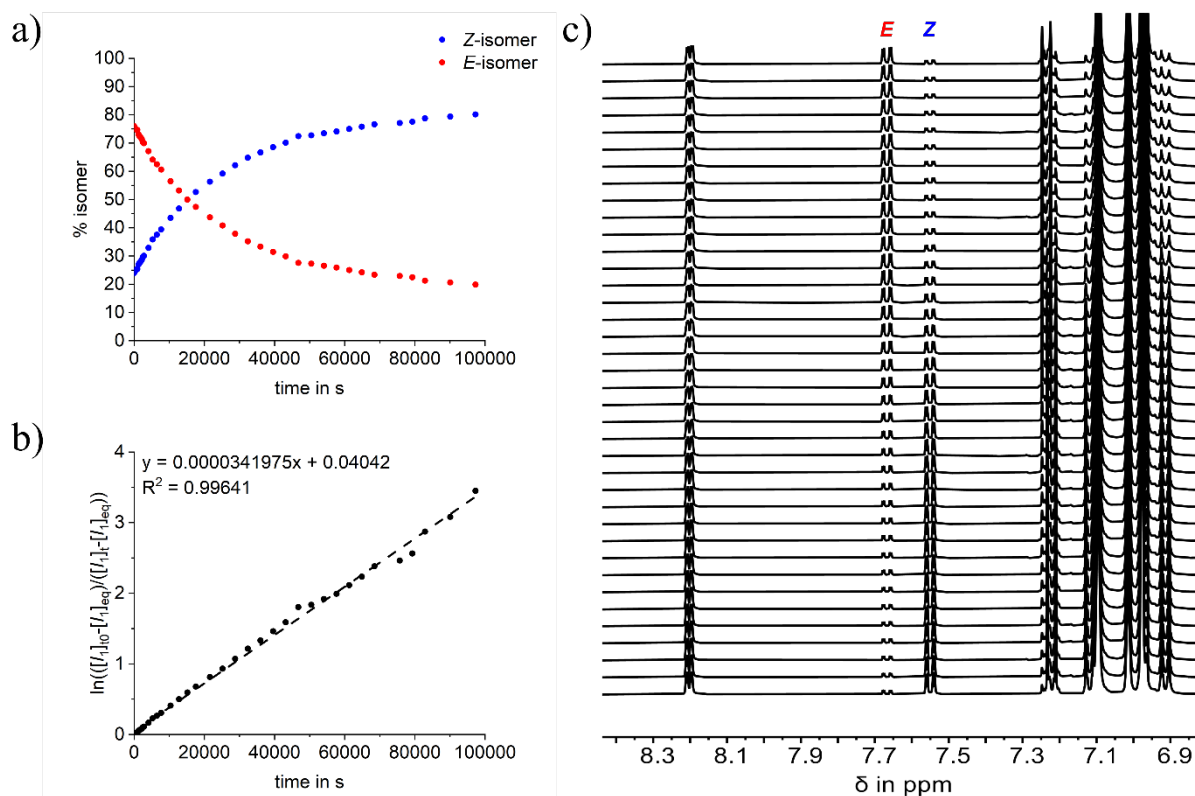


Figure S21: Thermal *E* to *Z* isomerization of diaryl-HTI **8** at 30 °C in toluene-*d*₈ solution in the dark. The metastable *E*-isomer was enriched with 450 nm light irradiation before the measurement; a) temporal change of the isomeric composition while heating at 30 °C. b) first order kinetic analysis of the thermal *E* to *Z* isomerization by plotting equation 9. The rate constant $k_{E/Z}$ is obtained from the slope of the linear fit. c) partial ¹H NMR spectra (400 MHz, toluene-*d*₈, 30 °C) measured in defined time intervals while heating the NMR-sample at 30 °C.

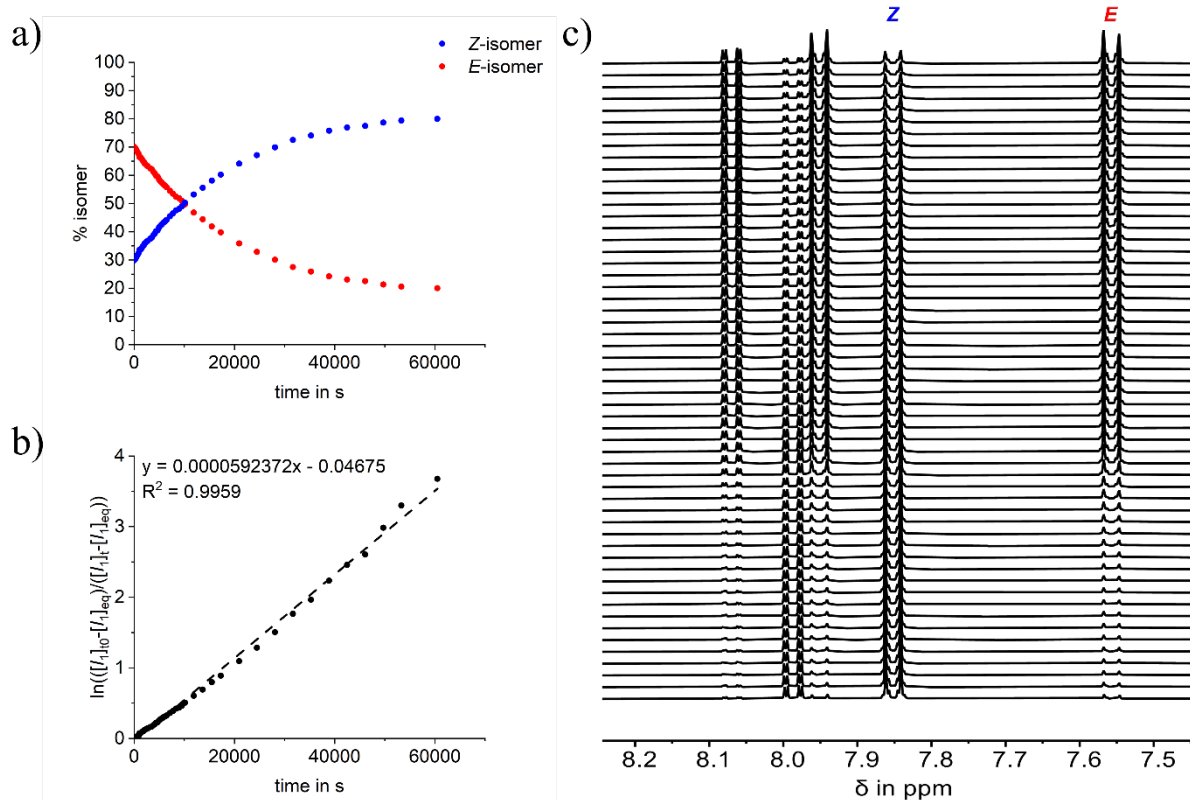


Figure S22: Thermal *E* to *Z* isomerization of diaryl-HTI **8** at 40 °C in DMSO-*d*₆ solution in the dark. The metastable *E*-isomer was enriched with 470 nm light irradiation before the measurement; a) temporal change of the isomeric composition while heating at 40 °C; b) first order kinetic analysis of the thermal *E* to *Z* isomerization by plotting equation 9. The rate constant $k_{E/Z}$ is obtained from the slope of the linear fit; c) partial ^1H NMR spectra (400 MHz, DMSO-*d*₆, 40 °C) measured in defined time intervals while heating the NMR-sample at 40 °C.

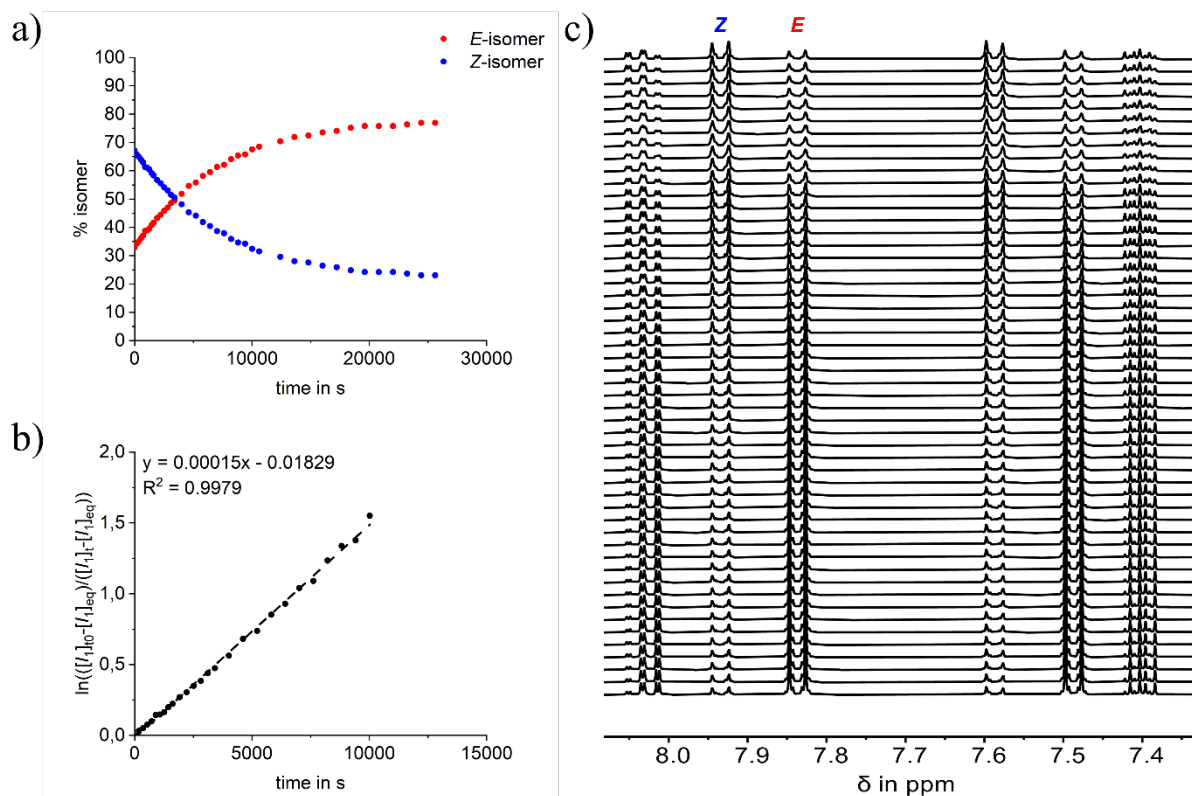


Figure S23: Thermal *Z* to *E* isomerization of diaryl-HTI **9** at 60 °C in DMSO-*d*₆ solution in the dark. The metastable *Z*-isomer was enriched with 435 nm light irradiation before the measurement; a) temporal change of the isomeric composition while heating at 60 °C; b) first order kinetic analysis of the thermal *Z* to *E* isomerization by plotting equation 9. The rate constant $k_{E/Z}$ is obtained from the slope of the linear fit; c) partial ¹H NMR spectra (500 MHz, DMSO-*d*₆, 60 °C) measured in defined time intervals while heating the NMR-sample at 60 °C.

Table S2: Gibbs energies of activation ΔG^\ddagger and corresponding half-lives (linearly extrapolated to 23 °C) for the thermal *E* to *Z* isomerization of diaryl-HTIs **2**, **3**, **4**, **7**, **8**, and **9** in toluene and/or DMSO solution.

Diaryl-HTI	Solvent	ΔG^\ddagger (thermal <i>E/Z</i> equil) kcal·mol ⁻¹	Equilibration half-life of pure <i>E</i> isomer at 23 °C	Slope of the linear fit (error)	Intercept of the linear fit (error)
8	toluene	24.054±0.006	16 h	3.4198·10 ⁻⁵ (± 3.42·10 ⁻⁷)	0.04042 (± 0.01456)
	DMSO	24.546±0.006	38 h	5.9237·10 ⁻⁵ (± 5.66·10 ⁻⁷)	-0.04675 (± 0.01172)
7	toluene	23.934±0.007	14 h	2.1475·10 ⁻⁴ (± 2.30·10 ⁻⁶)	-0.02094 (± 0.01445)
	DMSO	22.753±0.008	2 h	4.0142·10 ⁻⁴ (± 5.39·10 ⁻⁶)	0.07529 (± 0.02140)
3	toluene	23.181±0.004	4 h	5.2085·10 ⁻⁴ (± 3.46·10 ⁻⁶)	0.06590 (± 0.01248)
	DMSO	27.696±0.023	1 a	1.8015·10 ⁻⁴ (± 5.84·10 ⁻⁶)	0.01873 (± 0.04430)
2	toluene	25.704±0.006	12 d	4.7868·10 ⁻⁵ (± 4.39·10 ⁻⁷)	0.03893 (± 0.01470)
	DMSO	28.300±0.010	3 a	3.3844·10 ⁻⁴ (± 4.71·10 ⁻⁶)	-0.02211 (± 0.02603)
4	DMSO	27.773±0.012	1 a	2.1738·10 ⁻⁴ (± 3.67·10 ⁻⁶)	0.16367 (± 0.02842)
9	DMSO	25.577±0.008	16 d	1.5040·10 ⁻⁴ (± 1.38·10 ⁻⁶)	-0.01829 (± 0.00669)

Quantum Yield Determination

Quantum yield measurements were performed on the instrumental setup developed by the group of *E. Riedle*.^[6] A defined volume (2 mL) of toluene or benzene were filled in a cuvette and the illumination power P_{ill} was measured. Afterwards, diaryl-HTIs **2**, **3**, **4**, **7**, **8**, or **9** were added to the cuvette and the absorption was adjusted between 1.2 and 2.5 intensity. The solution was irradiated with 455 nm or 425 nm light in defined time intervals. After each irradiation cycle, the power readout of the solar cell detector was recorded and UV/Vis absorption spectra were measured. The change in concentration and therefore the number of isomerized molecules is calculated from the extinction coefficients.

The photochemical quantum yield Φ of a particular wavelength is calculated from the ratio between the number of isomerized molecules and the number of absorbed photons:

$$\Phi(\lambda) = \frac{N(\text{isomerized molecules})}{N(\text{absorbed photons})} \quad (\text{eq. 14})$$

The change in the number of isomerized molecules over a defined time interval is expressed by the following differential equations 15 and 16:

$$\begin{aligned} \frac{dN_Z(t)}{dt} = & -\Phi_{Z \rightarrow E} \int \frac{c_Z(t) \cdot \varepsilon_Z(\lambda)}{c_Z(t) \cdot \varepsilon_Z(\lambda) + c_E(t) \cdot \varepsilon_E(\lambda)} \cdot \frac{P_{\text{ill}} f(\lambda) \cdot \lambda}{h \cdot c} \cdot A(t, \lambda) d\lambda \quad (\text{eq. 15}) \\ & + \Phi_{E \rightarrow Z} \int \frac{c_E(t) \cdot \varepsilon_E(\lambda)}{c_Z(t) \cdot \varepsilon_Z(\lambda) + c_E(t) \cdot \varepsilon_E(\lambda)} \cdot \frac{P_{\text{ill}} f(\lambda) \cdot \lambda}{h \cdot c} \cdot A(t, \lambda) d\lambda \end{aligned}$$

$$\begin{aligned} \frac{dN_E(t)}{dt} = & -\Phi_{E \rightarrow Z} \int \frac{c_E(t) \cdot \varepsilon_E(\lambda)}{c_Z(t) \cdot \varepsilon_Z(\lambda) + c_E(t) \cdot \varepsilon_E(\lambda)} \cdot \frac{P_{\text{ill}} f(\lambda) \cdot \lambda}{h \cdot c} \cdot A(t, \lambda) d\lambda \quad (\text{eq. 16}) \\ & + \Phi_{Z \rightarrow E} \int \frac{c_Z(t) \cdot \varepsilon_Z(\lambda)}{c_Z(t) \cdot \varepsilon_Z(\lambda) + c_E(t) \cdot \varepsilon_E(\lambda)} \cdot \frac{P_{\text{ill}} f(\lambda) \cdot \lambda}{h \cdot c} \cdot A(t, \lambda) d\lambda \end{aligned}$$

with the number of molecules in *Z* configuration N_Z , the number of molecules in *E* configuration N_E , the concentration of the *Z*-isomer at time t $c_Z(t)$, the concentration of *E*-isomer at time t $c_E(t)$, the extinction coefficients at wavelength λ of the *Z*- and *E*-isomer $\varepsilon_Z(\lambda)$ and $\varepsilon_E(\lambda)$, respectively, the illumination power P_{ill} , the spectral distribution of the LED light $f(\lambda)$, the Planck's constant h ($6.62607 \cdot 10^{-34}$ J·s), the speed of light c ($2.99792 \cdot 10^8$ m·s⁻¹), and the absorbance at time t and wavelength λ $A(t, \lambda)$.

Furthermore, the absorbance depends on the thickness of the cuvette d , the concentration c of the Z - and E -isomer and the respective extinction coefficient ε :

$$A(t, \lambda) = 1 - 10^{-d(c_Z(t) \cdot \varepsilon_Z(\lambda) + c_E(t) \cdot \varepsilon_E(\lambda))} \quad (\text{eq. 16})$$

The forward and backward quantum yields $\Phi_{Z \rightarrow E}$ and $\Phi_{E \rightarrow Z}$ are both included in the calculation after modelling of the conversion. Therefore, only one measurement is required to extract the quantum yields for both photoisomerizations Z to E and vice versa.

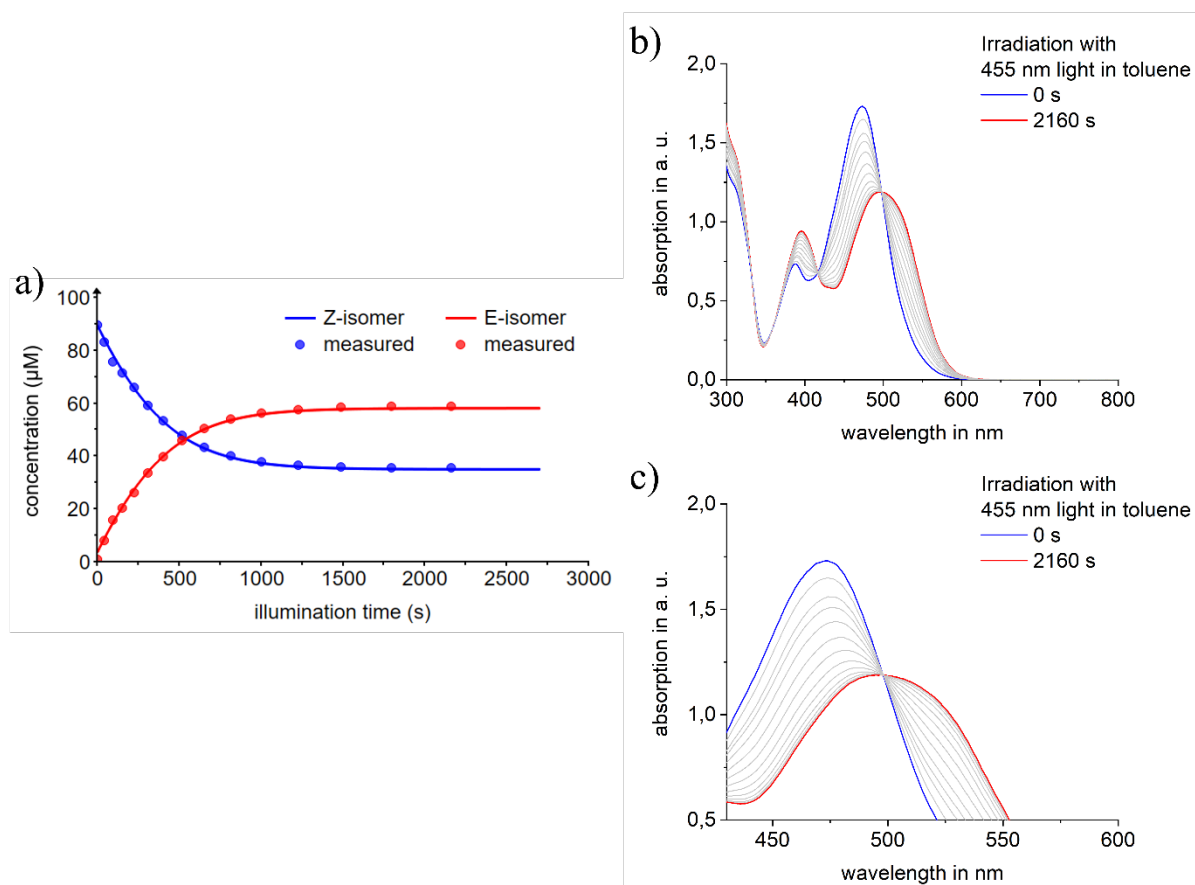


Figure S24: Quantum yield determination for the *Z* to *E* and *E* to *Z* photoisomerization of diaryl-HTI **2** in toluene solution during irradiation with 455 nm light; a) concentration change of *Z* and *E* isomer during the irradiation with 455 nm light; b) UV/Vis absorption spectra measured in defined time intervals during irradiation with 455 nm light; c) section of the UV/Vis absorption spectra depicting the isosbestic point at longer wavelengths.

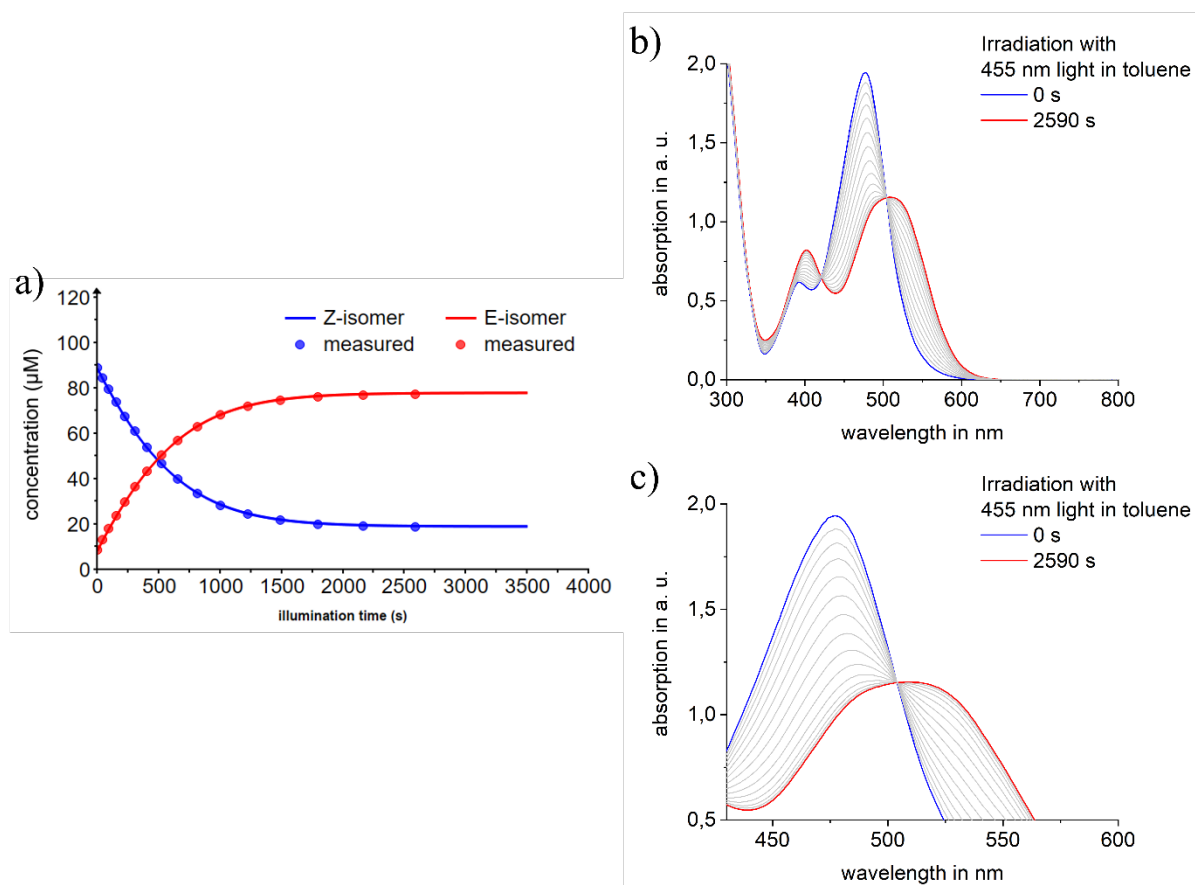


Figure S25: Quantum yield determination for the *Z* to *E* and *E* to *Z* photoisomerization of diaryl-HTI **3** in toluene solution during irradiation with 455 nm light; a) concentration change of *Z* and *E* isomer during the irradiation with 455 nm light; b) UV/Vis absorption spectra measured in defined time intervals during irradiation with 455 nm light; c) section of the UV/Vis absorption spectra depicting the isosbestic point at longer wavelengths.

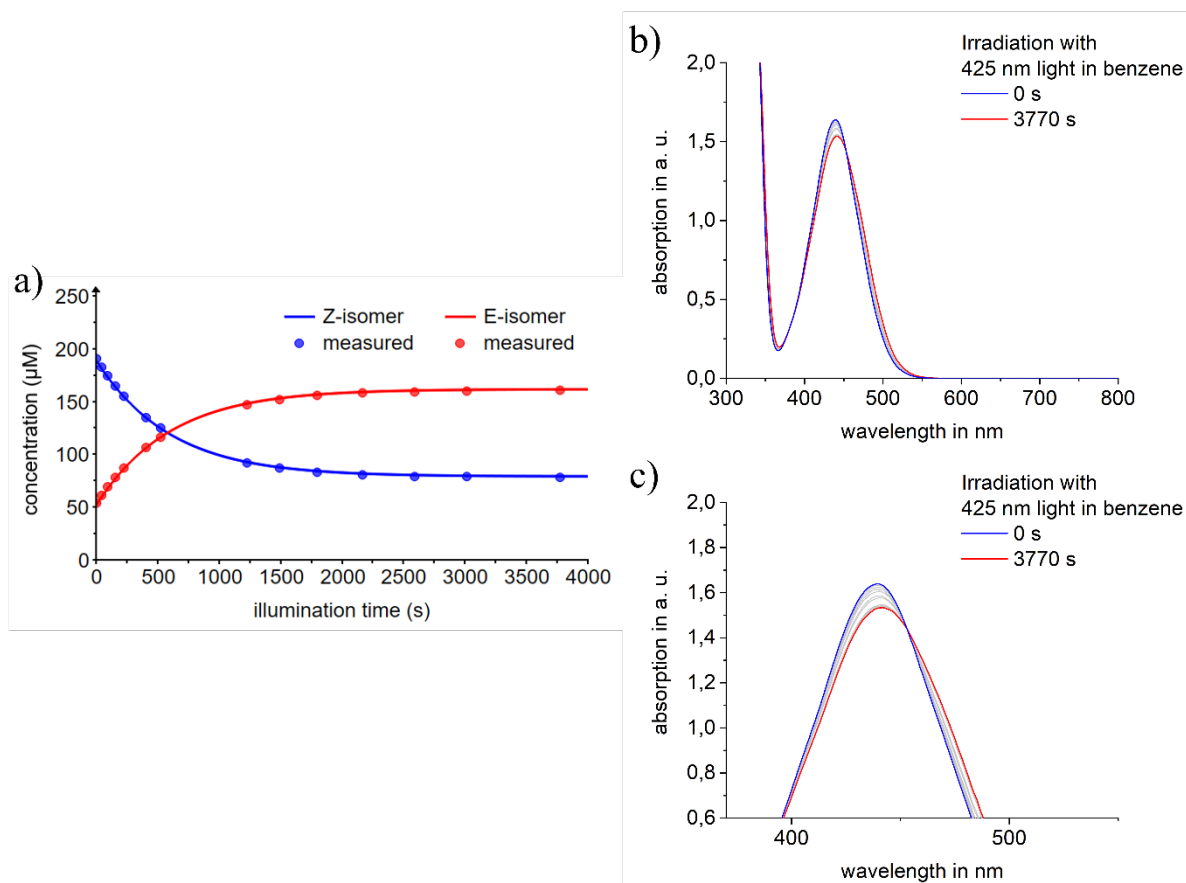


Figure S26: Quantum yield determination for the *Z* to *E* and *E* to *Z* photoisomerization of diaryl-HTI 4 in benzene solution during irradiation with 425 nm light; a) concentration change of *Z* and *E* isomer during the irradiation with 425 nm light; b) UV/Vis absorption spectra measured in defined time intervals during irradiation with 425 nm light; c) section of the UV/Vis absorption spectra depicting the isosbestic point at longer wavelengths.

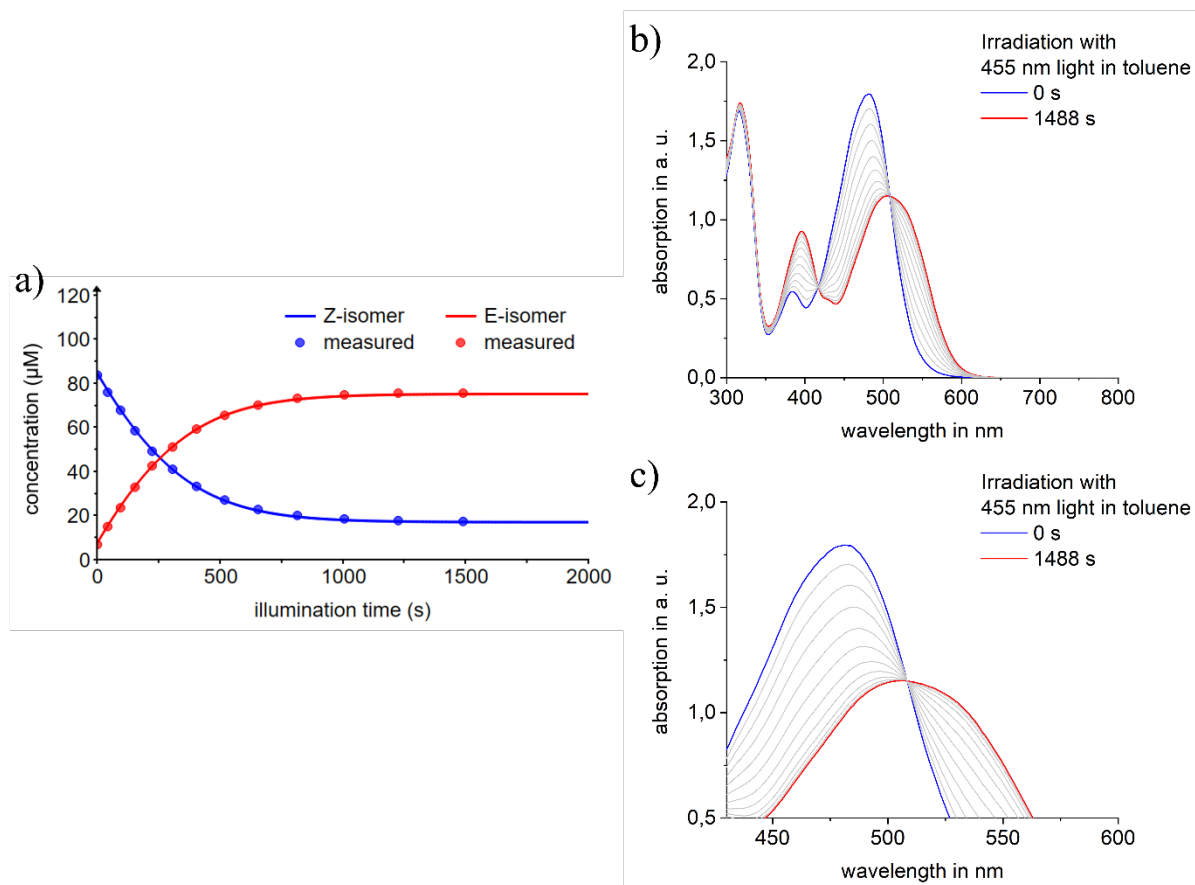


Figure S27: Quantum yield determination for the *Z* to *E* and *E* to *Z* photoisomerization of diaryl-HTI 7 in toluene solution during irradiation with 455 nm light; a) concentration change of *Z* and *E* isomer during the irradiation with 455 nm light; b) UV/Vis absorption spectra measured in defined time intervals during irradiation with 455 nm light; c) section of the UV/Vis absorption spectra depicting the isosbestic point at longer wavelengths.

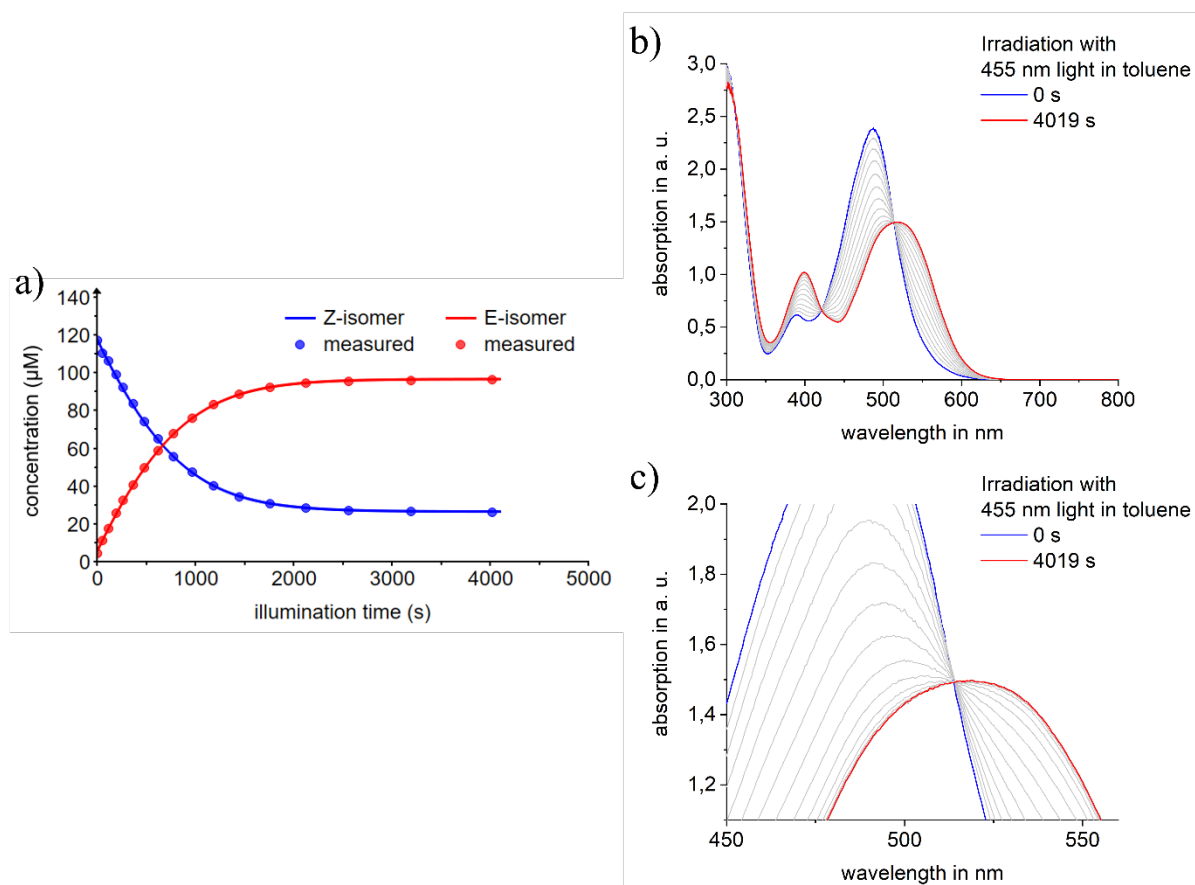


Figure S28: Quantum yield determination for the *Z* to *E* and *E* to *Z* photoisomerization of diaryl-HTI **8** in toluene solution during irradiation with 455 nm light; a) concentration change of *Z* and *E* isomer during the irradiation with 455 nm light; b) UV/Vis absorption spectra measured in defined time intervals during irradiation with 455 nm light; c) section of the UV/Vis absorption spectra depicting the isosbestic point at longer wavelengths.

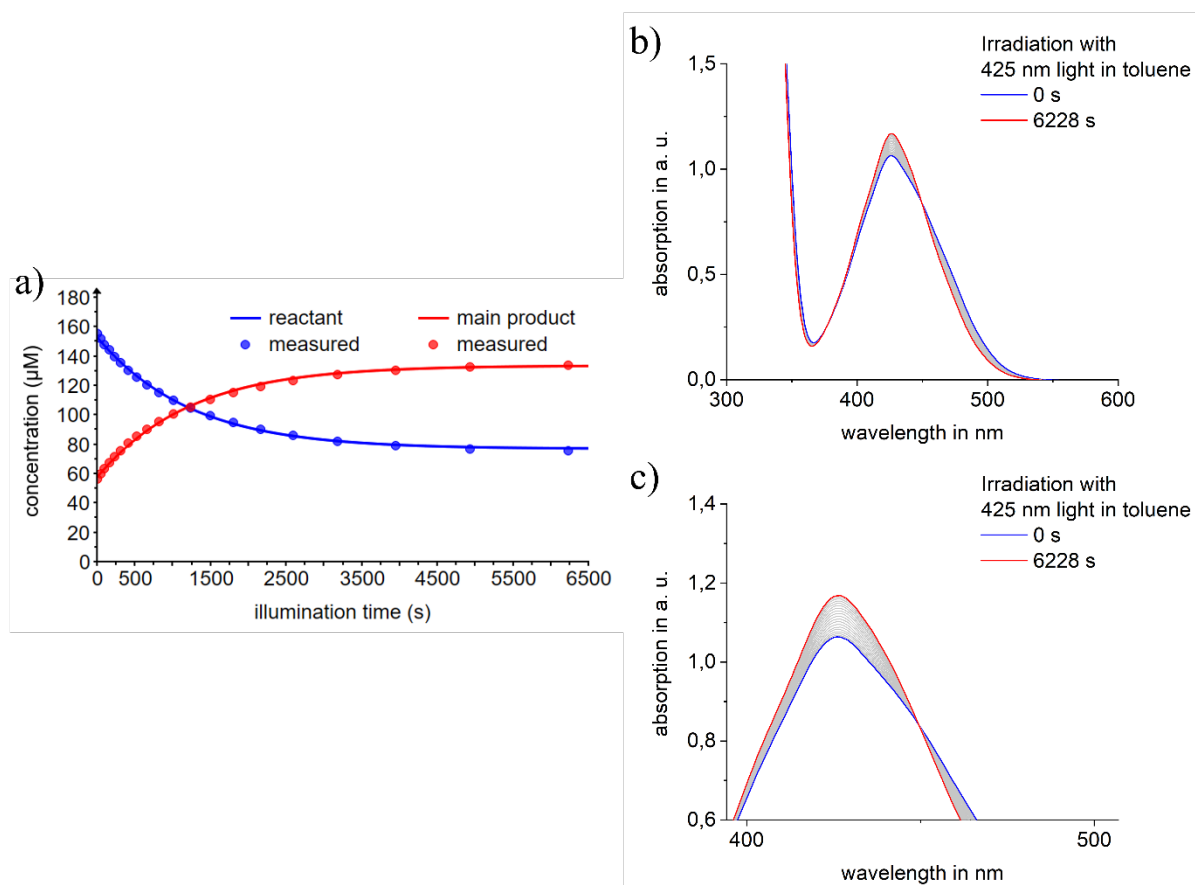


Figure S29: Quantum yield determination for the *Z* to *E* and *E* to *Z* photoisomerization of diaryl-HTI 9 in toluene solution during irradiation with 425 nm light; a) concentration change of *Z* and *E* isomer during the irradiation with 425 nm light; b) UV/Vis absorption spectra measured in defined time intervals during irradiation with 425 nm light; c) section of the UV/Vis absorption spectra depicting the isosbestic point at longer wavelengths.

Table S3: Measured quantum yields for the *Z* to *E* and *E* to *Z* photoisomerizations of diaryl-HTIs **2**, **3**, **4**, **7**, **8**, and **9** in toluene solution.

Diaryl-HTI	Solvent	Wavelength	$\Phi_{Z \text{ to } E}$	$\Phi_{E \text{ to } Z}$
9	toluene	425 nm	5%	
		425 nm		3%
8	toluene	455 nm	4%	
		455 nm		4%
7	toluene	455 nm	6%	
		455 nm		5%
4	benzene	425 nm	11%	
		425 nm		6%
3	toluene	455 nm	3%	
		455 nm		3%
2	toluene	455 nm	3%	
		455 nm		11%

Molecular Logic Application of Diaryl-HTIs **3** and **8** in Logic Gates and Keypad Locks

The behavior of diaryl-HTIs **3** and **8** under acidic conditions was investigated by UV/Vis absorption spectroscopy in toluene solution. Therefore, stock solutions of **3** and **8** with defined concentrations ($2.99 \cdot 10^{-5}$ mol/L and $3.03 \cdot 10^{-5}$ mol/L) were prepared and 2.0 mL were filled into a cuvette. A solution of trifluoroacetic acid (TFA) in toluene was added (0-2,000 equiv.) stepwise to the cuvette and UV/Vis absorption spectra were recorded until no changes were observed.

Diaryl-HTI **8** bears two protonation sites on the pyridine-nitrogen and the dimethylamine moiety. After protonation, two new absorption maxima at 420 nm and 549 nm evolved associated with protonation on both the amine and the pyridine. Due to the lack of separate addressability of only one protonation side at the one time further studies regarding the use of diaryl-HTI **8** in logic gates were not carried out.

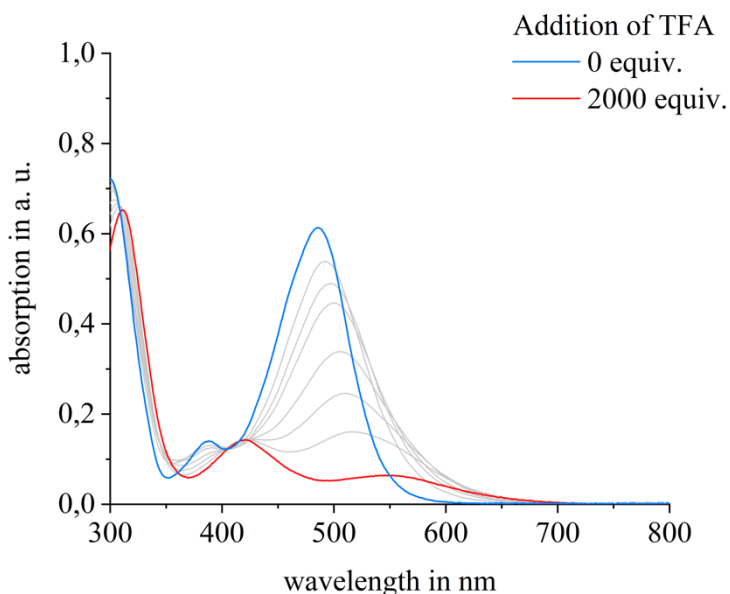


Figure S30: UV/Vis absorption spectra of diaryl-HTI **8** in toluene solution recorded after stepwise addition of TFA (0-2,000 equiv. grey to red spectra).

In diaryl-HTI **3** only the dimethylamine moiety is predestined for protonation with TFA. The absorption changes during stepwise protonation with TFA were investigated by UV/Vis absorption spectroscopy in toluene solution. Deprotonation of protonated diaryl-HTI **3** was

carried out by the addition of 2,000 equiv. triethylamine (TEA) to recover unprotonated diaryl-HTI **3**. After one protonation and deprotonation cycle, irradiation with 470 nm and 617 nm light induced enrichment of the *E*- and *Z*-isomer, respectively. Thus, the photoswitching properties were recovered after acid and base induced changes and the application of diaryl-HTI **3** in logic gates could be further investigated.

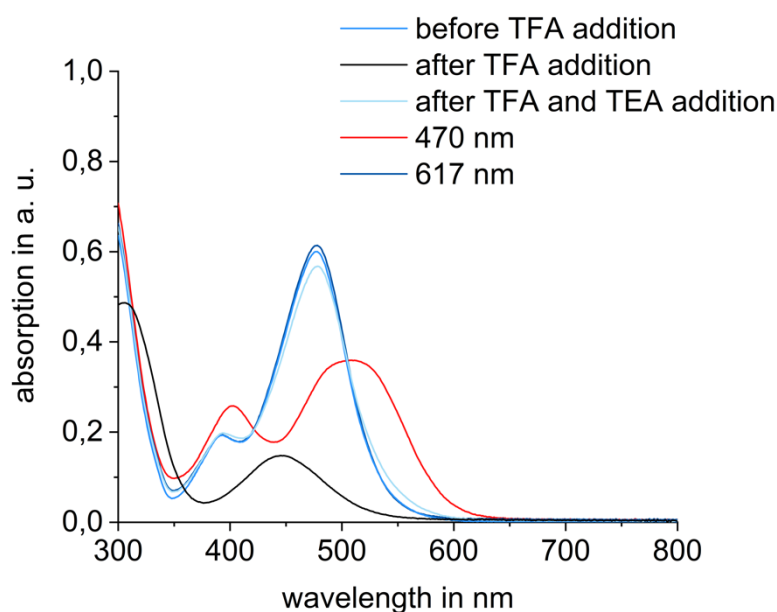


Figure S31: UV/Vis absorption spectra of diaryl-HTI **3** in toluene solution before addition of TFA, after addition of TFA, after addition of TFA and TEA, and after irradiation with 470 nm and 617 nm light following the protonation and deprotonation cycle.

With the presence of a protonation site at the dimethylamine moiety and the photoisomerizable double-bond as independently triggerable units in diaryl-HTI **3**, a system composed of three states (*E*-**3**, *Z*-**3**, and *Z*-**3H**⁺) can be setup. By using four different orthogonal inputs (470 nm light, 617 nm light, TFA and TEA) the three states are reversibly interconverted. For protonation and deprotonation 2,000 equiv. of TFA and TEA are used. The difference in the absorption spectra of *E*-**3**, *Z*-**3**, and *Z*-**3H**⁺ allows the definition of four threshold limits at different output readouts (Absorption (A)>0.05 at 580 nm, A>0.2 at 500 nm, A>0.5 at 480 nm, and A>0.27 at 328 nm). Therefore, a variety of different molecular logic operations can be elicited with diaryl-HTI **3** as outlined below.

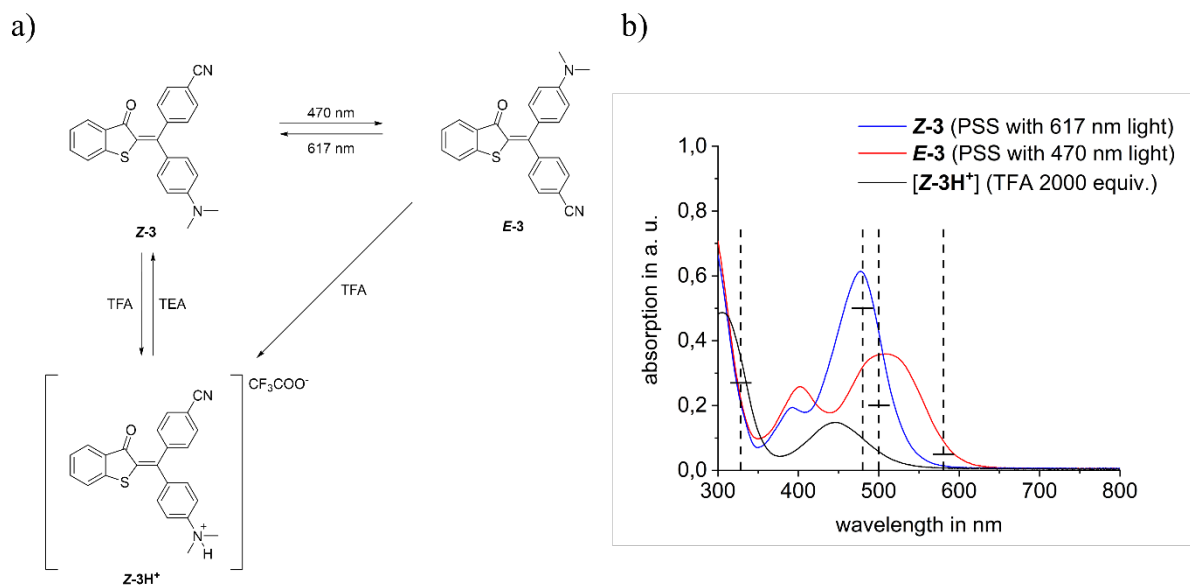


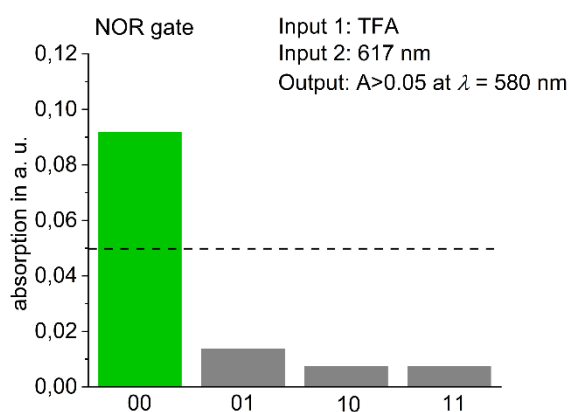
Figure S32: Overview of a three-state molecular logic system composed of *E-3*, *Z-3*, and *Z-3H⁺*; a) schematic representation for the interconversion of *E-3*, *Z-3*, and *Z-3H⁺* with 470 nm light, 617 nm light, TFA and TEA as orthogonal inputs; b) UV/Vis absorption spectra of *E-3*, *Z-3*, and *Z-3H⁺* in toluene solution with the output readouts (vertical dashed lines) and the threshold levels (horizontal lines).

Five different 2-bit logic gates are generated starting from *E-3* and *Z-3H⁺*. A NOR, NOT, SAND and Identity gate are setup with *E-3* as initial state and TFA and 617 nm light as orthogonal inputs. As reset the two triggers TEA and 470 nm light have to be given. Furthermore, a AND, SAND, Identity and NOT gate can be constructed from *Z-3H⁺* as starting state with TEA and 470 nm light serving as inputs. As reset the two triggers TFA and 617 nm light have to be given in this case.

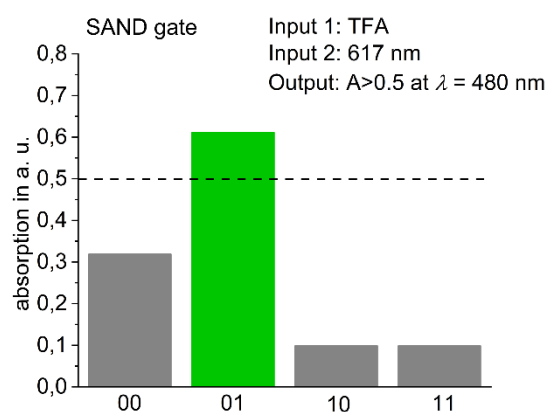
a)

Input 1 TFA 2000 equiv.	Input 2 617 nm light	Out 1: NOR A>0.05 at 580 nm	Out 2: SAND A>0.4 at 480 nm	Out 3: NOT A>0.2 at 500 nm	Out 4: Identity A>0.27 at 328 nm
0	0	1	0	1	0
0	1	0	1	1	0
1	0	0	0	0	1
1	1	0	0	0	1

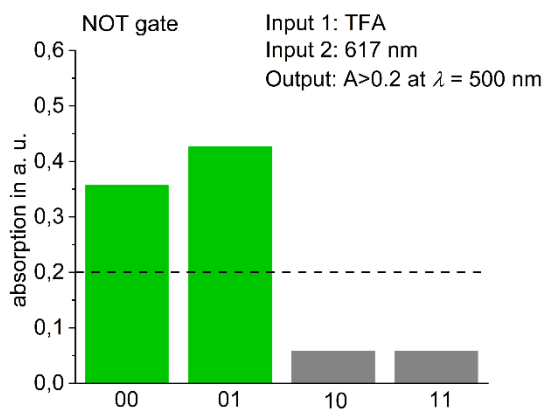
b)



c)



d)



e)

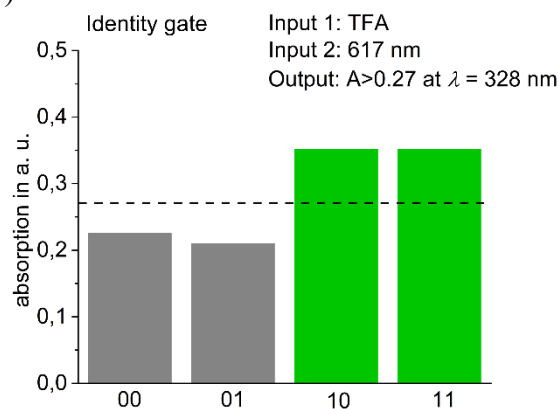
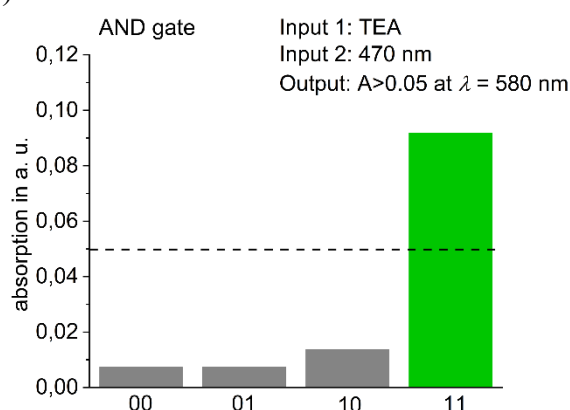


Figure S33: Overview for 2-bit molecular logic systems starting from *E-3* and using TFA (2,000 equiv.) and 617 nm light as inputs; a) truth table for the NOR-, SAND-, NOT-, and Identity gates; b) absorptions at output readout 580 nm (threshold level shown as horizontal dashed line) representing a NOR-gate (truth output colored in green and false output colored in grey); c) absorptions at output readout 480 nm (threshold level shown as horizontal dashed line) representing a SAND-gate (truth output colored in green and false output colored in grey); d) absorptions at output readout 500 nm (threshold level shown as horizontal dashed line) representing a NOT-gate (truth output colored in green and false output colored in grey); e) absorptions at output readout 328 nm (threshold level shown as horizontal dashed line) representing an Identity gate (truth output colored in green and false output colored in grey).

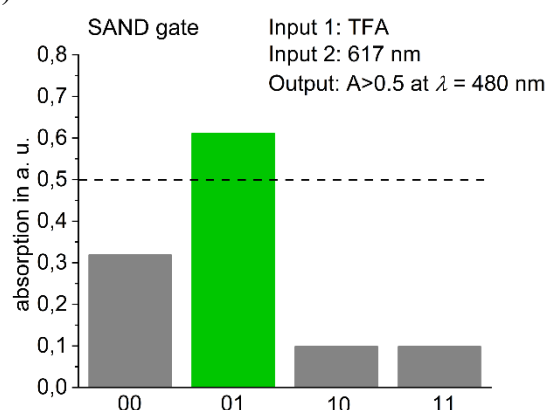
a)

Input 1 TEA 2000 equiv.	Input 2 470 nm light	Out 1: AND A>0.05 at 580 nm	Out 2: SAND A>0.4 at 480 nm	Out 3: Identity A>0.2 at 500 nm	Out 4: NOT A>0.27 at 328 nm
0	0	0	0	0	1
0	1	0	0	0	1
1	0	0	1	1	0
1	1	1	0	1	0

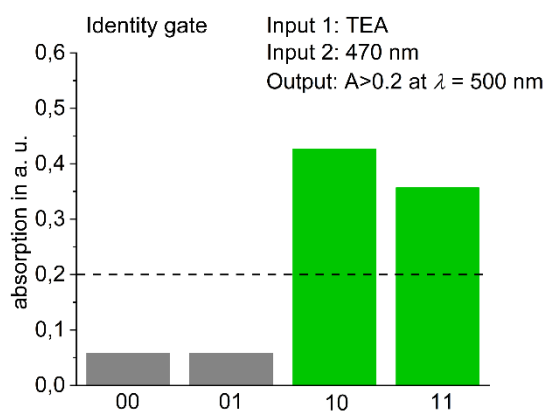
b)



c)



d)



e)

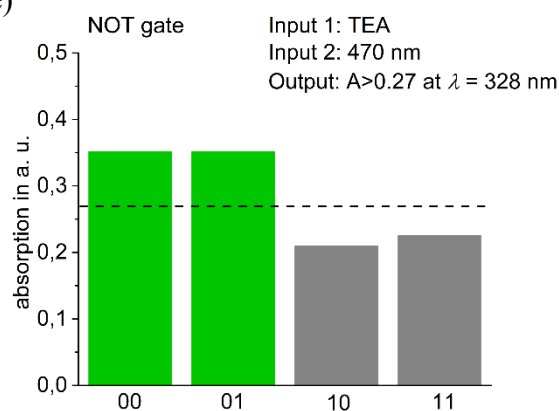


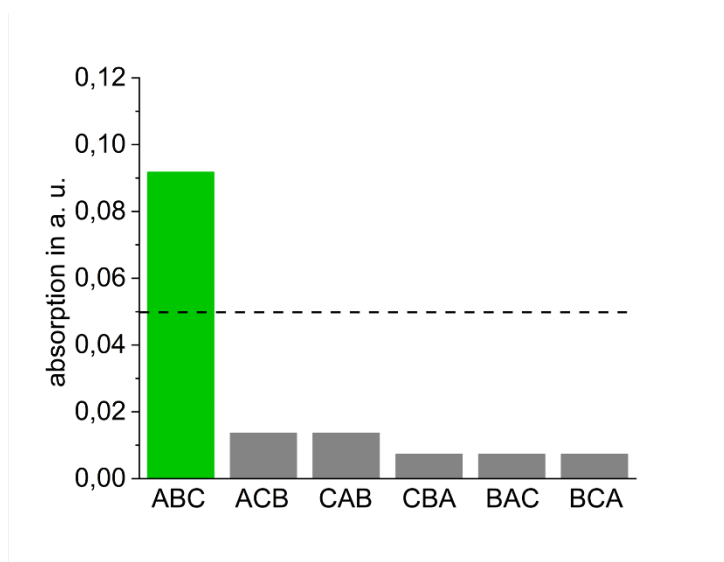
Figure S34: Overview for 2-bit molecular logic systems starting from **Z-3H⁺** and using TEA (2,000 equiv.) and 470 nm light as inputs; a) truth table for the AND, SAND, Identity, and NOT gates; b) absorptions at output readout 580 nm (threshold level shown as horizontal dashed line) representing an AND gate (truth output colored in green and false output colored in grey); c) absorptions at output readout 480 nm (threshold level shown as horizontal dashed line) representing a SAND gate (truth output colored in green and false output colored in grey); d) absorptions at output readout 500 nm (threshold level shown as horizontal dashed line) representing an Identity gate (truth output colored in green and false output colored in grey); e) absorptions at output readout 328 nm (threshold level shown as horizontal dashed line) representing a NOT gate (truth output colored in green and false output colored in grey).

A molecular binary multiplier can be setup with two inputs (TEA and 470 nm light) and the output readout at 580 nm ($A > 0.05$). Herein, the binary numbers of the two inputs are multiplied to give the binary combination of the corresponding binary products. The binary products are finally translated to the decimal values.

Table S4: Truth table for a binary multiplier with TEA and 470 nm light as inputs and the output readout at 580 nm.

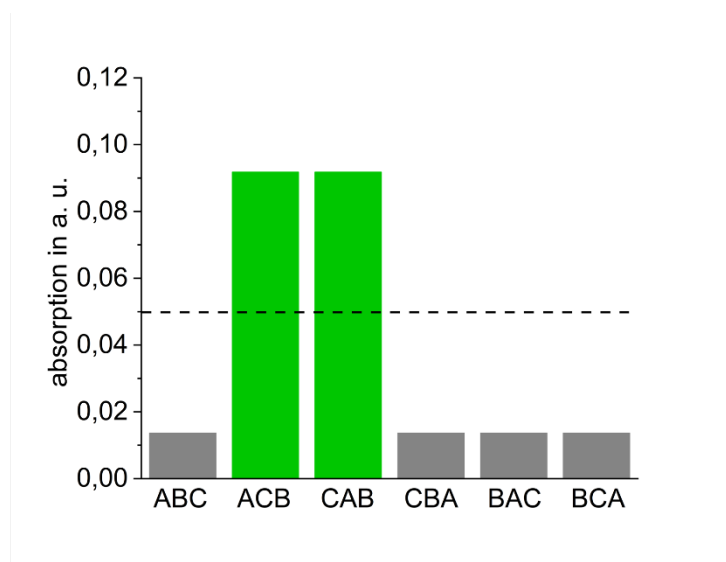
Input 1 TEA 2000 equiv.	Input 2 470 nm light	Out 1: A>0.05 at 580 nm	Binary Product	Decimal Value
0	0	0	00	0
0	1	0	00	0
1	0	0	00	0
1	1	1	01	1

The irradiation (470 nm and 617 nm light) and protonation/deprotonation (TFA and TEA) inputs are further utilized to realize 3-input and 4-input molecular keypad locks starting from the **Z-3H⁺** state. For this purpose, TFA (2,000 equiv.), TEA (2,000 equiv.) and 470 nm light are used to generate a 3-input molecular keypad lock with one true input combination (one out of six) and a 3-input molecular keypad lock with two true input combinations (two out of six) using TEA, 470 nm and 617 nm light. At last, all four inputs are integrated into a 4-input molecular keypad lock with three true input combinations (three out of 24).



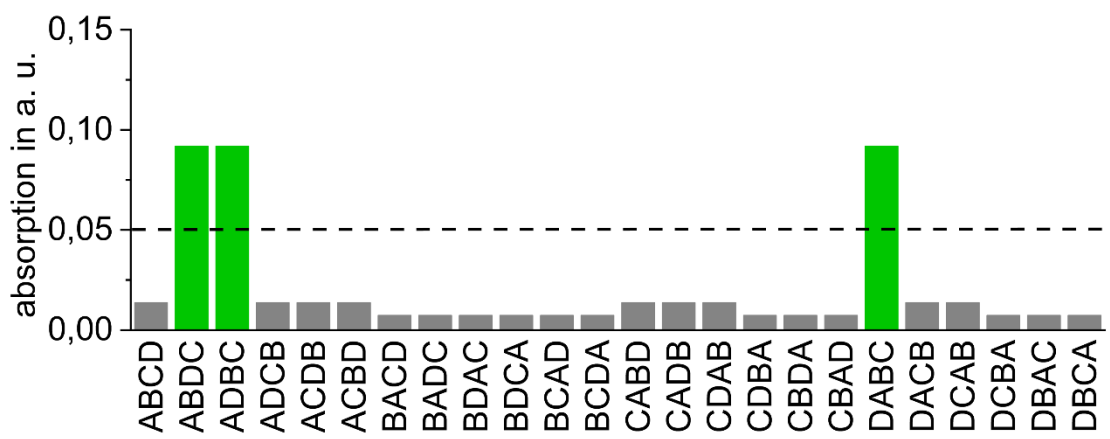
Sequence	State after input 1	State after input 1 and 2	State after input 1, 2, and 3	Output A>0.05 at 580 nm
ABC	Z-3H ⁺	Z-3	E-3	1
ACB	Z-3H ⁺	Z-3H ⁺	Z-3	0
CAB	Z-3H ⁺	Z-3H ⁺	Z-3	0
CBA	Z-3H ⁺	Z-3	Z-3H ⁺	0
BAC	Z-3	Z-3H ⁺	Z-3H ⁺	0
BCA	Z-3	E-3	Z-3H ⁺	0

Figure S35: Output readouts at 580 nm and the threshold limit at A>0.05 (dashed line) for a molecular keypad lock with three inputs, A (addition of TFA (2,000 equiv.)), B (addition of TEA (2,000 equiv.)), and C (irradiation with 470 nm light), beginning from **Z-3H⁺**. True and false readouts are colored in green and grey, respectively. The input sequences and states after each input are summarized in the table.



Sequence	State after input 1	State after input 1 and 2	State after input 1, 2, and 3	Output A>0.05 at 580 nm
ABC	Z-3	E-3	Z-3	0
ACB	Z-3	Z-3	E-3	1
CAB	Z-3H ⁺	Z-3	E-3	1
CBA	Z-3H ⁺	Z-3H ⁺	Z-3	0
BAC	Z-3H ⁺	Z-3	Z-3	0
BCA	Z-3H ⁺	Z-3H ⁺	Z-3	0

Figure S36: Output readouts at 580 nm and the threshold limit at A>0.05 (dashed line) for a molecular keypad lock with three inputs, A (addition of TEA (2,000 equiv.)), B (irradiation with 470 nm light), and C (irradiation with 617 nm light), beginning from **Z-3H⁺**. True and false readouts are colored in green and grey, respectively. The input sequences and states after each input are summarized in the table.



Sequence	State after input 1	State after input 1 and 2	State after input 1, 2, and 3	State after input 1, 2, 3, and 4	Output A>0.05 at 580 nm
ABCD	Z-3H ⁺	Z-3	E-3	Z-3	0
ABDC	Z-3H ⁺	Z-3	Z-3	E-3	1
ADBC	Z-3H ⁺	Z-3H ⁺	Z-3	E-3	1
ADCB	Z-3H ⁺	Z-3H ⁺	Z-3H ⁺	Z-3	0
ACDB	Z-3H ⁺	Z-3H ⁺	Z-3H ⁺	Z-3	0
ACBD	Z-3H ⁺	Z-3H ⁺	Z-3	Z-3	0
BACD	Z-3	Z-3H ⁺	Z-3H ⁺	Z-3H ⁺	0
BADC	Z-3	Z-3H ⁺	Z-3H ⁺	Z-3H ⁺	0
BDAC	Z-3	Z-3	Z-3H ⁺	Z-3H ⁺	0
BDCA	Z-3	Z-3	E-3	Z-3H ⁺	0
BCAD	Z-3	E-3	Z-3H ⁺	Z-3H ⁺	0
BCDA	Z-3	E-3	Z-3	Z-3H ⁺	0
CABD	Z-3H ⁺	Z-3H ⁺	Z-3	Z-3	0
CADB	Z-3H ⁺	Z-3H ⁺	Z-3H ⁺	Z-3	0
CDAB	Z-3H ⁺	Z-3H ⁺	Z-3H ⁺	Z-3	0
CDBA	Z-3H ⁺	Z-3H ⁺	Z-3	Z-3H ⁺	0
CBDA	Z-3H ⁺	Z-3	Z-3	Z-3H ⁺	0
CBAD	Z-3H ⁺	Z-3	Z-3H ⁺	Z-3H ⁺	0
DABC	Z-3H ⁺	Z-3H ⁺	Z-3	E-3	1
DACB	Z-3H ⁺	Z-3H ⁺	Z-3H ⁺	Z-3	0
DCAB	Z-3H ⁺	Z-3H ⁺	Z-3H ⁺	Z-3	0
DCBA	Z-3H ⁺	Z-3H ⁺	Z-3	Z-3H ⁺	0
DBAC	Z-3H ⁺	Z-3	Z-3H ⁺	Z-3H ⁺	0
DBCA	Z-3H ⁺	Z-3	E-3	Z-3H ⁺	0

Figure S37: Output readouts at 580 nm and threshold limit at $A > 0.05$ (dashed line) for a molecular keypad lock with four inputs, A (addition of TFA (2,000 equiv.)), B (addition of TEA (2,000 equiv.)), C (irradiation with 470 nm light), and D (irradiation with 617 nm light), beginning from **Z-3H⁺**. True and false readouts are colored in green and grey, respectively. The input sequences and states after each input sequence are summarized in the table.

Theoretical Description of Diaryl-HTI **3** and Diaryl-HTI **8**

The structures for the *Z*- and *E*-isomer of diaryl-HTI **3** and **8** in toluene were optimized on the B3LYP level of theory using the IEFPCM solvent model. The basis set 6-311+G(d,p) with ultrafine integration grid and tight optimization thresholds was employed. The minima were confirmed by frequency analysis of the obtained structures. Molecular Orbitals (MOs) were visualized from the fchk file.

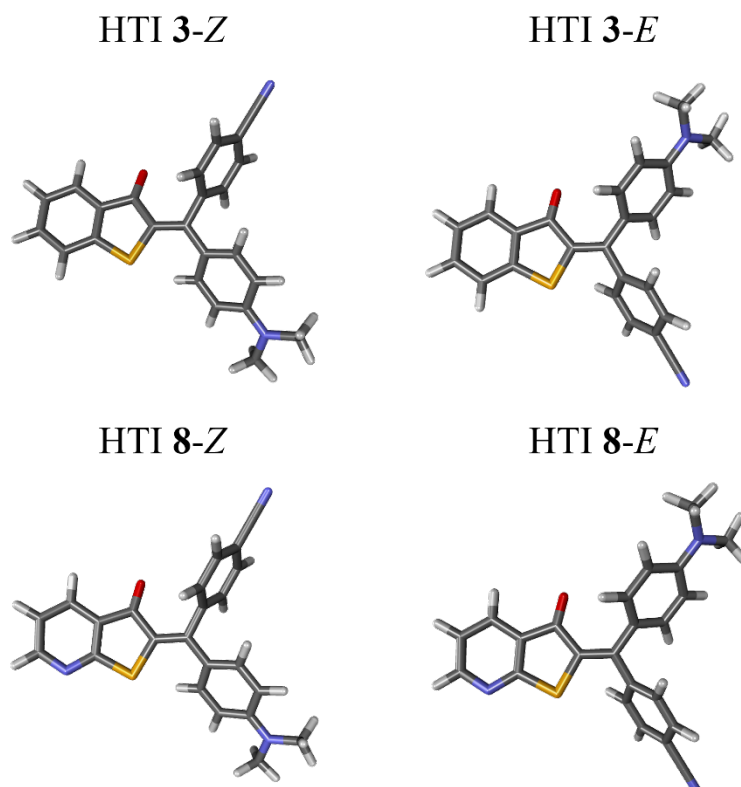


Figure S38: Theoretically obtained optimized molecular structures for the *Z*- and *E*-isomers of diaryl-HTIs **3** and **8** in toluene calculated on the B3LYP/6-311G(d,p) level of theory using the IEFPCM solvent model. Calculated ΔG differences between the *E* and *Z* isomers, i.e. $\Delta G_{E-Z}(\mathbf{3}) = 1.1$ kcal/mol and $\Delta G_{E-Z}(\mathbf{8}) = 1.4$ kcal/mol, are in good agreement with the experimental values obtained at 40 °C and 30 °C, respectively.

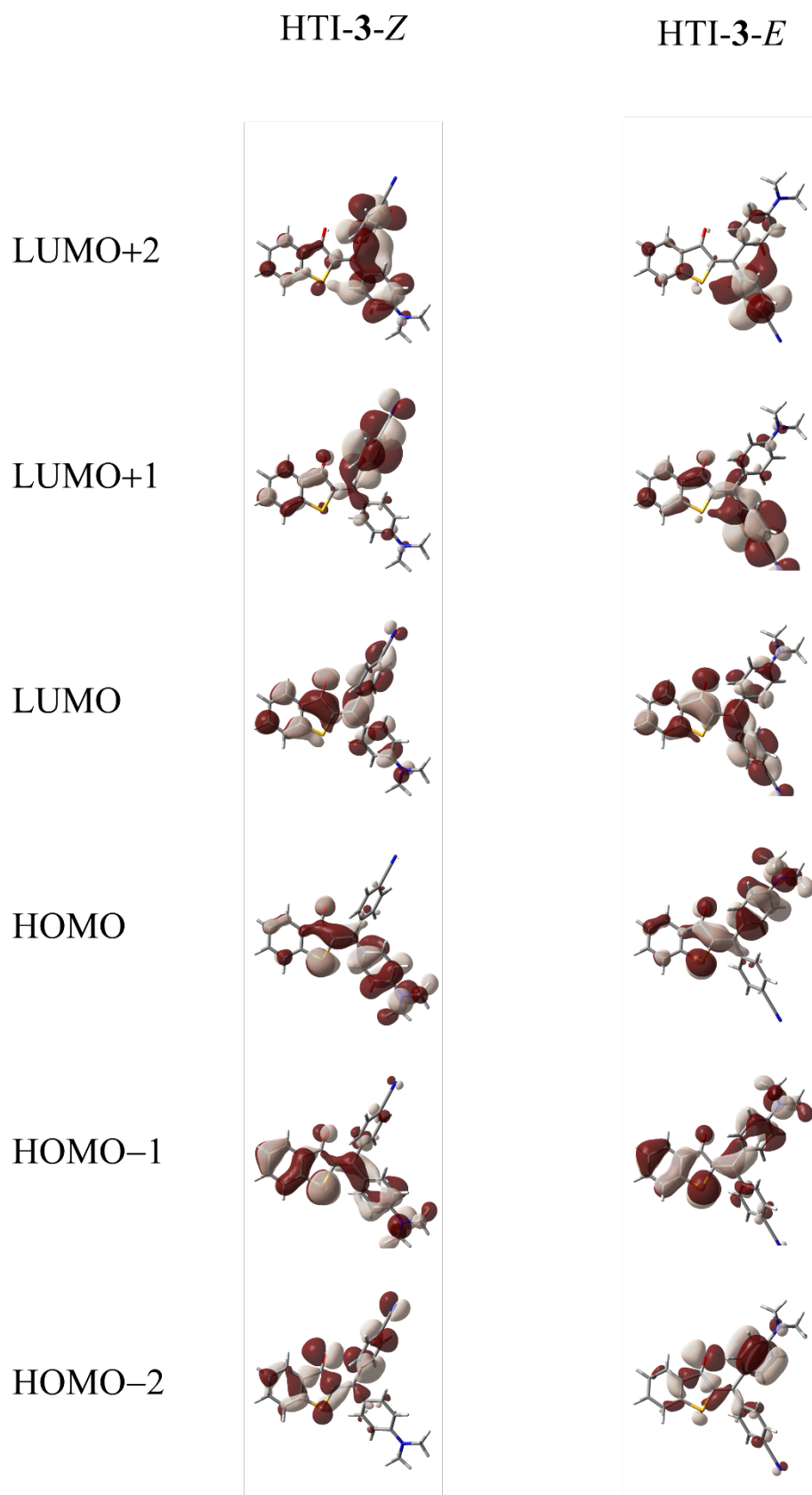


Figure S39: Theoretically obtained MOs for the *Z*- and *E*-isomer of diaryl-HTI **3** in toluene calculated on the B3LYP/6-311G(d,p) level of theory using the IEFPCM solvent model

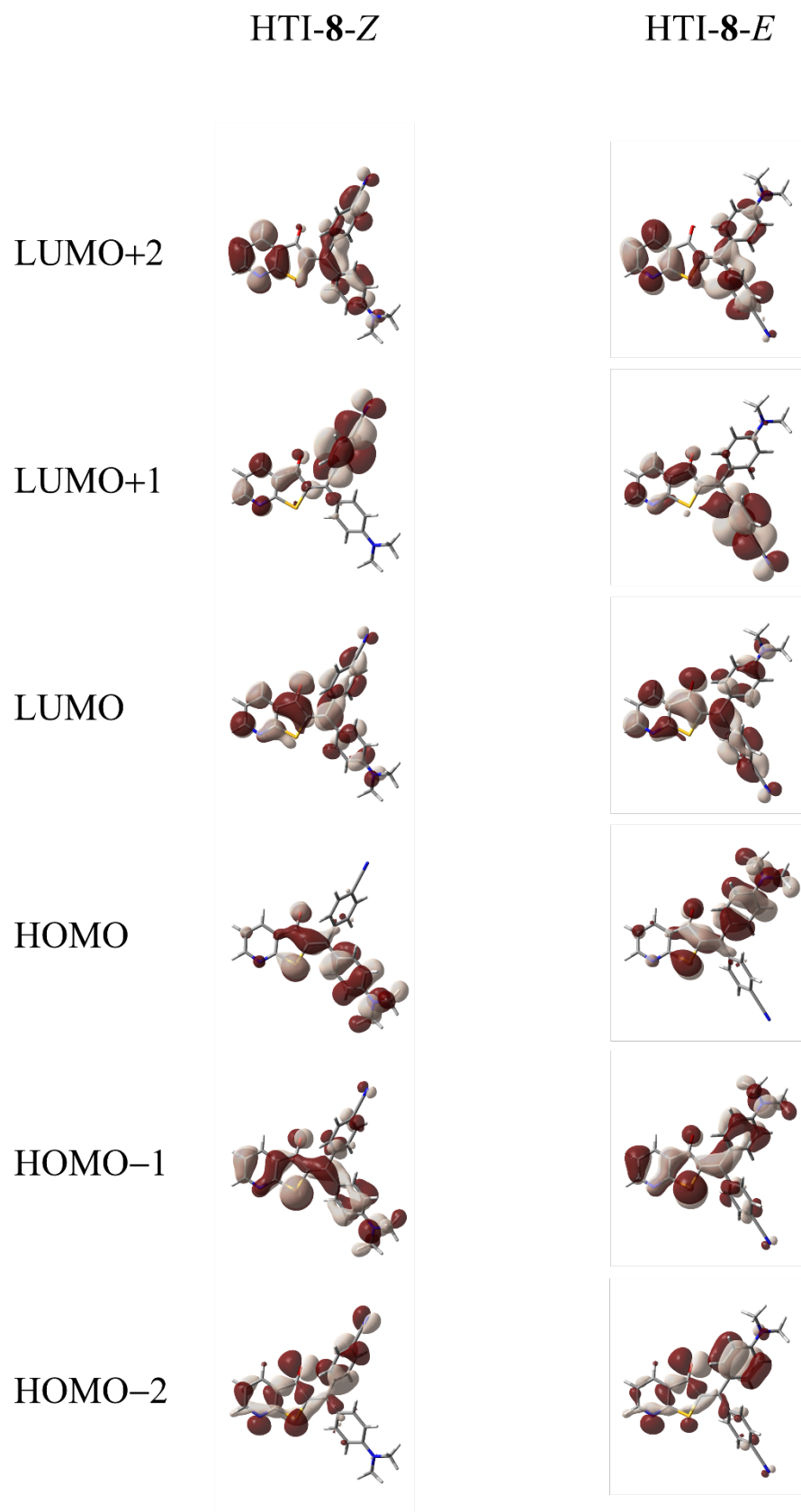


Figure S40: Theoretically obtained MOs for the *Z*- and *E*-isomer of diaryl-HTI **8** in toluene calculated on the B3LYP/6-311G(d,p) level of theory using the IEFPCM solvent model.

1D NOE NMR Spectra for Determination of Isomer Configuration

For elucidation of the double bond configuration of diaryl-HTIs 1D NOE NMR experiments were performed. Samples with 2-5 mg of substance were dissolved in deuterated solvents and the samples were irradiated with specific frequencies to observe through-space coupling from the aryl substituents to the benzothiophenone fragment of the diaryl-HTIs.

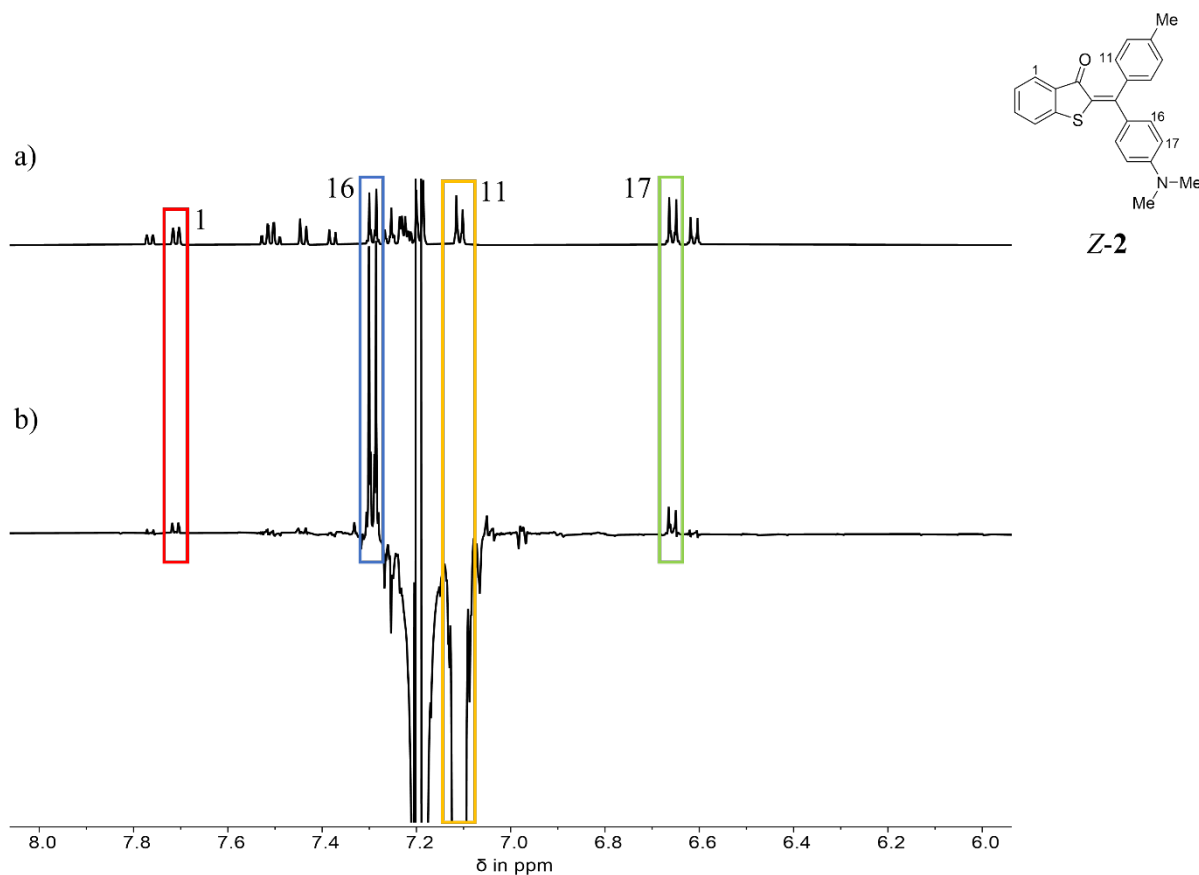


Figure S41: Aromatic region of the NMR spectra of diaryl-HTI **2** (mixture of *E* and *Z* isomer). Irradiation of the proton H(11) (yellow) leads to a through-space coupling to H(1) (red), H(16) (blue) and H(17) (green); a) ^1H NMR spectrum (601 MHz, CD_2Cl_2 , 0°C); b) 1D NOE NMR spectrum (601 MHz, CD_2Cl_2 , 0°C).

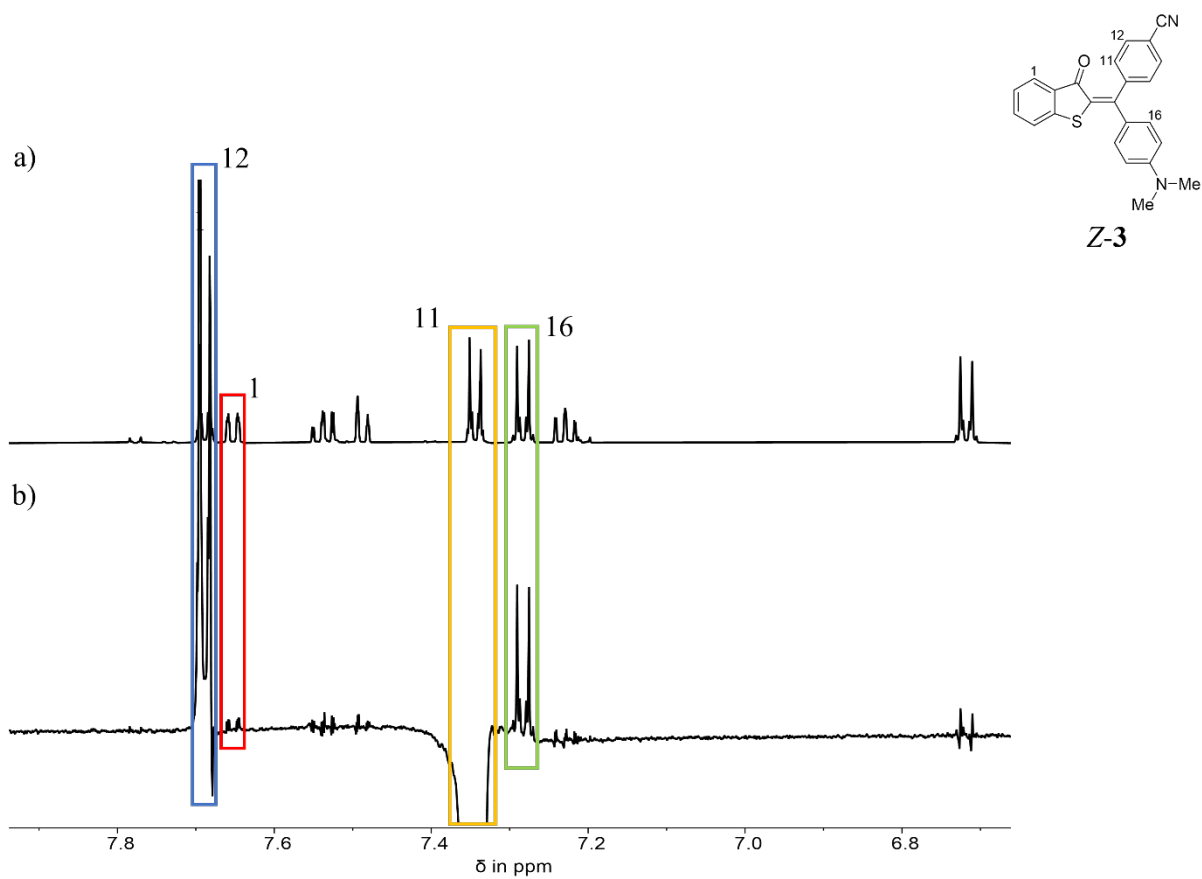


Figure S42: Aromatic region of the NMR spectra of diaryl-HTI **3** (mixture of *E* and *Z* isomer). Irradiation of the proton H(11) (yellow) leads to a trough-space coupling to H(1) (red), H(12) (blue) and H(16) (green); a) ^1H NMR spectrum (601 MHz, $\text{THF-}d_8$, 25°C); b) 1D NOE NMR spectrum (601 MHz, $\text{THF-}d_8$, 25°C).

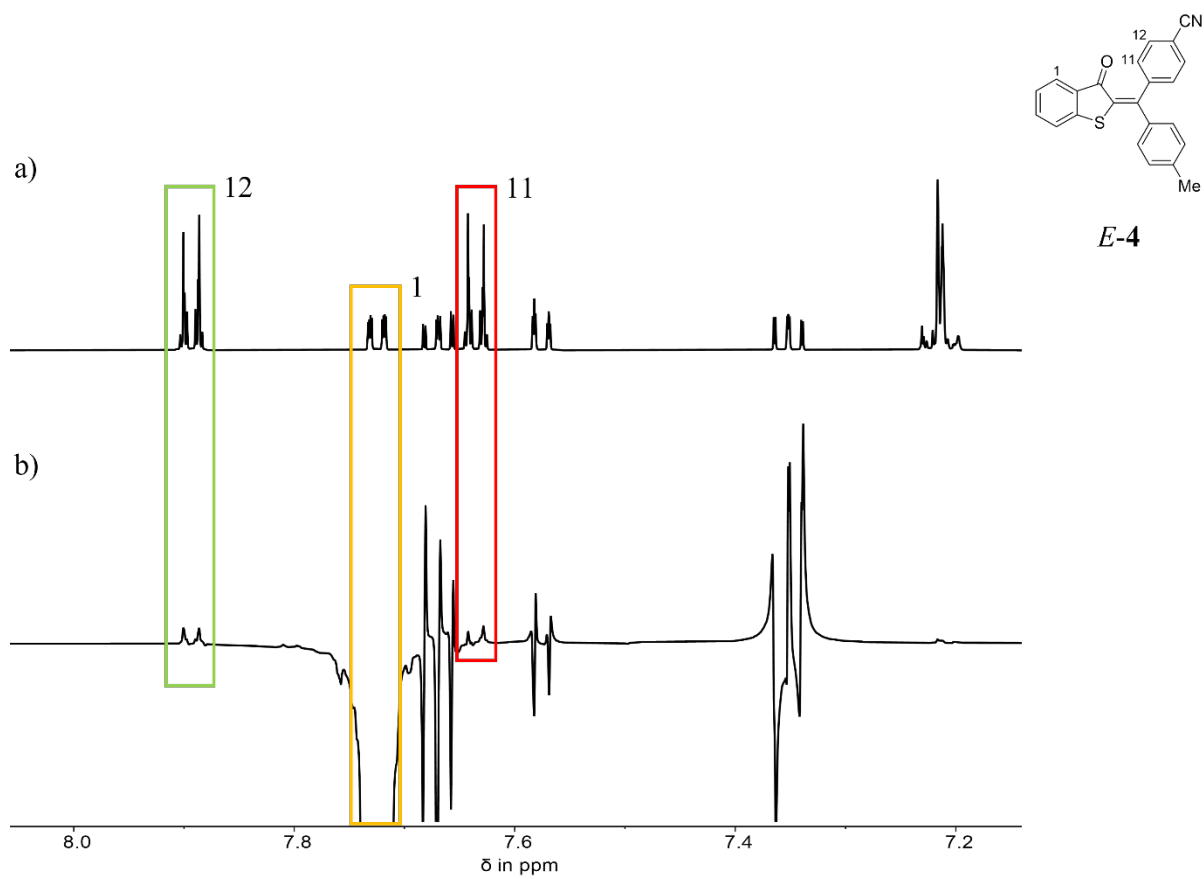


Figure S43: Aromatic region of the NMR spectra of diaryl-HTI **4** (*E*-isomer). Irradiation of the proton H(1) (yellow) leads to a trough-space coupling to H(11) (red) and H(12) (green); a) ^1H NMR spectrum (601 MHz, $(\text{CD}_3)_2\text{CO}$, 25°C); b) 1D NOE NMR spectrum (601 MHz, $(\text{CD}_3)_2\text{CO}$, 25°C).

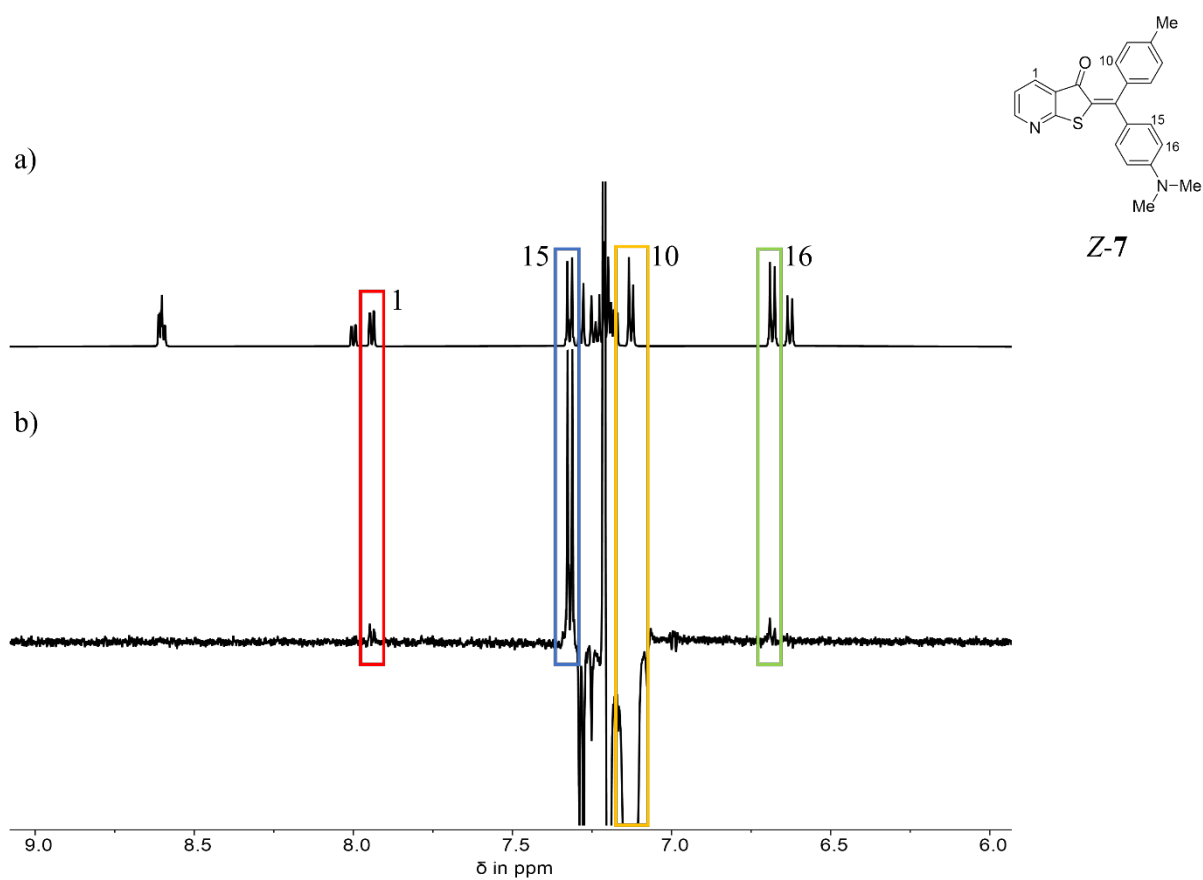


Figure S44: Aromatic region of the NMR spectra of diaryl-HTI 7 (mixture of *E* and *Z* isomer). Irradiation of the proton H(10) (yellow) leads to a trough-space coupling to H(1) (red), H(15) (blue) and H(16) (green); a) ¹H NMR spectrum (601 MHz, CD₂Cl₂, 25°C); b) 1D NOE NMR spectrum (601 MHz, CD₂Cl₂, 25°C).

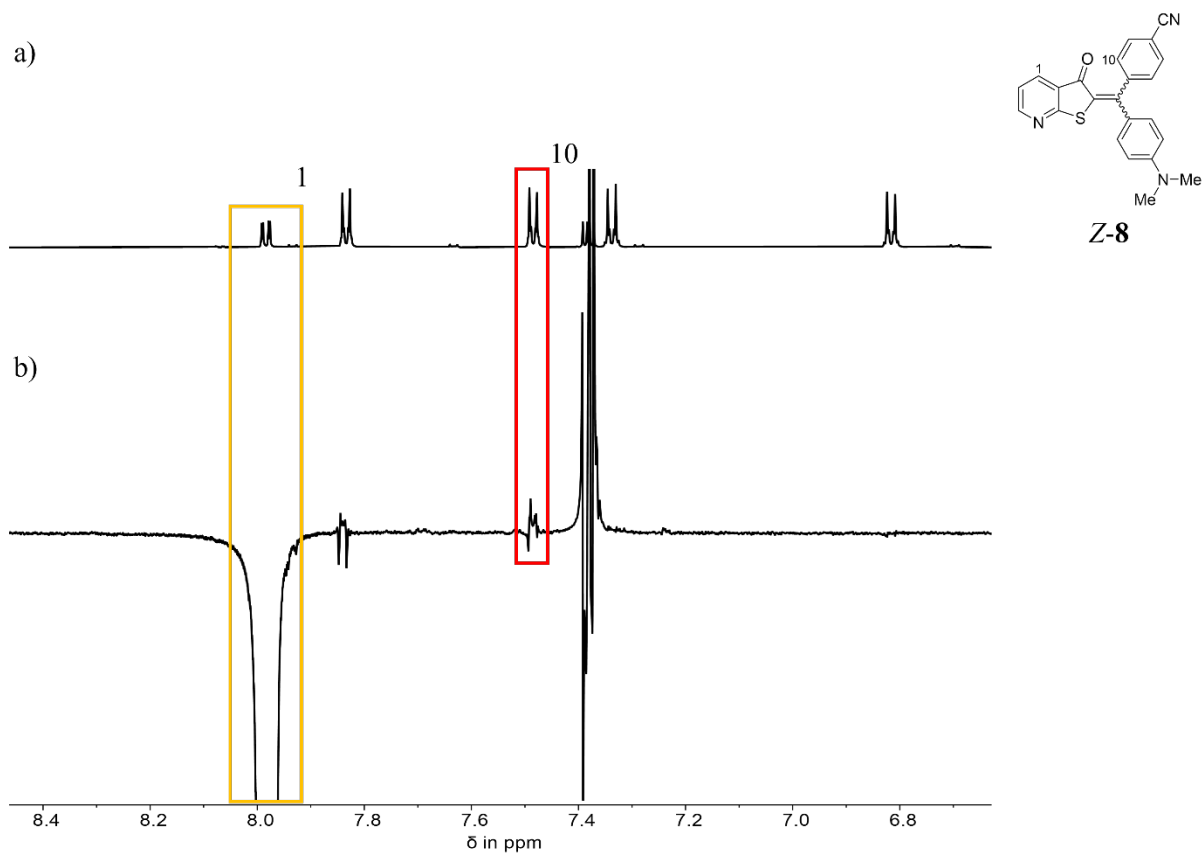


Figure S45: Aromatic region of the NMR spectra of diaryl-HTI **8** (mixture of *E* and *Z* isomer). Irradiation of the proton H(1) (yellow) leads to a trough-space coupling to H(10) (red); a) ^1H NMR spectrum (601 MHz, $(\text{CD}_3)_2\text{CO}$, 25°C); b) 1D NOE NMR spectrum (601 MHz, $(\text{CD}_3)_2\text{CO}$, 25°C).

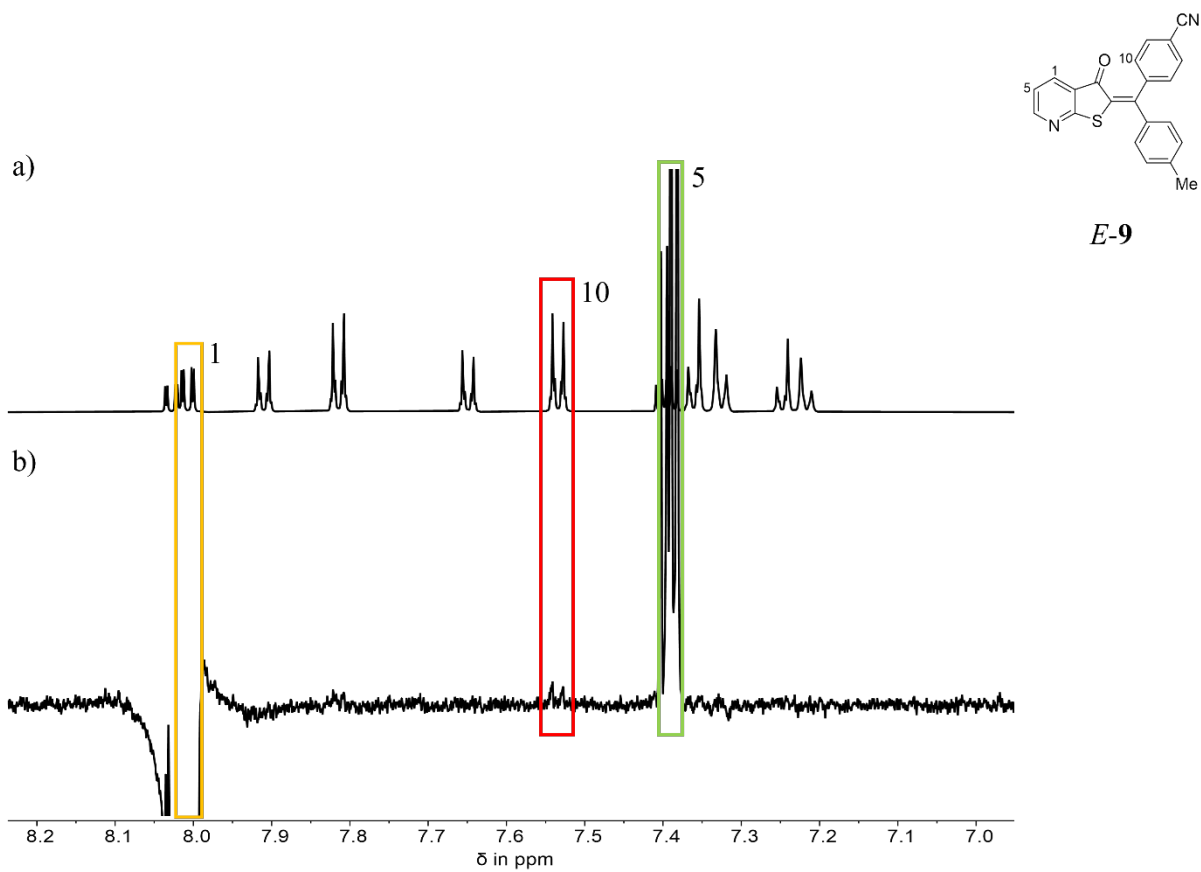
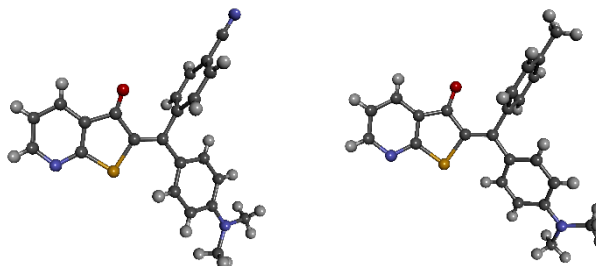
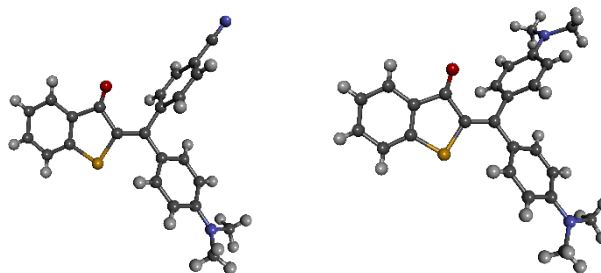


Figure S46: Aromatic region of the NMR spectra of diaryl-HTI **9** (mixture of *E* and *Z* isomer). Irradiation of the proton H(1) (yellow) leads to a trough-space coupling to H(10) (red) and H(5) (green); a) ^1H NMR spectrum (601 MHz, $(\text{CD}_3)_2\text{CO}$, 25°C); b) 1D NOE NMR spectrum (601 MHz, $(\text{CD}_3)_2\text{CO}$, 25°C).

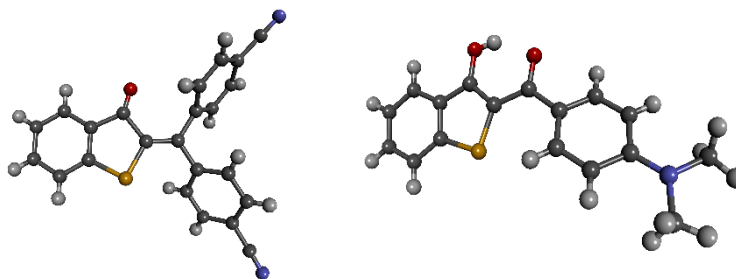
Crystal Structural Data



Compound	Diaryl-HTI 8 CCDC 2227018	Diaryl-HTI 7 CCDC 2227017
Formula	C ₂₃ H ₁₇ N ₃ OS	C ₂₃ H ₂₀ N ₂ OS
$D_{calc.}$ / g cm ⁻³	1.333	1.286
μ /mm ⁻¹	1.648	1.601
Formula Weight	383.45	372.47
Colour	light red	clear reddish red
Shape	plate-shaped	plate-shaped
Size/mm ³	0.33×0.31×0.08	0.24×0.12×0.10
T /K	153(1)	153.00(10)
Crystal System	orthorhombic	monoclinic
Flack Parameter	0.03(2)	0.14(7)
Hoof Parameter	0.024(15)	0.16(2)
Space Group	$P2_12_12_1$	$P2_1$
$a/\text{Å}$	7.1543(2)	5.5494(8)
$b/\text{Å}$	11.4783(4)	12.9584(18)
$c/\text{Å}$	23.2717(9)	13.437(2)
α°	90	90
β°	90	95.222(13)
γ°	90	90
$V/\text{Å}^3$	1911.05(11)	962.3(2)
Z	4	2
Z'	1	1
Wavelength/Å	1.54184	1.54184
Radiation type	Cu K α	Cu K α
θ_{min}°	3.799	3.303
θ_{max}°	72.180	71.330
Measured Refl's.	6676	6457
Indep't Refl's	3658	3595
Refl's $I \geq 2 \sigma(I)$	3376	2974
R_{int}	0.0347	0.0532
Parameters	255	259
Restraints	0	3
Largest Peak	0.390	0.238
Deepest Hole	-0.449	-0.230
GooF	1.065	1.087
wR_2 (all data)	0.1355	0.2346
wR_2	0.1307	0.2222
R_1 (all data)	0.0535	0.0930
R_1	0.0493	0.0816



Compound	Diaryl-HTI 3 CCDC 2227015	Diaryl-HTI 1 CCDC 2227014
Formula	C ₂₄ H ₁₈ N ₂ OS	C ₂₅ H ₂₄ N ₂ OS
$D_{calc.}/\text{g cm}^{-3}$	1.309	1.297
μ/mm^{-1}	1.605	1.537
Formula Weight	382.46	400.52
Colour	clear light red	clear reddish red
Shape	block-shaped	needle-shaped
Size/mm ³	0.23×0.20×0.10	0.25×0.05×0.05
T/K	154(4)	152.95(10)
Crystal System	monoclinic	monoclinic
Space Group	$P2_1/n$	$P2_1/c$
$a/\text{Å}$	8.7409(2)	9.9704(8)
$b/\text{Å}$	13.9118(3)	21.4506(10)
$c/\text{Å}$	15.9596(4)	9.7628(5)
α°	90	90
β°	89.742(2)	100.735(6)
γ°	90	90
$V/\text{Å}^3$	1940.69(8)	2051.4(2)
Z	4	4
Z'	1	1
Wavelength/Å	1.54184	1.54184
Radiation type	Cu K α	Cu K α
$\theta_{min}/^\circ$	4.216	4.514
$\theta_{max}/^\circ$	71.634	69.260
Measured Refl's.	6519	6287
Indep't Refl's	3641	3658
Refl's $I \geq 2 \sigma(I)$	3397	3060
R_{int}	0.0215	0.0275
Parameters	255	266
Restraints	0	0
Largest Peak	0.870	0.602
Deepest Hole	-0.678	-0.495
GooF	1.025	1.049
wR_2 (all data)	0.1445	0.1891
wR_2	0.1416	0.1780
R_1 (all data)	0.0557	0.0789
R_1	0.0530	0.0677



Compound	Diaryl-HTI 5 CCDC 2227016	Compound 15 CCDC 2227451
Formula	C ₂₃ H ₁₂ N ₂ OS	C ₁₇ H ₁₅ NO ₂ S
$D_{calc.}/\text{g cm}^{-3}$	1.351	1.391
μ/mm^{-1}	1.718	2.053
Formula Weight	364.41	297.36
Colour	clear light orange	clear light yellow
Shape	block-shaped	block-shaped
Size/mm ³	0.41×0.33×0.27	0.26×0.21×0.16
T/K	153.00(10)	153.00(10)
Crystal System	monoclinic	monoclinic
Space Group	$P2_1/n$	$P2_1/c$
$a/\text{Å}$	12.1913(2)	15.6601(2)
$b/\text{Å}$	22.6255(3)	7.17100(10)
$c/\text{Å}$	13.0947(2)	12.72030(10)
α°	90	90
β°	97.3090(10)	96.1630(10)
γ°	90	90
$V/\text{Å}^3$	3582.62(9)	1420.22(3)
Z	8	4
Z'	2	1
Wavelength/Å	1.54184	1.54184
Radiation type	Cu K α	Cu K α
θ_{min}°	3.924	2.838
θ_{max}°	73.191	71.537
Measured Refl's.	13496	8644
Indep't Refl's	6961	2717
Refl's $I \geq 2 \sigma(I)$	6064	2611
R_{int}	0.0276	0.0191
Parameters	488	194
Restraints	0	0
Largest Peak	0.709	0.284
Deepest Hole	-0.571	-0.203
GooF	1.020	1.068
wR_2 (all data)	0.1164	0.0850
wR_2	0.1111	0.0842
R_1 (all data)	0.0513	0.0309
R_1	0.0446	0.0301

NMR spectra

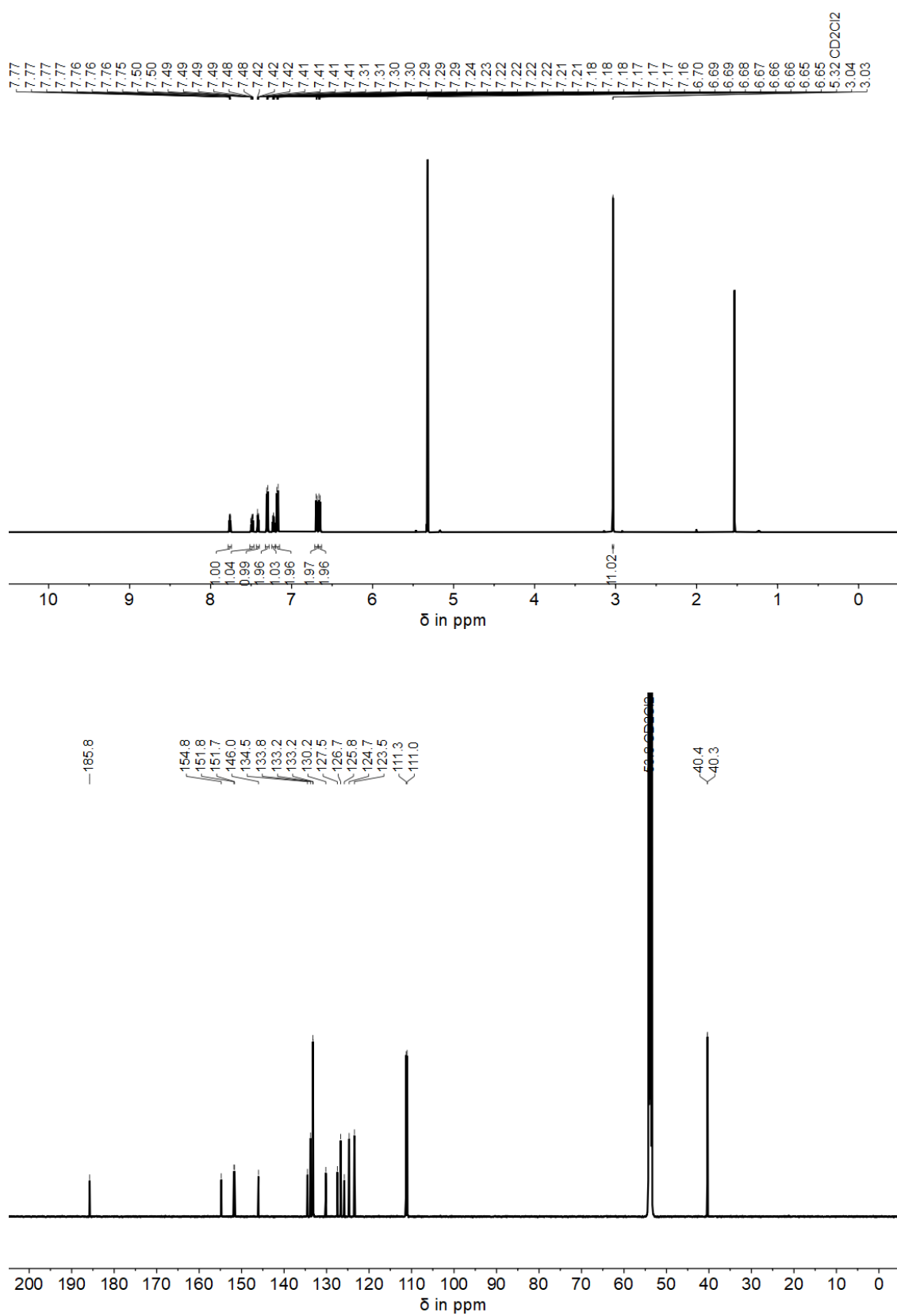


Figure S47: NMR spectra of diaryl-HTI 1; ¹H NMR spectrum (601 MHz, CD₂Cl₂, 23 °C) (top); ¹³C NMR spectrum (151 MHz, CD₂Cl₂, 23 °C) (bottom).

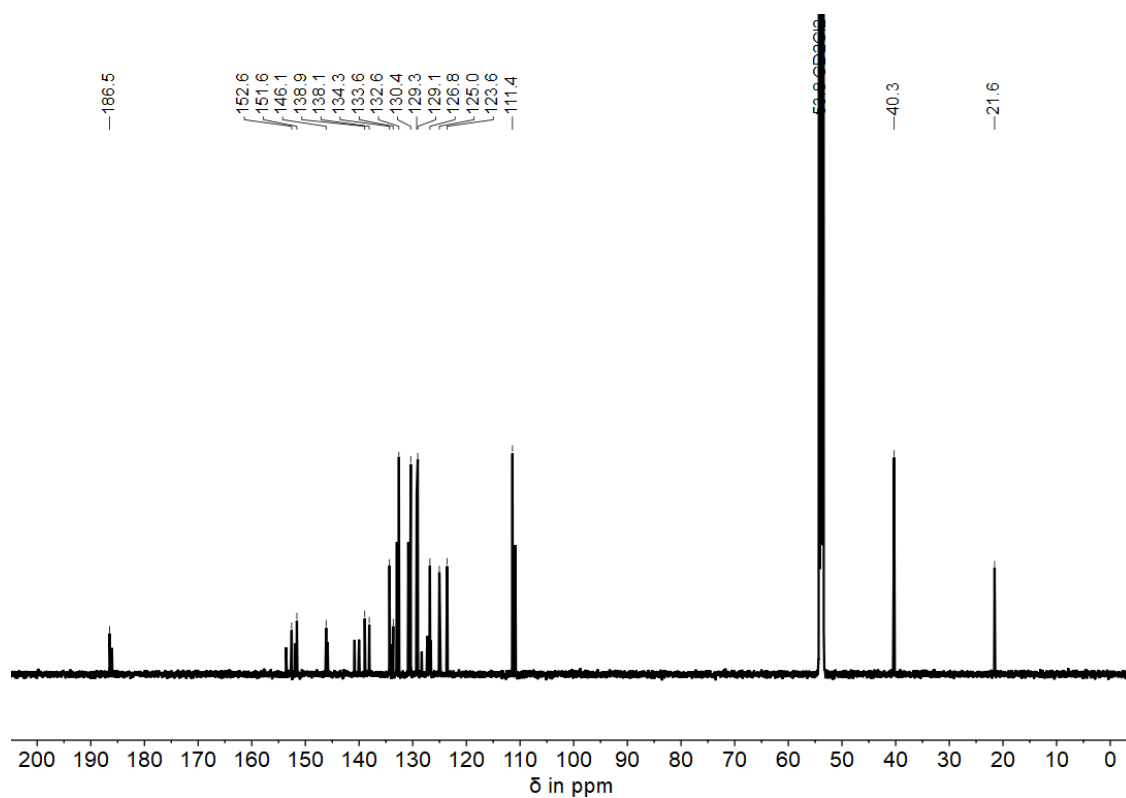
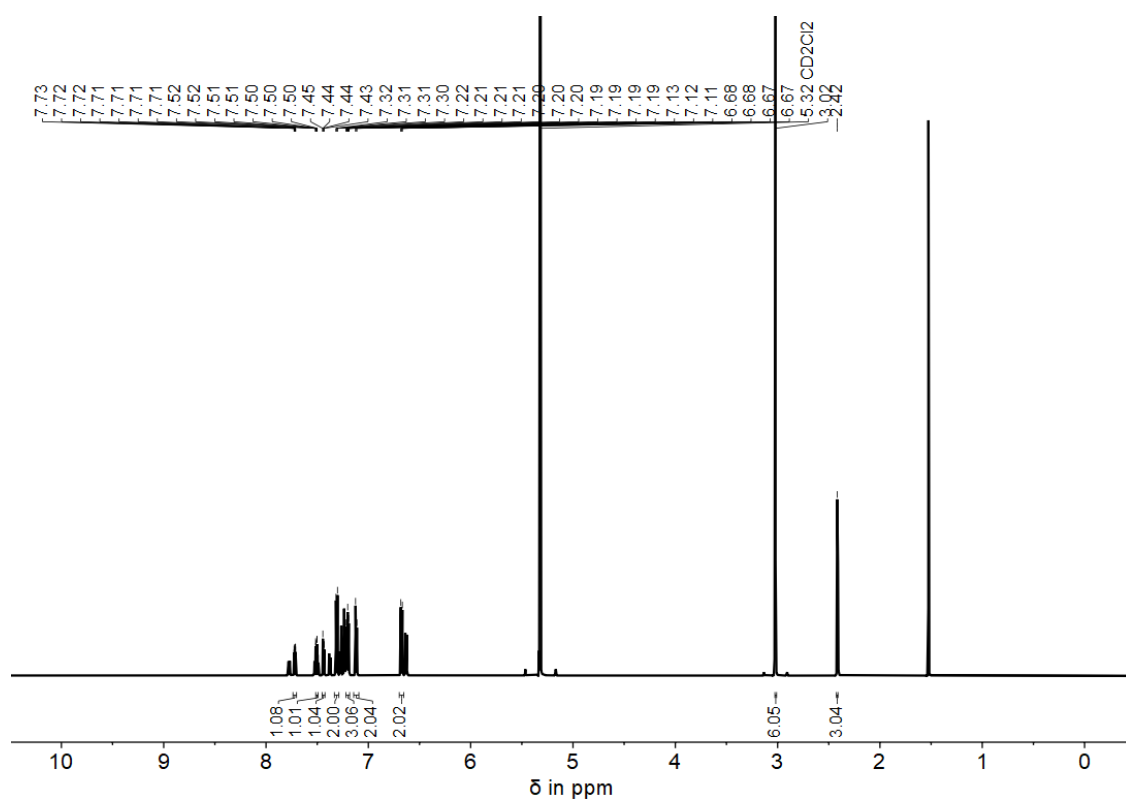


Figure S48: NMR spectra of diaryl-HTI **2** (mixture of *E* and *Z* isomer); ¹H NMR spectrum (601 MHz, CD₂Cl₂, 23 °C) (top); ¹³C NMR spectrum (151 MHz, CD₂Cl₂, 23 °C) (bottom).

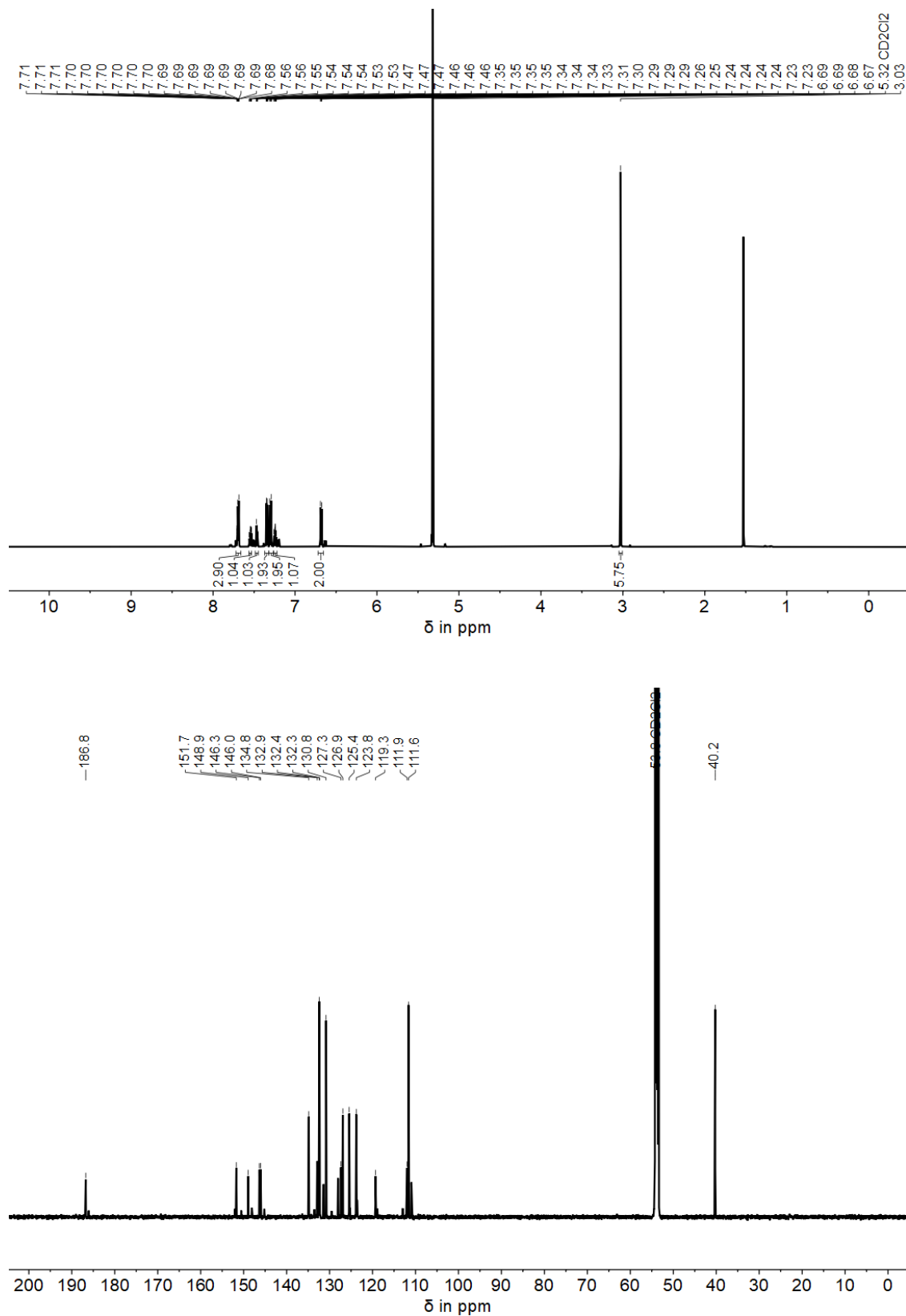


Figure S49: NMR spectra of diaryl-HTI **3** (mixture of *E* and *Z* isomer); ¹H NMR spectrum (601 MHz, CD₂Cl₂, 23 °C) (top); ¹³C NMR spectrum (151 MHz, CD₂Cl₂, 23 °C) (bottom).

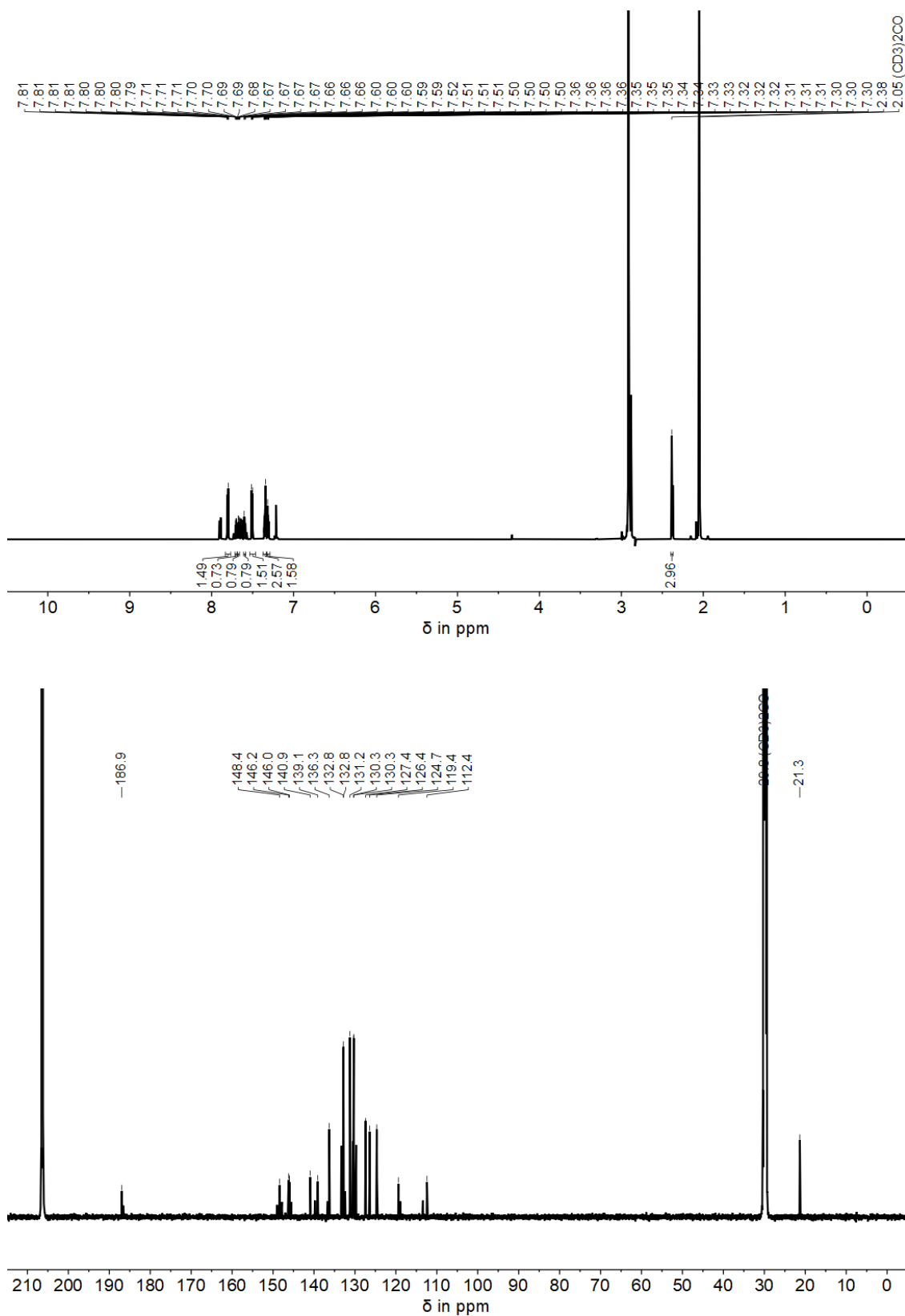


Figure S50: NMR spectra of diaryl-HTI **4** (mixture of *E* and *Z* isomer); ^1H NMR spectrum (601 MHz, $(\text{CD}_3)_2\text{CO}$, 23 °C) (top); ^{13}C NMR spectrum (151 MHz, $(\text{CD}_3)_2\text{CO}$, 23 °C) (bottom).

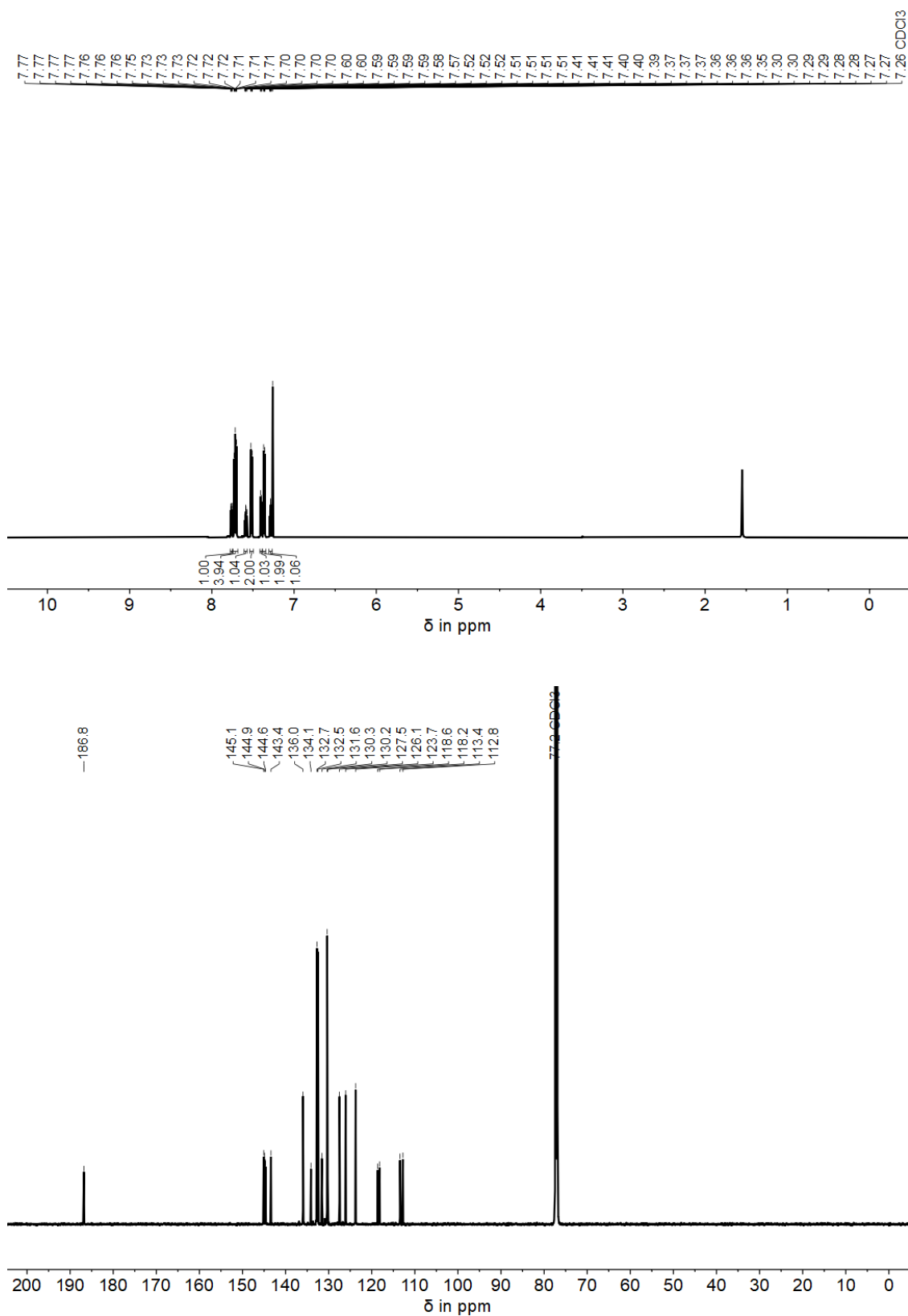


Figure S51: NMR spectra of diaryl-HTI 5; ^1H NMR spectrum (601 MHz, CDCl_3 , 23 °C) (top); ^{13}C NMR spectrum (151 MHz, CDCl_3 , 23 °C) (bottom).

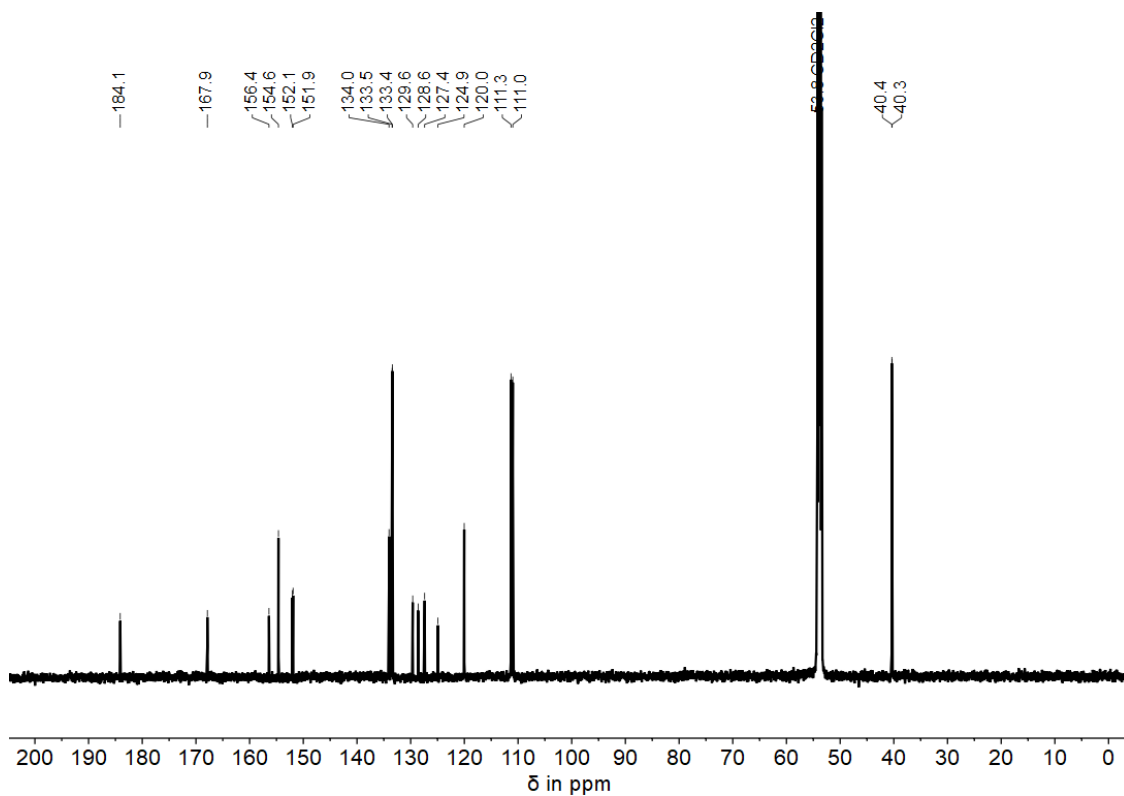
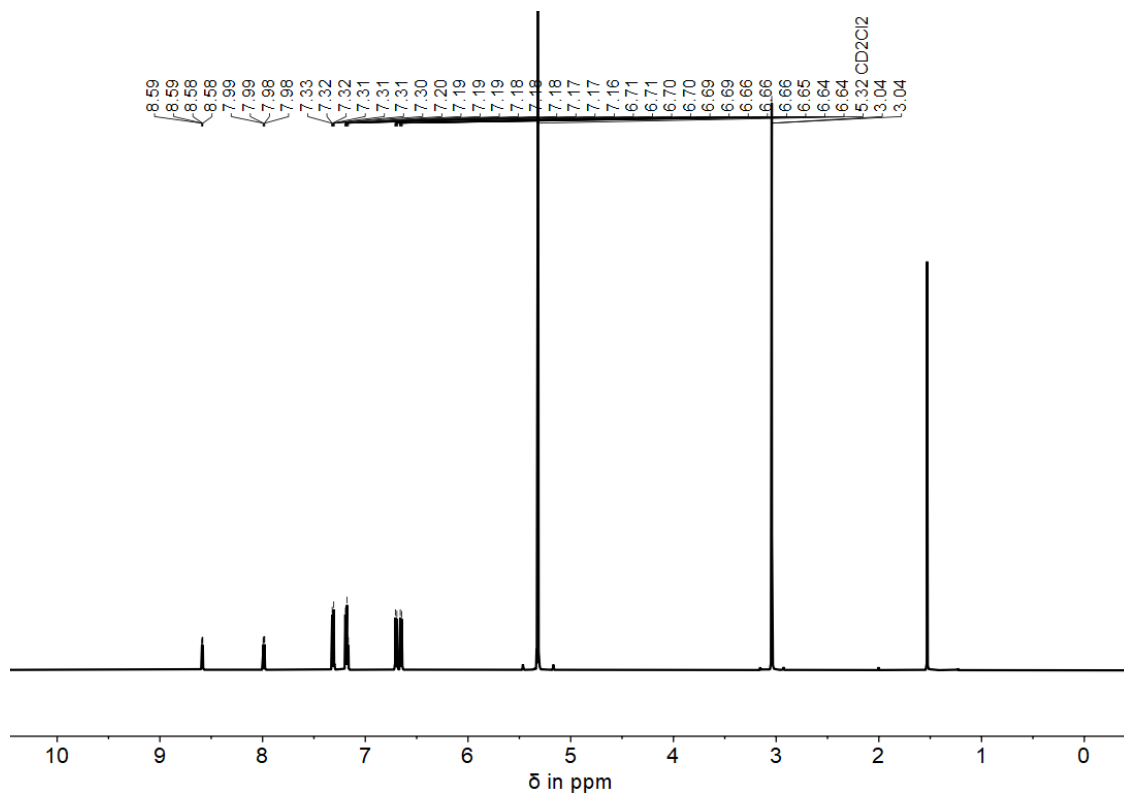


Figure S52: NMR spectra of diaryl-HTI **6**; ^1H NMR spectrum (601 MHz, CD_2Cl_2 , 23 °C) (top); ^{13}C NMR spectrum (151 MHz, CD_2Cl_2 , 23 °C) (bottom).

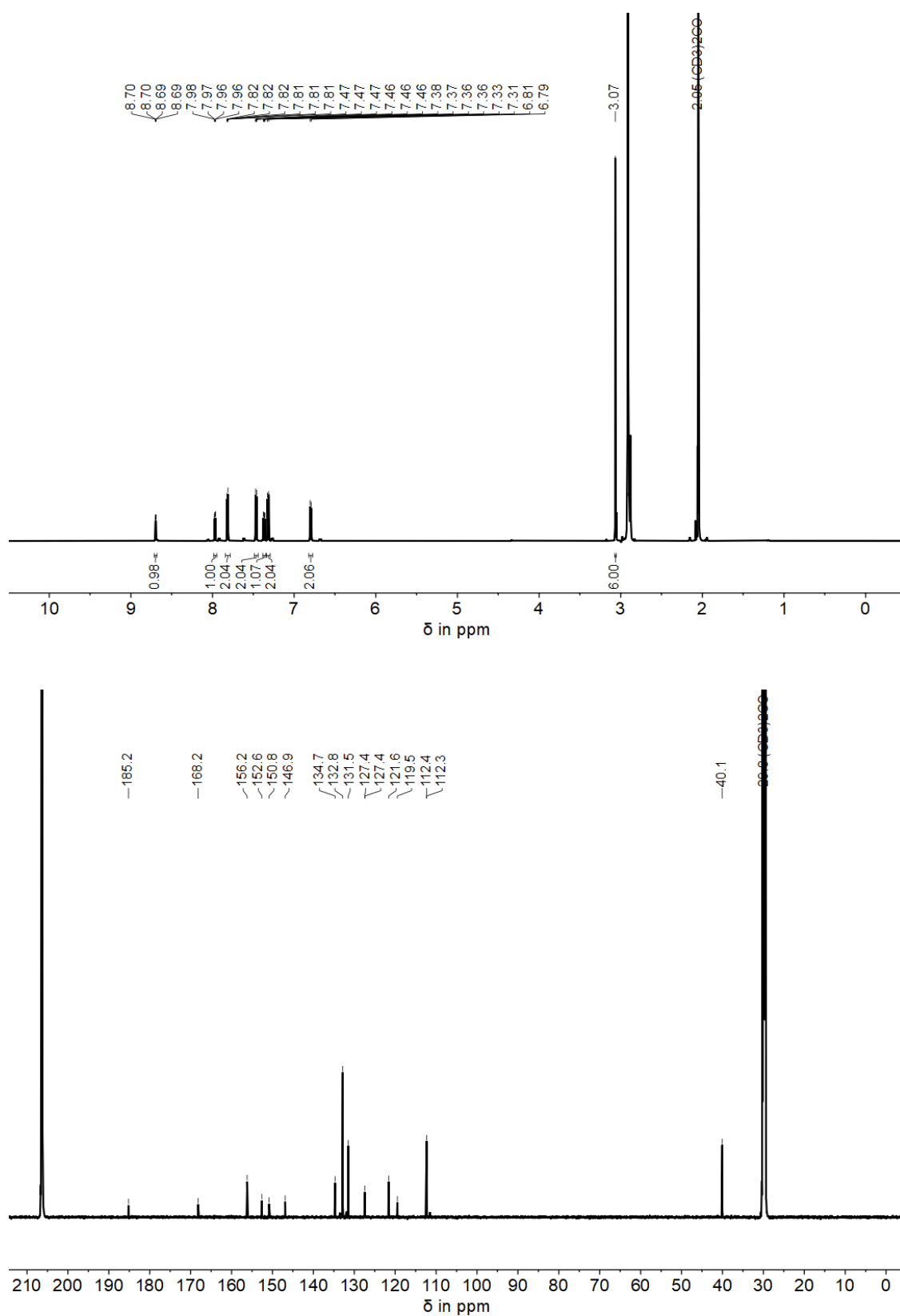


Figure S54: NMR spectra of diaryl-HTI **8** (mixture of *E* and *Z* isomer); ^1H NMR spectrum (601 MHz, $(\text{CD}_3)_2\text{CO}$, 23 °C) (top); ^{13}C NMR spectrum (151 MHz, $(\text{CD}_3)_2\text{CO}$, 23 °C) (bottom).

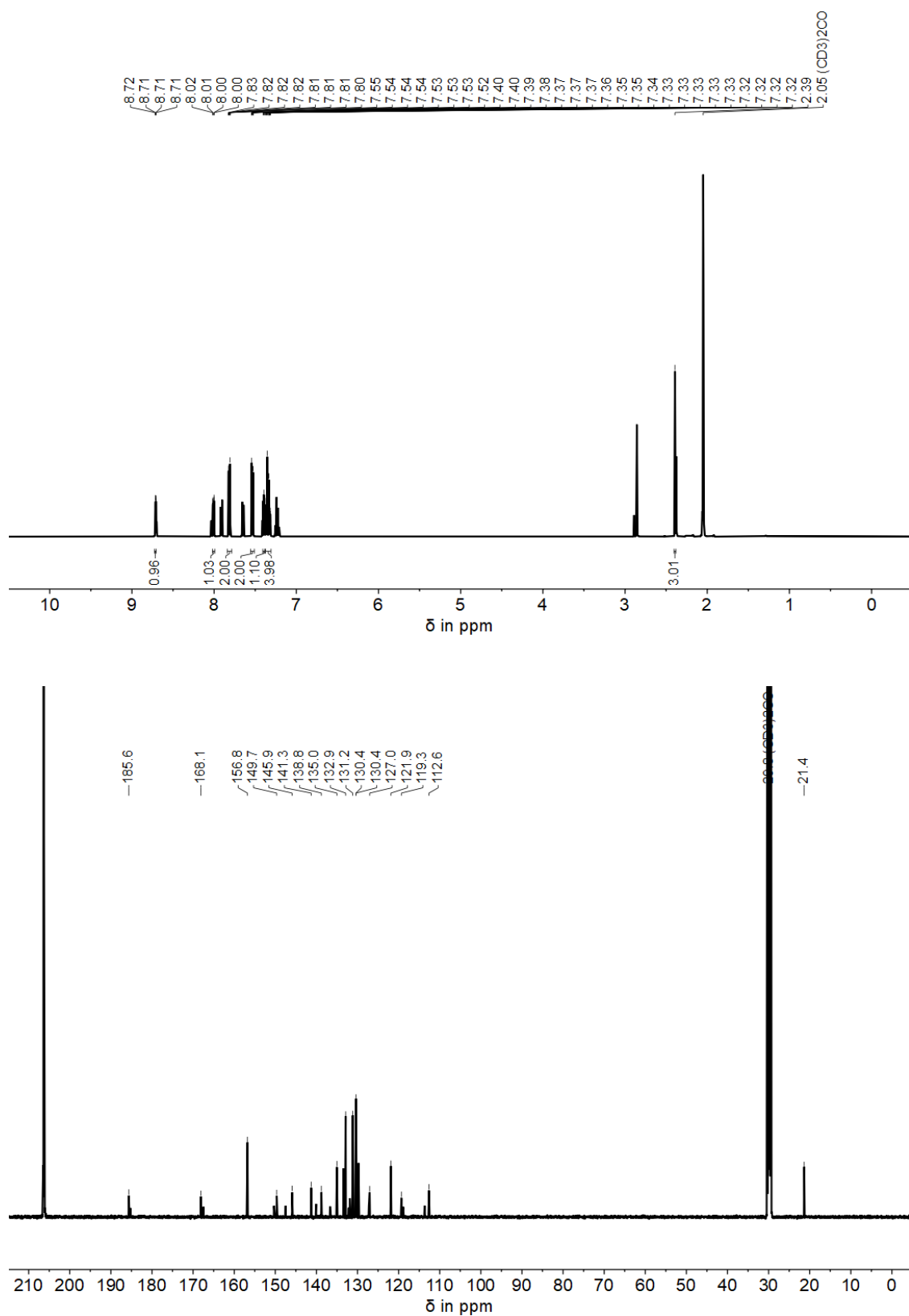


Figure S55: NMR spectra of diaryl-HTI **9** (mixture of *E* and *Z* isomer); ¹H NMR spectrum (500 MHz, (CD₃)₂CO, 23 °C) (top); ¹³C NMR spectrum (126 MHz, (CD₃)₂CO, 23 °C) (bottom).

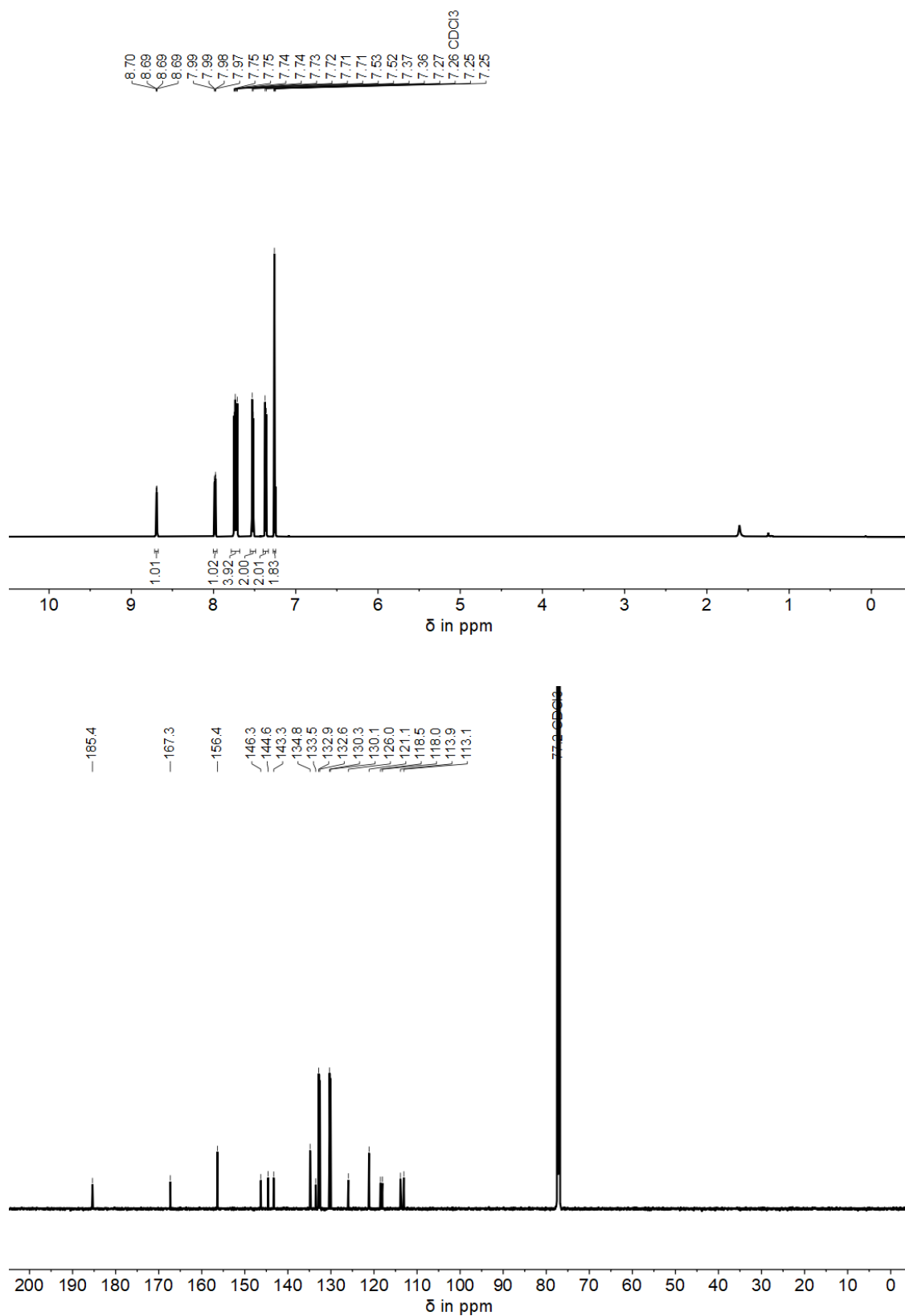


Figure S56: NMR spectra of diaryl-HTI 10; ¹H NMR spectrum (601 MHz, CDCl₃, 23 °C) (top); ¹³C NMR spectrum (151 MHz, CDCl₃, 23 °C) (bottom).

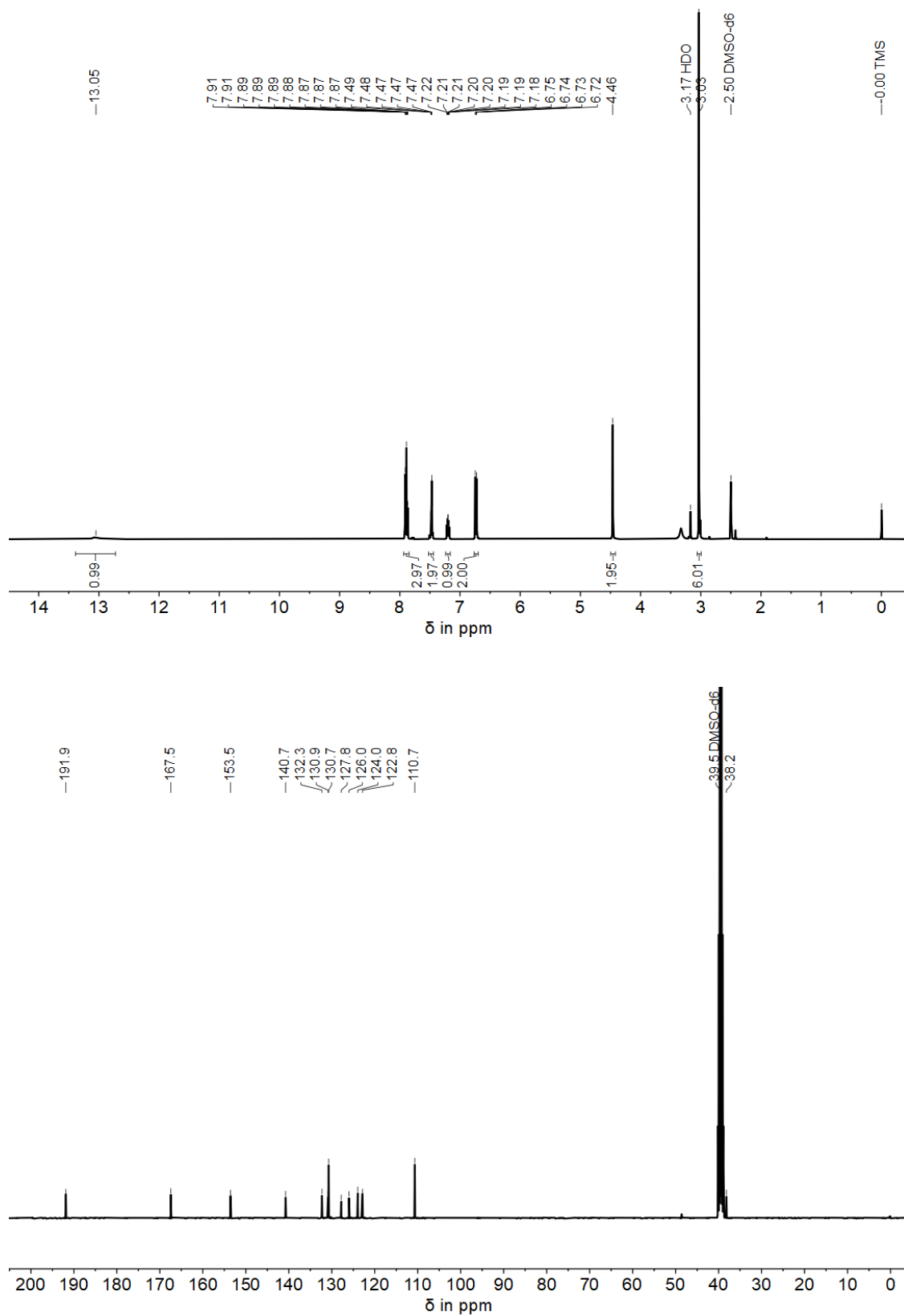


Figure S57: NMR spectra of compound **12**; ¹H NMR spectrum (400 MHz, (CD₃)₂SO, 23 °C) (top); ¹³C NMR spectrum (101 MHz, (CD₃)₂SO, 23 °C) (bottom).

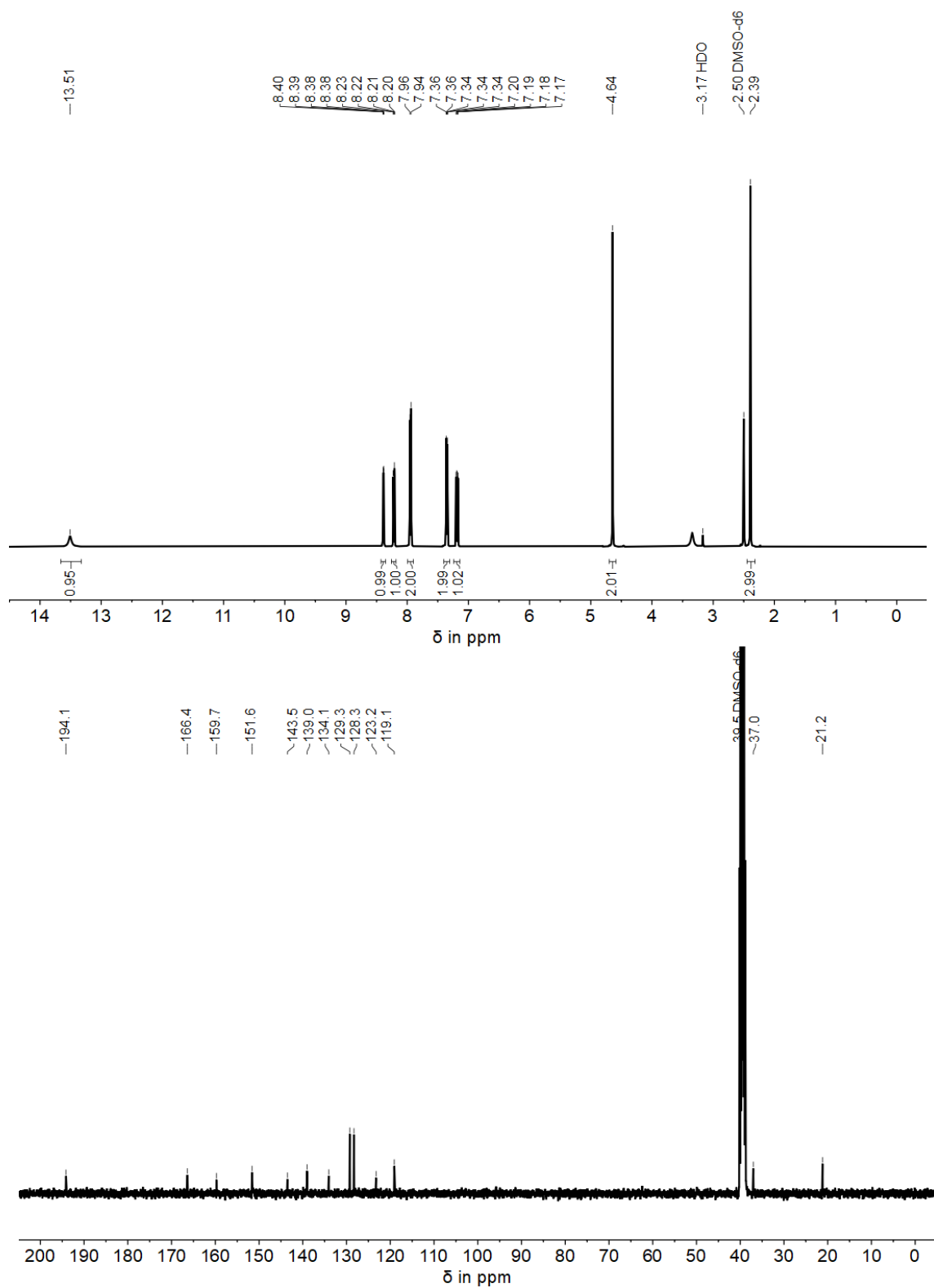


Figure S58: NMR spectra of compound **13**; ^1H NMR spectrum (400 MHz, $(\text{CD}_3)_2\text{SO}$, 23 °C) (top); ^{13}C NMR spectrum (101 MHz, $(\text{CD}_3)_2\text{SO}$, 23 °C) (bottom).

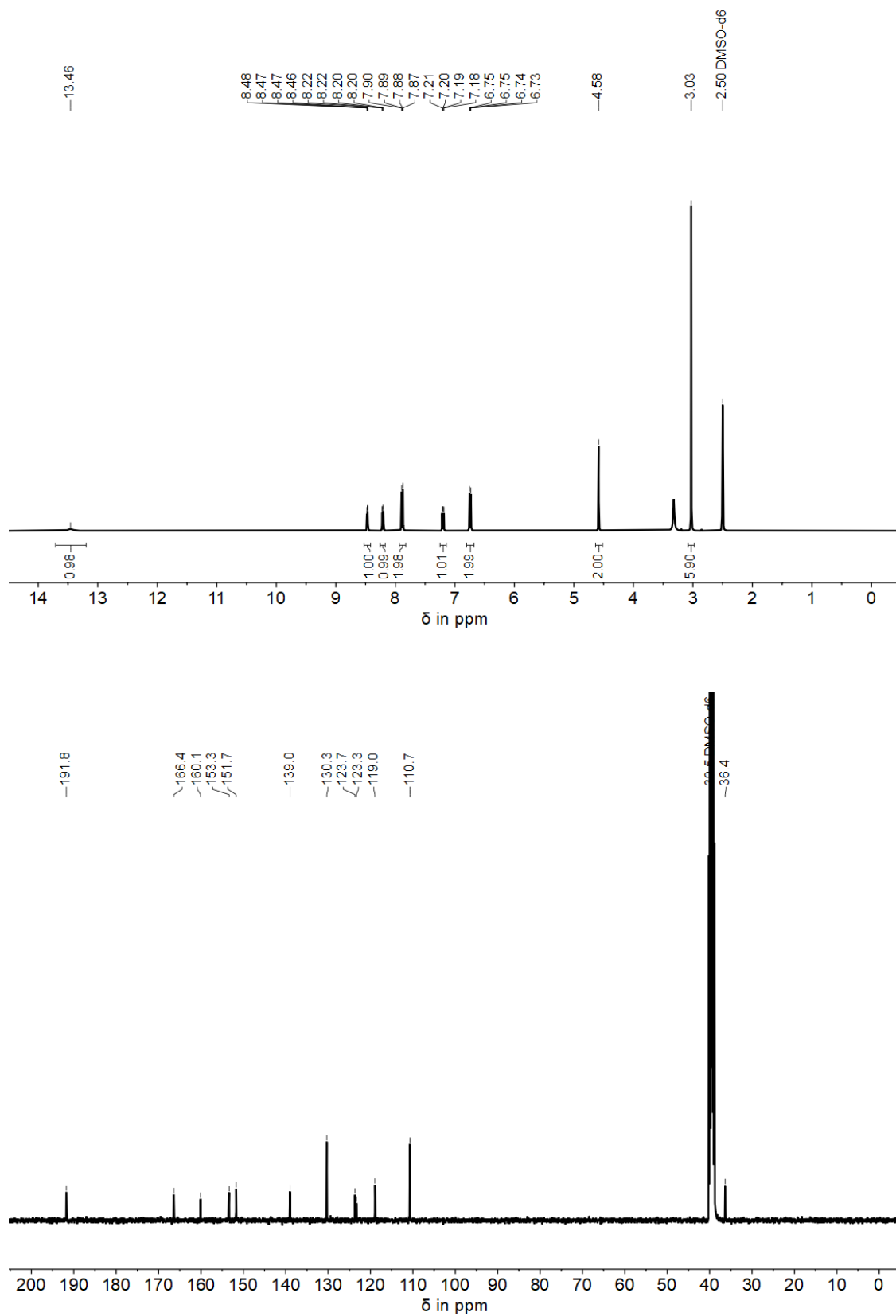


Figure S59: NMR spectra of compound **14**; ¹H NMR spectrum (400 MHz, (CD₃)₂SO, 23 °C) (top); ¹³C NMR spectrum (101 MHz, (CD₃)₂SO, 23 °C) (bottom).

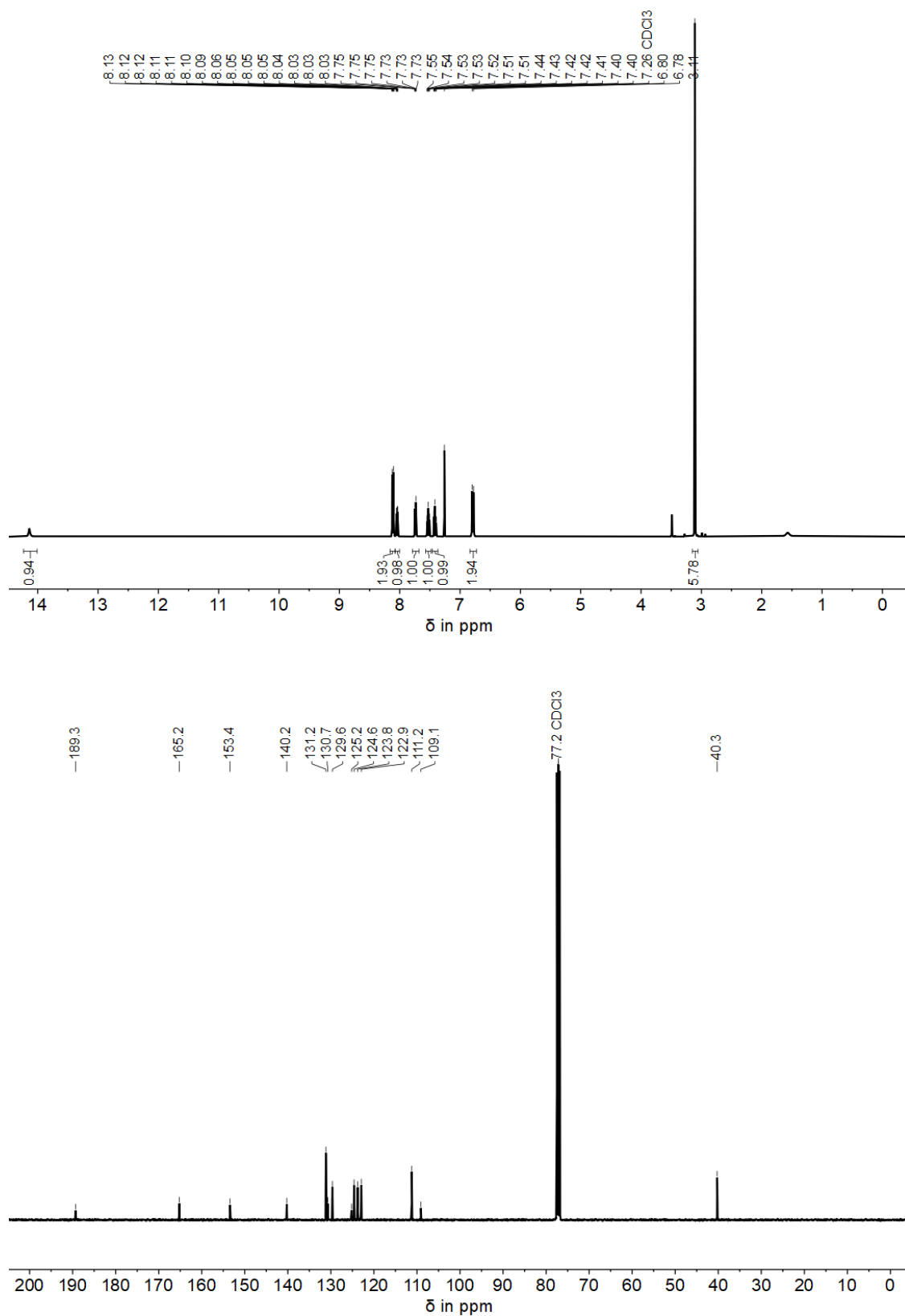


Figure S60: NMR spectra of compound **15**; ¹H NMR spectrum (400 MHz, CDCl₃, 23 °C) (top); ¹³C NMR spectrum (101 MHz, CDCl₃, 23 °C) (bottom).

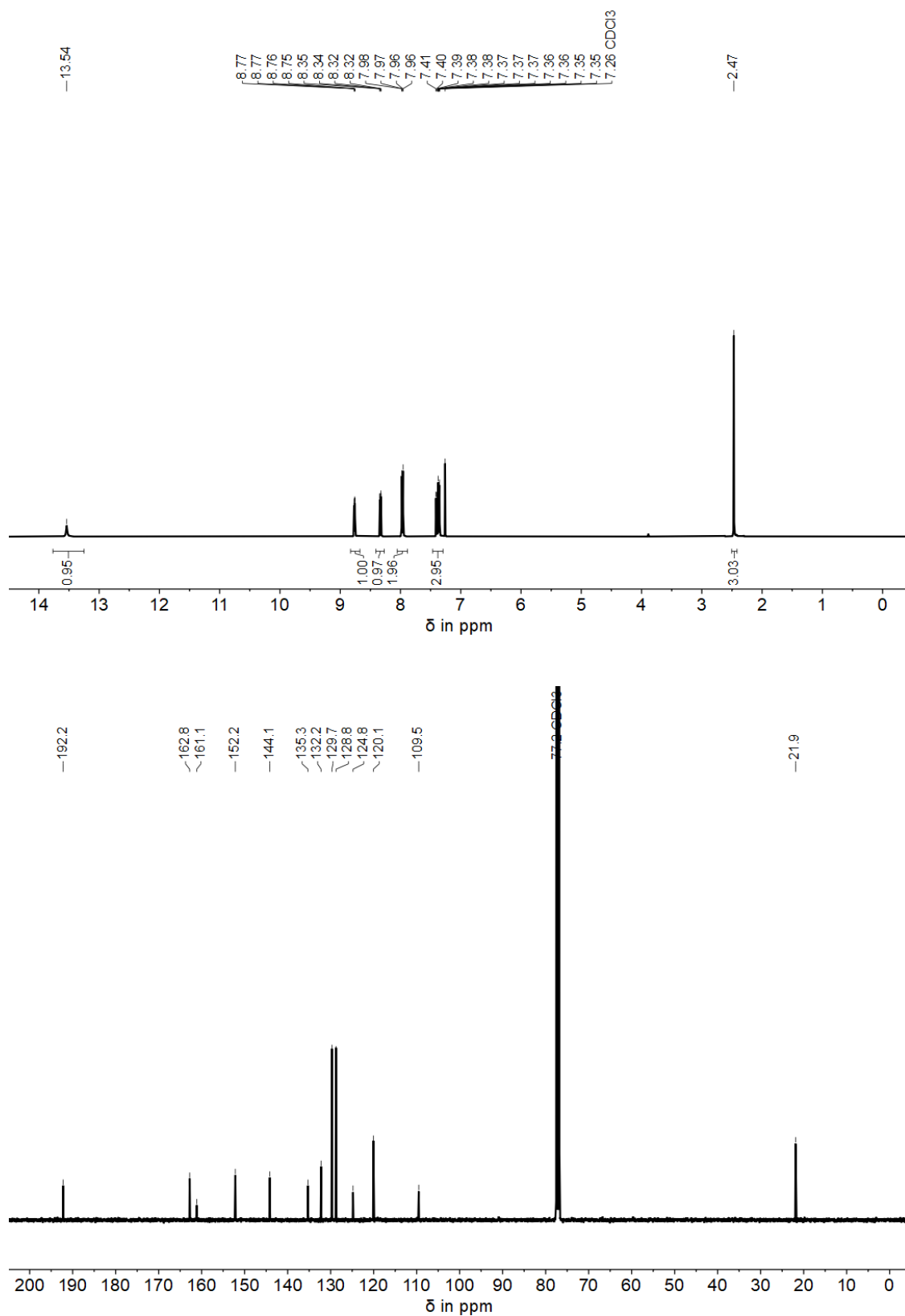


Figure S61: NMR spectra of compound **16**; ¹H NMR spectrum (400 MHz, CDCl₃, 23 °C) (top); ¹³C NMR spectrum (101 MHz, CDCl₃, 23 °C) (bottom).

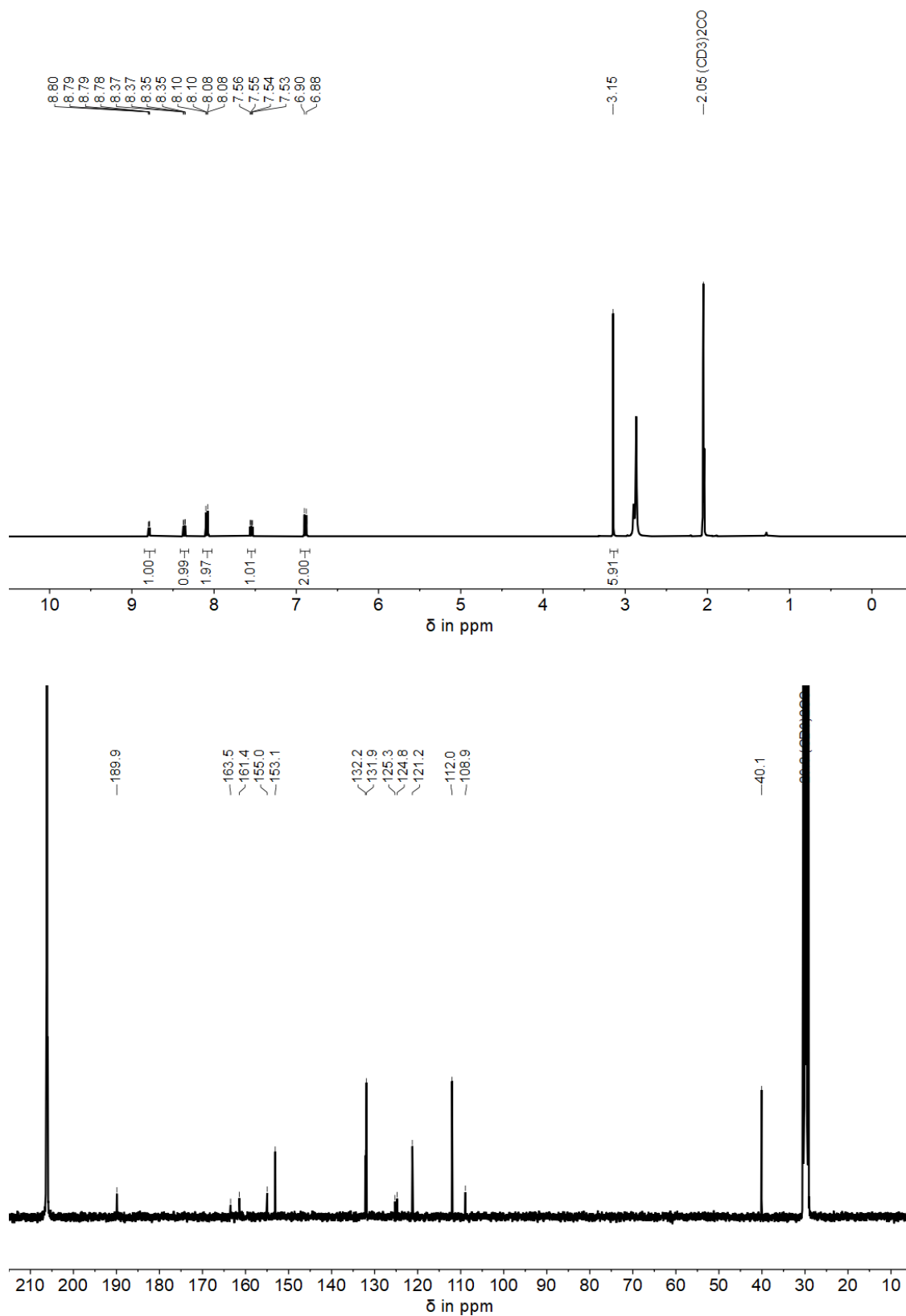


Figure S62: NMR spectra of compound 17; ^1H NMR spectrum (400 MHz, $(\text{CD}_3)_2\text{CO}$, 23 °C) (top); ^{13}C NMR spectrum (101 MHz, $(\text{CD}_3)_2\text{CO}$, 23 °C) (bottom).

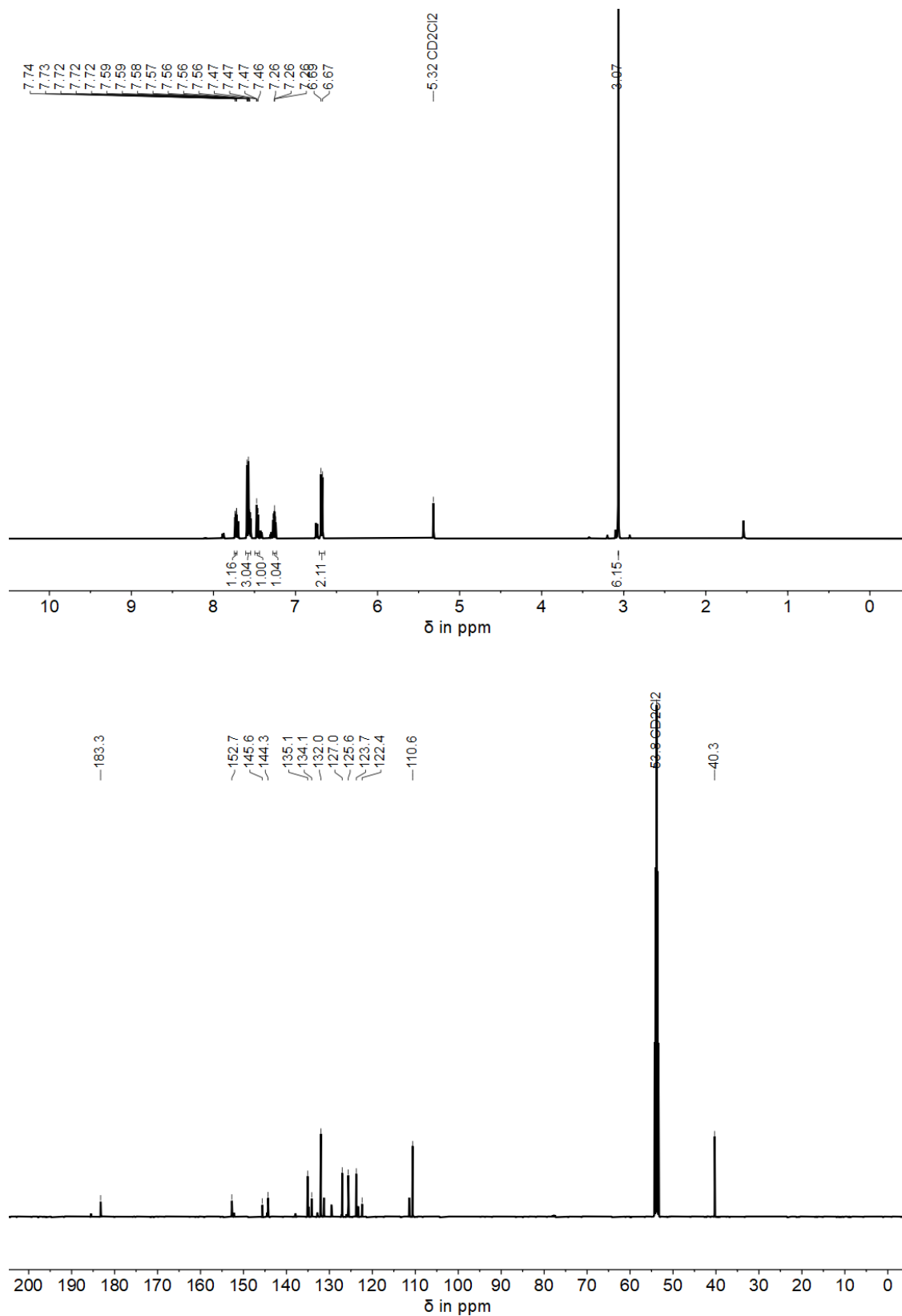


Figure S63: NMR spectra of compound **18** (mixture of *E* and *Z* isomer); ¹H NMR spectrum (500 MHz, CD₂Cl₂, 23 °C) (top); ¹³C NMR spectrum (126 MHz, CD₂Cl₂, 23 °C) (bottom).

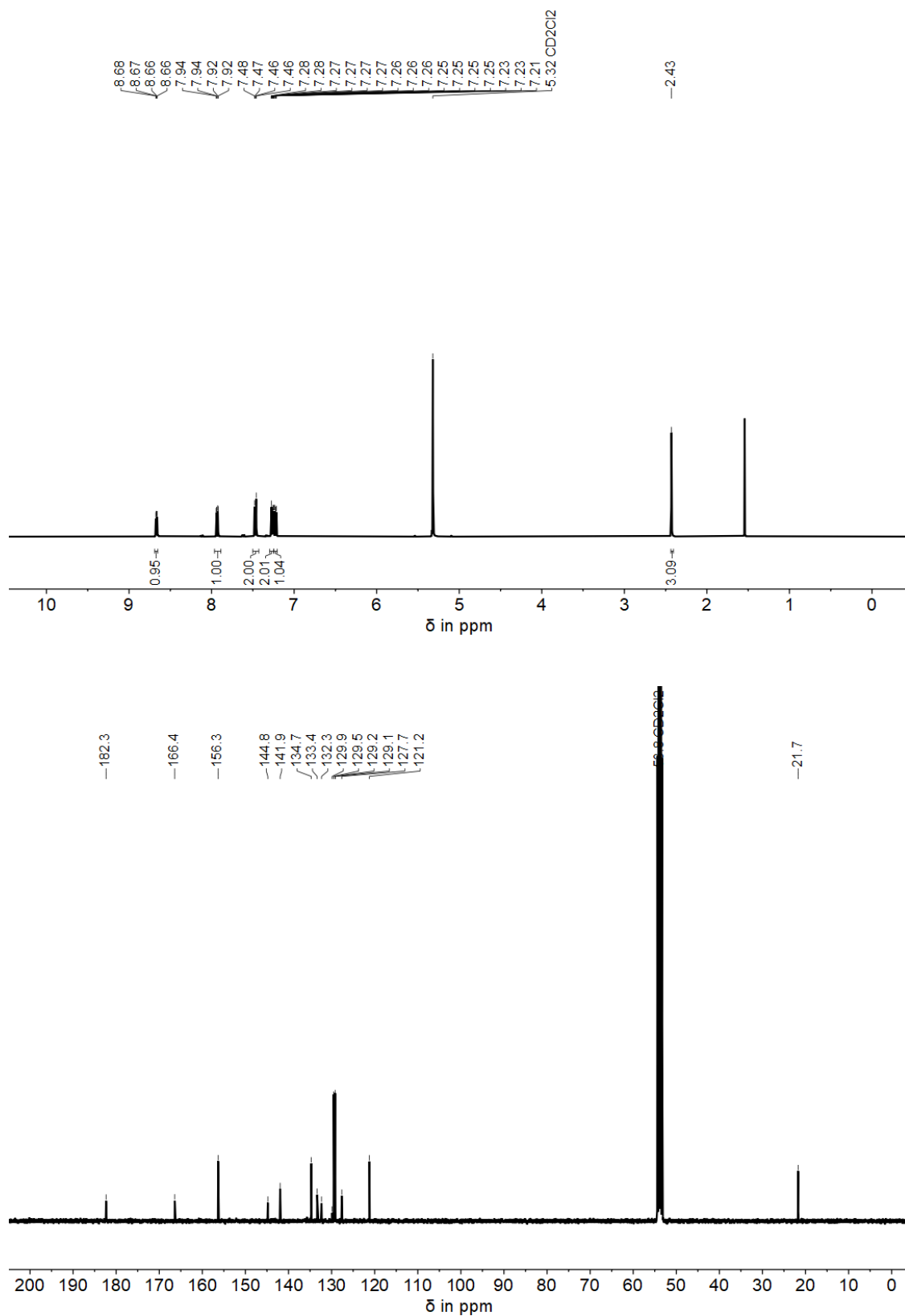


Figure S64: NMR spectra of compound **19**; ^1H NMR spectrum (400 MHz, CD_2Cl_2 , 23 °C) (top); ^{13}C NMR spectrum (101 MHz, CD_2Cl_2 , 23 °C) (bottom).

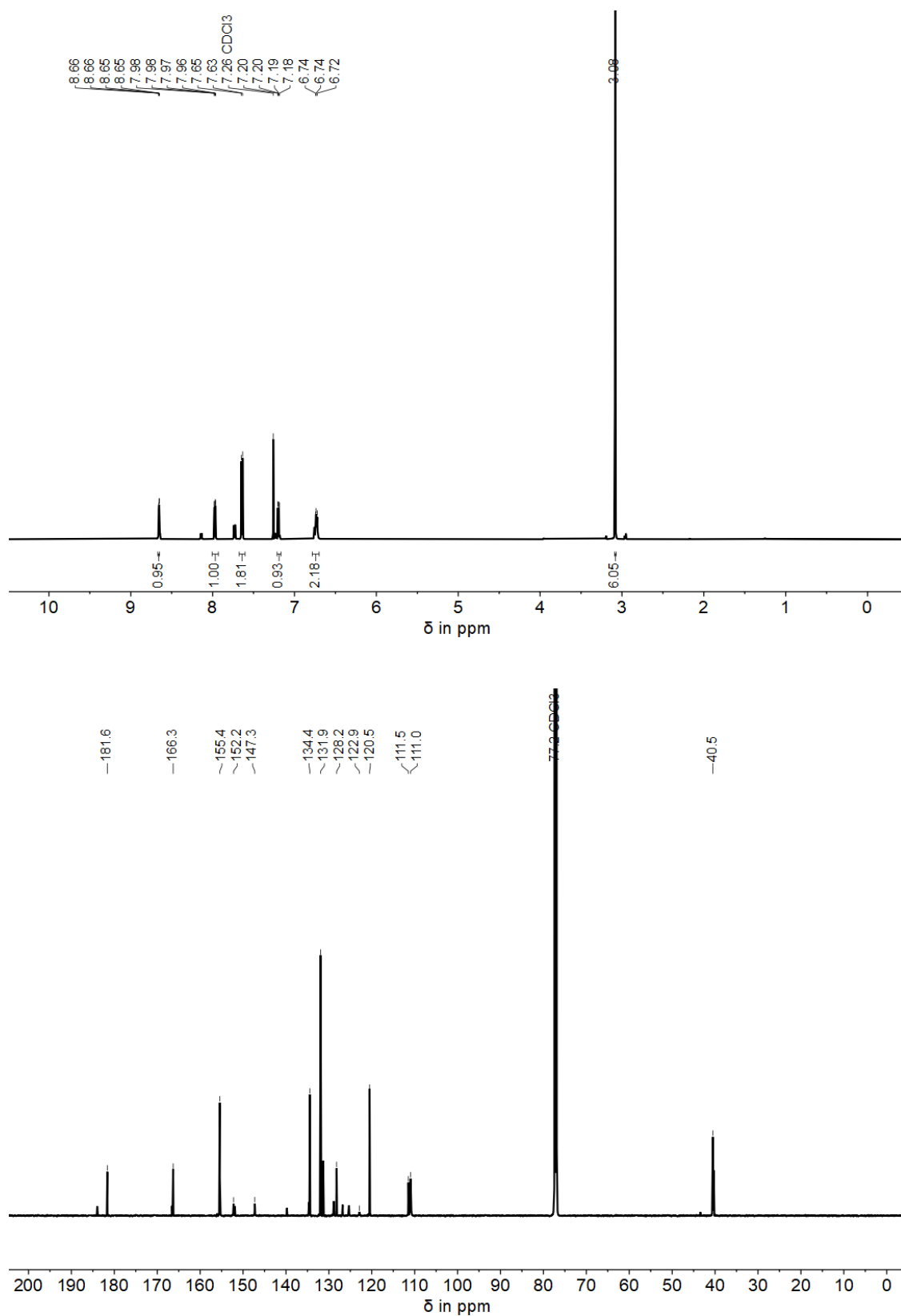


Figure S65: NMR spectra of compound **20** (mixture of *E* and *Z* isomer); ¹H NMR spectrum (601 MHz, CDCl₃, 23 °C) (top); ¹³C NMR spectrum (151 MHz, CDCl₃, 23 °C) (bottom).

References

- [1] G. R. Fulmer, A. J. M. Miller, N. H. Sherden, H. E. Gottlieb, A. Nudelman, B. M. Stoltz, J. E. Bercaw, K. I. Goldberg, *Organometallics* **2010**, *29*, 2176.
- [2] A. Gerwien, T. Reinhardt, P. Mayer, H. Dube, *Organic Letters* **2018**, *20*, 232.
- [3] L. C. King, G. K. Ostrum, *The Journal of Organic Chemistry* **1964**, *29*, 3459.
- [4] J. E. Zweig, T. R. Newhouse, *Journal of the American Chemical Society* **2017**, *139*, 10956.
- [5] B. Zhong, L. Sun, H. Shi, J. Li, C. Chen, Z. Chen, WO2017176812, **2017**.
- [6] H. Volfova, Q. Hu, Riedle Eberhard, *EPA Newsletter* **2019**, 51.